

MINISTRY OF HEALTH OF UKRAINE
ZAPORIZHZHIA STATE MEDICAL UNIVERSITY
Internal Medicine Department no2

O. E. Berezin, V. A. Vizir, O. V. Demidenko

CARDIOVASCULAR DISEASES.

TOPICS FOR STUDENTS' SELF-EDUCATION.

(«INTERNAL MEDICINE». MODULE 2)

PART 1

The executive task force for students of of medical faculty 5th course

Zaporizhzhia

2019

UDC 616.1(075.8)

B 45

*Ratified on meeting of the Central methodical committee
of Zaporizhzhia State Medical University
and it is recommended for the use in educational process for foreign students.
(Protocol no 2 from 28.11.2019.)*

Reviewers:

V. V. Syvolap - MD, PhD, professor, Head of Department of Multimodal Diagnostics and Propedeutics, Zaporizhzhia State Medical University;

O. V. Kraydashenko - MD, PhD, professor, Head of Department of Clinical Pharmacology, Pharmacy and Pharmacotherapy with the Course of Cosmetology, Zaporizhzhia State Medical University.

Authors:

O. E. Berezin - MD, PhD, professor, Department of Internal Diseases 2;

V. A. Vizir - MD, PhD, professor, Department of Internal Diseases 2;

O. V. Demidenko -MD, PhD, Head of Department of Internal Diseases 2.

Berezin O. E.

B45 Cardiovascular diseases («Internal Medicine». Modul 2). Topics for self-education of students: Part 1 : The executive task force for self-education of students of 5th course of medical faculty / O. E. Berezin, V. A. Vizir, O. V. Demidenko. – ZSMU, 2019. – 139 p.

Березін О. Є.

Захворювання серцево-судинної системи. Питання для самостійної роботи студентів («Внутрішня медицина». Модуль 2). Ч. 1 : навчальний посібник для самостійної роботи студентів 5 курсу медичного факультету / О. Є. Березін, В. А. Візір, О. В. Деміденко. – ЗДМУ, 2019. – 139 с.

The executive task force is provided to the students of 5th courses of medical faculties for self-education on some topics in the fields of cardiovascular diseases incorporated into the discipline «Internal Medicine». There is the information about the most important topics regarding diagnosis of cardiac diseases.

UDC 616.1(075.8)

©Berezin A. E., Vizir V. A., Demidenko O. V., 2019

©Zaporizhzhia State Medical University, 2019

Content

1. **Topic 1. Practical skills for the topic №1 «Normal ECG, normal echocardiogram».....6**
 - 1.1.Acquiring methodology of ECG registration and interpretation.
 - 1.2.Mastering the skills of echocardiogramms' interpretation in the field of the topic.
2. **Topic 2. Practical skills for the topics №2, №3 and №4 «Primary arterial hypertension. Secondary arterial hypetension. Neurocirculatory dystonia»..... 58**
 - 2.1.Acquiring methodology of blood pressure measure.
 - 2.2.Mastering the skills of risk stratification in patients with arterial hypertension
 - 2.3.Mastering the skills of ECGs' interpretation in the field of the topic.
3. **Topic 3. Practical skills for the topics №5, №6 and № 7 «Atherosclerosis. Chronic coronary artery disease. Acute coronary syndrome (unstable angina, acute myocardila infarction)»..... 71**
 - 3.1.Mastering the skills of cardiovascular risk stratification.
 - 3.2.Mastering the skills of lipid profile interpretation.
 - 3.3.Mastering the skills of biochemistry data interpretation (biomarkers of myocardial necrosis).
 - 3.4.Mastering the skills of ECG interpretation in the field of the topic.
4. **Topic 4. Practical skills for the topic №8 «Inheried heart diseases in adults. Aquired heart diseases»..... 96**
 - 4.1.Mastering the skills of thoracic X-ray data interpretation in the field of the topic.
 - 4.2.Mastering the skills of EchoCG interpretation in the field of the topic.

List of abbreviations

ACS	acute coronary syndrome
APAH	associated pulmonary arterial hypertension
ASD	atrial septal defect
AV	atrioventricular
CAD	coronary artery disease
CHD	coronary heart disease
CT	computed tomography
CV	cardiovascular diseases
ECG	electrocardiogram
EF	ejection fraction
ESC	European cardiology Association
HCM	hypertrophic cardiomyopathy
HDL- C	high-density lipoprotein cholesterol
HF	heart failure
HIV	human immunodeficiency virus
IPAH	idiopathic pulmonary arterial hypertension
ISH	isolated systolic hypertension
IVUS	intravascular ultrasound
JET	functional ectopic tachycardia
LA	left arm
LAFB	left anterior fascicular block
LBBB	left bundle branch block
LL	left leg
LMWH	low molecular weight heparin
LQTS	long-QT syndrome
LV	left ventricle / ventricular
LVH	left ventricular hypertrophy
LVNC	left ventricular non-compaction
LVOT	left ventricular outflow tract
MBC	minimum bactericidal concentration
MHC	myosin heavy chain
MI	myocardial infarction
MR	mitral regurgitation
MRI	magnetic resonance imaging
NSTEMI	non ST-elevation MI
PAC	pulmonary artery catheter
PAP	pulmonary arterial pressure
PH	pulmonary hypertension
PP	pulse pressure

PPCM	peripartum cardiomyopathy
PVCs	premature ventricular complexes
PVD	peripheral vascular disease
PVE	prosthetic valve endocarditis
PVR	pulmonary vascular resistance
PVT	prosthetic valve thrombosis
RA	right arm
RAP	right atrial pressure
RBBB	right bundle branch block
RCM	restricted cardiomyopathy
RCT	randomized controlled trial
RHC	right heart catheterization
RV	right ventricle/ventricular
SVT	supraventricular tachycardia
TAPSE	tricuspid annular plane systolic excursion
TDI	tissue Doppler imaging
TEE	transesophageal echography
TEE	transesophageal echography
VA	ventriculoatrial
WPW	Wolff-Parkinson-White syndrome

1. Topic 1: Preparation for class №1 «Normal ECG and normal echocardiogram».

1.1. Acquiring methodology of ECG registration and interpretation

What is commonly called an electrocardiogram (ECG) is the graph obtained when the electrical potentials of an electrical field originating in the heart are recorded at the body surface. Although the ECG gives very useful clinical information, it only provides an approximation of the voltage produced by the source. The ECG has not been able to achieve interesting new insights into its own basic theoretic limitations, which some have considered as the solutions of the "forward" problem and the "inverse" problem of electrocardiography. Whereas the former seeks the description of a specific electrocardiographic pattern in response to a specific local or regional intracardiac change in electrical activity, the latter seeks to predict the behavior of the cardiac generator from potentials recorded at the body surface. Nevertheless, recent experimental studies have provided new information capable of expanding the clinical usefulness of the ECG, as will be discussed throughout this chapter. The ECG has many uses: It may serve as an in-dependent marker of myocardial disease; it may reflect anatomic, hemodynamic, molecular, ionic, and drug-induced abnormalities of the heart; and it may provide information that is essential for the proper diagnosis and therapy of many cardiac problems. In fact, it is the most commonly used laboratory procedure for the diagnosis of heart disease. Underreading or misreading due to insufficient knowledge of pathologic conditions, overreading due to an inability to recognize technical errors, and most important, failure to correlate ECG findings with the clinical findings may result in iatrogenic heart disease. Every physician interpreting ECGs as well as those learning electrocardiographic interpretation should read the Guidelines for Electrocardiography of the American College of Cardiology, American Heart Association; European Cardiology Society Task Force.

Ventricular depolarization and repolarization

Fluxes of ions across the cell membranes cause the differences in voltage between resting and activated myocardial cells. To understand the electrical forces produced by the heart as a whole at the body surface, it has been conventional to first

discuss the electrical properties of a hypothetical muscle strip from the free wall of the left ventricle extending from endocardium to epicardium. In the resting or polarized state, the charges are at rest. A unipolar electrode facing the epicardial side of the strip, such as V6, registers an isoelectric line. If activation of this relatively large muscle strip starts in the endocardial side, it initiates the process called depolarization. The sequence of this process is thus from endocardium to epicardium. Depolarization has been described as a moving wave with the positive charges in front of the negative charges. The previously mentioned lead V6 overlying the epicardium of the left ventricle will record a positivity because it consistently faces positive charges throughout the entire depolarization sequence. On the other hand, the sequence of ventricular repolarization is from epicardium to endocardium. The negative charges, however, travel in front because repolarization tends to reestablish the resting, polarized state of the previously depolarized cells. As a consequence of the latter, V6 will record a positive deflection (T wave) because it constantly faces positive charges throughout the entire repolarization sequence. The earlier epicardial end of repolarization has been attributed to the shorter duration of repolarization that epicardial cells have in comparison with endocardial cells. Thus repolarization finishes at the epicardium while it still has not been completed at the endocardium. Hence the sequence of repolarization is, as noted previously, from epicardium to endocardium. M cells play a determining role in the inscription of the T wave because currents flowing down voltage gradients on either side of the usual (but not necessarily) mid-myocardial cells determine both the height and width of the T wave, as well as the degree to which the ascending or descending limbs of the T wave are interrupted.

Electrocardiographic leads

To record an ECG, an electric circuit between the heart and the electrocardiograph must be completed. For this purpose, electrodes are placed on different parts of the body surface and are connected to the instrument by means of cables. Thus the whole system consists of an instrument, electrodes, cables, and leads.

Bipolar Standard Leads

An ECG lead can be defined as a pair of terminals with designated polarity, each of which is connected either directly or via a passive-active network to recording electrodes. In 1913, Einthoven developed a method of studying the electrical activity of the heart by representing it graphically in a two-dimensional geometric figure, namely, an equilateral triangle. There are several simplifying assumptions on which Einthoven's hypothesis is founded:

1. The body is a homogeneous volume conductor. Although the conductivity of the various tissues is not the same, the differences are not great enough to invalidate that the body can be considered as a homogeneous volume conductor.

2. The sum of all the electric forces, or the mean of all the forces generated during the cardiac cycle, can be considered as originating in a dipole located in the electrical center of the heart.

3. Electrodes placed on the right arm (RA), left arm (LA), and left leg (LL) are used to pick up the potential variations on these extremities. Standard (bipolar) leads (I, II, and III) are obtained by recording, respectively, the potential differences between LA and RA, LL and RA, and LL and LA. These leads record potential variations in a single frontal plane only.

4. Attachment between these limb electrodes, on the forearms and limbs, corresponds to a position in the root of the corresponding limb. For example, an electrode in the right forearm records the electrical activity that reaches the right shoulder. It should be pointed out that when the electrodes are placed proximally to the roots of the extremities, they lose their relatively "far" distance from the heart.

Hence Einthoven's equilateral theory does not hold. The latter is of importance to understand why leads placed proximally to the roots of the extremities, such as those used for exercise testing and coronary care unit and Holter monitoring, by being only "equivalent" to the corresponding bipolar leads, are in some cases markedly different from the "true" standard bipolar leads.

Wilson Central Terminal

The sum of the potentials from the right arm (RA), left arm (LA), and left leg (LL) is equal to zero throughout the cardiac cycle with respect to any point at the body surface. Lead wires attached to electrodes on each limb are connected together,

through 5000-Ω resistors, at a point. When this common point-Wilson's central terminal-is attached to the negative pole of the ECG machine and an "exploring" electrode is connected to the positive pole, the potential variations recorded will be those of the latter only. A lead taken by this method is called a unipolar lead. Actually, the central terminal is not zero because the RA, LA, and LL are not equidistant from each other and from the heart, the body tissues vary in resistance, and the heart and extremities do not lie in exactly the same plane in the body. The potential of the central terminal has been said to average around 0.3 mV.

Unipolar Extremity Leads

At present, unipolar extremity leads are obtained by disconnecting the input to the central terminal of Wilson from the extremity being explored. This results in a one-and-a-half increase in their voltage. These augmented (a) extremity leads are the ones usually used for clinical electrocardiography and are labeled aVR, aVL, and aVF.

Unipolar Precordial Leads

The unipolar precordial ECG is obtained by placing the exploring electrode (connected to the positive pole of the ECG machine) on the classic six locations of the anterior and left portions of the chest. The central terminal is used as the indifferent electrode. Precordial (V) leads yield a positive deflection when facing positive charges and negative deflections when facing negative charges. They do this according to what Wilson called the solid-angle concept. A solid angle is merely an imaginary cone extending from the site in the chest throughout the heart. The precordial electrode is at its apex, and its base is at the opposite epicardial surface. This concept is most important to understand precordial lead morphologies. According to Wilson's scalar concept of electrocardiography, this occurs because the solid angle subtended by the corresponding lead records the electrical activity from the regions of the heart over which the lead is placed as well as from distant regions.

Thus, if V₂ is placed over (thereby facing) the right ventricle, part of the initial positive ventricular deflection reflects right ventricular activation, with the corresponding electrical forces moving toward the electrode. Most portions of the terminal S wave represent activation of muscle other than the right ventricle (septum and free left ventricular wall), reflecting electrical forces moving away from the

electrode. Acceptance that the amount of muscle activity recorded by various unipolar leads is not the same implies different "real" duration of depolarization and repolarization, irrespective of that supposedly resulting from the projections of a vector on an idealized horizontal lead axis (see sections on QT dispersion and vectorcardiography). For practical purposes, the peak of the r (or R) wave in precordial leads gives a rough estimate of the moment of arrival of excitation (intrinsicoid deflection) at the muscle underneath the electrode. This encompasses a considerable number of muscle fibers (given by the solid-angle concept), however-in fact, a greater number than if the electrode is placed directly on the epicardial surface. In the latter case, the moment of arrival of excitation at the electrode affects a lesser number of fibers and is thus given by the intrinsic deflection.

Special Leads

Some leads are not considered part of the standard ECG but are useful in specific circumstances. Posterior leads (V7, V8, and V9) increase the ECG sensitivity for injury in the posterior wall. Right precordial leads (V3R, V4R) are particularly useful for the diagnosis of right ventricular infarcts and of some congenital abnormalities. A routine use of the negative aVR (at 30 degrees) would add useful information to the standard ECG, and it would be less likely to be overlooked during routine ECG interpretation.

The P wave is not always distinctly seen in the 12-lead ECG, but it may be easily identified with special leads. Distinct P waveforms can be seen by placing the right and left arm leads in various chest positions (if possible, parallel to the vector of atrial depolarization) while recording lead I (the Lewis lead). Atrial activity can also be recorded semiinvasively from leads placed in the esophagus because the anterior wall of the esophagus lies against the left atrium. In patients with dual-chamber pacemakers, atrial electrograms can be recorded by telemetry from the pacing electrodes. In patients recovering from cardiac surgery, the placement of temporary epicardial pacing electrodes allows the direct recording of atrial activity.

Equipment

Electrocardiographers are calibrated to give a deflection of 10 mm/mV (this calibration is seen at the beginning or end of the ECG). ECG paper is graph paper

divided in little squares of 1 mm each and bigger squares of 5 mm each. The paper speed is standardized to 25 mm/second. One mm equals 0.1 mV.

Commercial systems provide ECG programs with stereotyped methodologies of measurement. The only limb ECG leads that digital electrocardiographs record are leads I and II; the remaining limb leads are calculated in real time based on the Einthoven law ($I + III = II$) and using relationships derived from lead vectors for the aV leads. For the calculation of the electrical QRS axis, the entire QRS complex area is used. This is an advantage over the manual QRS axis estimation, based mainly on R-wave measurements.

Current electrocardiographs use digital technology. Analog data are converted into digital signals that are later processed. The use of compression techniques allows storage and subsequent retrieval of serial ECG recordings, as well as remote transmission of ECG data

Normal activation of the heart: ventricular depolarization

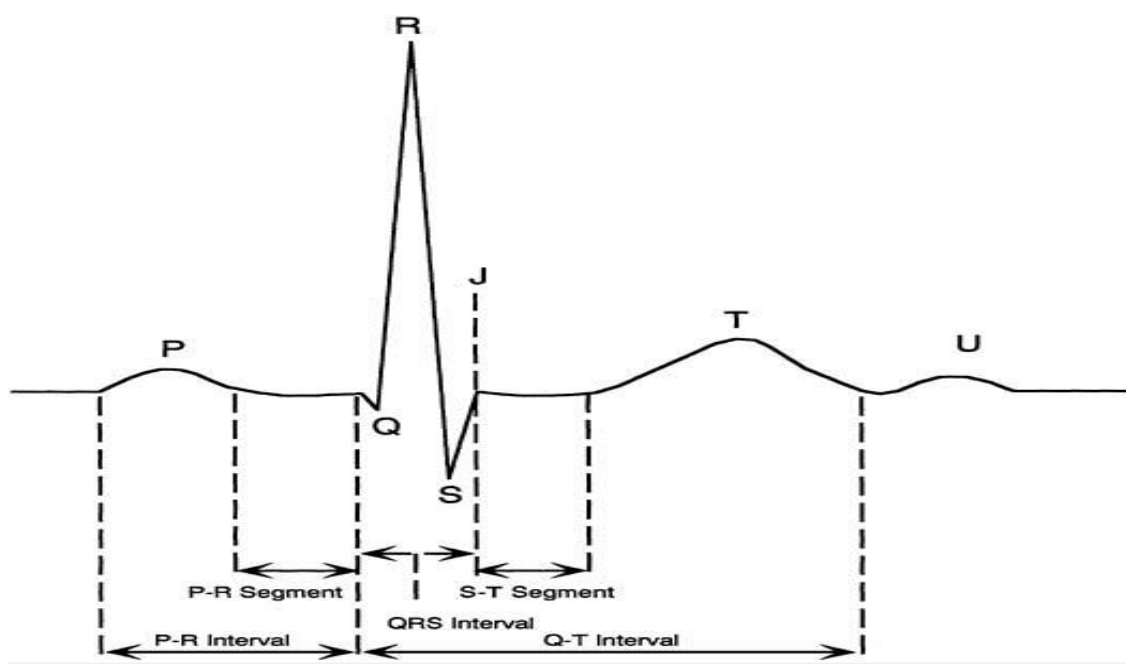
After emerging from the sinus node, the cardiac impulse propagates throughout the atria in its journey toward the atrioventricular (AV) node. The normal P wave (resulting from activation of the myocardium of both atria) is a consequence of, but does not directly represent, sinus node activity. During sinus rhythm, the right atrium is activated before the left atrium. This explains why high-fidelity recordings of the P waves of some normal persons show a small notch at the top. The latter simply reflects the normal asynchrony existing between the atria. Because of the anatomic position of the sinus node, the sequence of atrial depolarization occurs in an inferior, leftward, and somewhat posterior direction. The normal P waves are always positive in leads I, II, aVF, and V3 to V6 and negative in lead aVR. According to the anatomic position of the heart, the P wave may be diphasic in V1 and aVL or negative in the latter lead.

Atrial repolarization, also called Ta, is directly opposite in polarity to the P wave. It is usually not seen because it coincides with the PR segment (not to be confused with the PR interval) and QRS complex. The PR interval (used to estimate AV conduction time) includes conduction through the "true" AV structures (AV node, His bundle, bundle branches, and main divisions of the left bundle branch), as

well as through those parts of the atria located between sinus and AV nodes. The onset of ventricular depolarization (given by the beginning of the normal q wave) reflects activation of the left side of the interventricular septum. This has been attributed to the fact that the left bundle system is shorter than the right bundle branch.

In addition, the large fanlike distribution of the ramifications of the fascicles of the left bundle branch on the left septal surface produces activation of a greater number of ordinary muscle cells per unit of time. For this reason, the normal initial depolarization is oriented from left to right, therefore explaining the small q wave in lead V6 and the small r wave in lead V1. After the cardiac impulse descending through the right bundle branch reaches the right septal surface, the interventricular septum is activated in both directions. Septal activation is thereafter encompassed within or neutralized by free-wall activation. The most distal ramifications of both bundle branches (Purkinje fibers) form networks within the subendocardial regions of both ventricular walls. The latter are activated as soon as the multiple ramifications emerge from the Purkinje fibers. The greater mass of the left ventricular (LV) free wall explains why LV free-wall events overpower those of the interventricular septum and right ventricular free wall. Normal intervals and waves on ECG are presented in Figure 1.

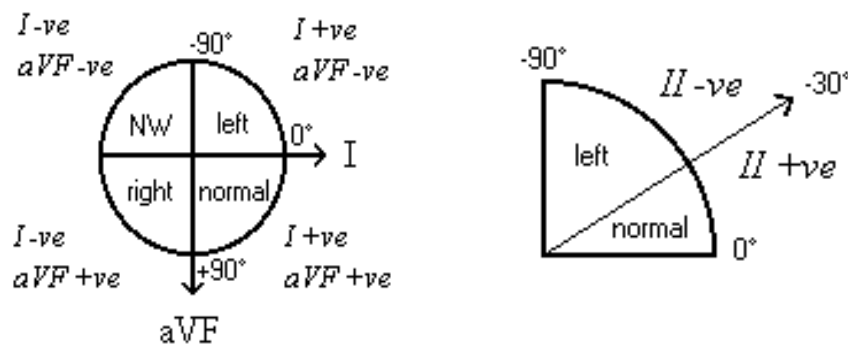
Figure 1: Normal intervals and waves on ECG



Electrical axis

The electrical axis (EA) may be defined as a vector originating in the center of Einthoven's equilateral triangle (Figure 2). A vector is a mathematical value expressed as an arrow that has magnitude, sense, and direction. On the other hand, scalar values only have magnitude

Figure 2: Determination of the electrical axis



Notes:

- both I and aVF +vector = normal axis
- both I and aVF - vector = axis in the Northwest Territory
- lead I - vector and aVF + vector = right axis deviation
- lead I + vector and aVF - vector
 - lead II + vector = normal axis
 - lead II - vector = left axis deviation

Noted that using leads I and aVF the axis can be calculated to within one of the four quadrants at a glance. If the axis is in the "left" quadrant take your second glance at lead II.

When applied to the EA of the QRS complexes, the vector that represents it also gives the direction of the activation process as projected in the plane of the limb leads. Its length represents the manifest potential of the dipole in the center of the triangle. These general considerations apply either to the instantaneous EA (the vector indicating the direction of the impulse at the instant at which it is determined) or to the mean EA (which is the resultant of all instantaneous electrical axes). Although the term EA can be used in reference to any of the major components of the ECG (P, T, or QRS), it is generally applied to the QRS. There are many methods for determining the mean EA. The one recommended by electrocardiographers of the classical school consists of calculating the net areas enclosed by the QRS complex in leads I, II, and III. The net area is the absolute sum of the positive and negative areas of the QRS complex in the corresponding lead. One of the drawbacks of this method is that the absolute values of the net area cannot be determined accurately by

inspection. Since the absolute magnitude of the EA is not of fundamental clinical importance, it has been recommended that arbitrary units be used.

When this is done, the results can be counterchecked by using Einthoven's law. For example, if in a given case lead I is +4 units, lead II is +2 units, and lead III is -2 units, the calculation is accurate because the sum of leads I and III (+4 plus -2) must always equal lead II (+2). After having determined the net area, the results are plotted on the sides of the triangle, and perpendiculars are dropped from two or all three leads. The perpendiculars will meet at a point away from the center of the triangle. A line drawn from the latter to the former defines the mean EA. A simpler, though less precise, method of calculating the quadrant (or parts of a quadrant) in which the EA is located consists of using the maximal QRS deflection in leads I and aVF and, when necessary, lead II. This method is inexact from the mathematical viewpoint but has the value of simplicity. The main causes of axis deviation are presented in Table 1.

Table 1: The main causes of axis deviation

The type of axis deviation	Main causes of axis deviation
Northwest axis	<ul style="list-style-type: none"> • emphysema • hyperkalaemia • lead transposition • artificial cardiac pacing • ventricular tachycardia
Left axis deviation	<ul style="list-style-type: none"> • left anterior hemiblock • Q waves of inferior myocardial infarction • artificial cardiac pacing • emphysema • hyperkalaemia • Wolff-Parkinson-White syndrome - right sided accessory pathway • tricuspid atresia • ostium primum ASD • injection of contrast into left coronary artery
Right axis deviation	<ul style="list-style-type: none"> • normal finding in children and tall thin adults • right ventricular hypertrophy • chronic lung disease even without pulmonary hypertension • anterolateral myocardial infarction • left posterior hemiblock • pulmonary embolus • Wolff-Parkinson-White syndrome - left sided accessory pathway

- | | |
|--|--|
| | <ul style="list-style-type: none">• atrial septal defect• ventricular septal defect |
|--|--|

Ventricular gradient

The relationship between the EA of the QRS complex and the T wave was referred to by Wilson as the ventricular gradient. In contrast to what occurs in an epicardial-to-endocardial muscle strip (as mentioned previously), in the isolated muscle strip, the sequence of ventricular depolarization occurs in the same direction as that of repolarization. Although the QRS and T deflections have opposite polarity, the algebraic sum of QRS and T areas is zero. In the human heart, however, not only is the sequence different, but the pathways of ventricular depolarization and repolarization are not exactly the same. Thus the algebraic sum of QRS and T areas is no longer zero.

Therefore, a gradient is said to exist. The ventricular gradient can be calculated by determining the electrical axis of the QRS and T (using areas) and then obtaining the resultant by the parallelogram method. Wilson considered that the ventricular gradient could be of help in differentiating between T-wave inversion of various causes (primary changes) and the obligatory secondary T-wave changes resulting from abnormalities in depolarization, such as bundle branch block, ventricular hypertrophy, ventricular pacing, and preexcitation syndromes. In practice, calculation of the ventricular gradient is difficult and time consuming because it has to be determined by areas and not maximal amplitude.

The type was attributed to modulated electrotonic interactions occurring during cardiac activation in such a way that repolarization was accelerated at ventricular sites where depolarization begins and delayed in areas where depolarization terminates. T-wave changes appearing after prolonged depolarization was no longer present showed accumulation and (fading) long-term memory for variable time.

Cardiac Rhythm

The rhythm is sinus if there is a P wave in front of every QRS and if the P wave is upright in leads I and aVF (Figure 3). The rhythm is low right atrial if there is a P wave in front of every QRS but if the P wave is upright in lead I and inverted in lead aVF (Figure 4). This is not an abnormal rhythm. It is a variant of normal and requires

no special evaluation or treatment. The rhythm is left atrial if there is a P wave in front of every QRS and the P wave is inverted in lead I (Figure 5). This rhythm can be associated with situs inversus totalis, in which the morphologic right atrium and the normal sinus node are to the left of the left atrium. In this case, the rhythm requires no treatment. A left atrial rhythm can also occur with normal situs when a left atrial electric focus supplants the normal sinus rhythm. In the absence of a left atrial ectopic focus tachycardia associated with this condition, no treatment is required.

Figure 3: Sinus rhythm

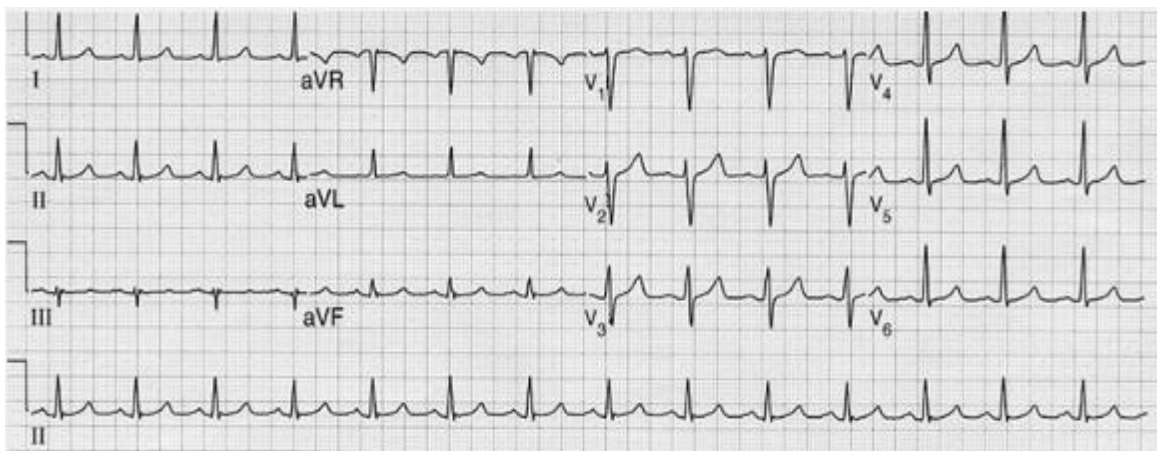


Figure 4: Low right atrial rhythm

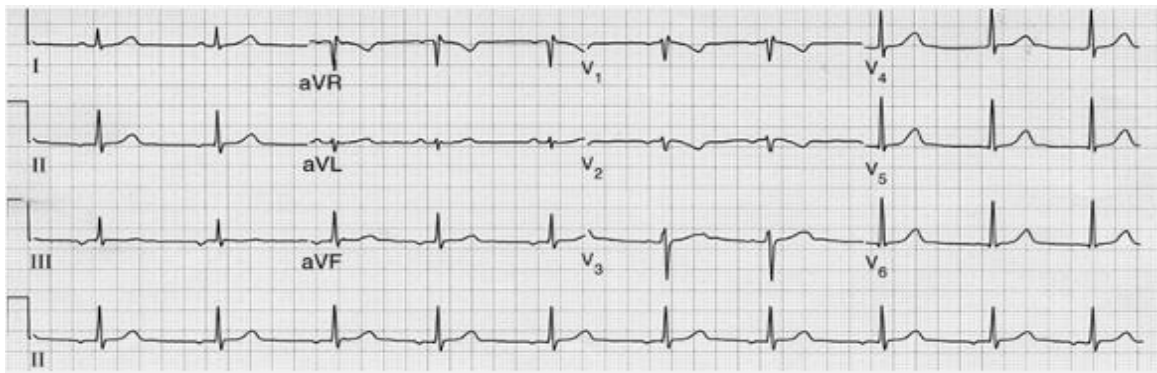
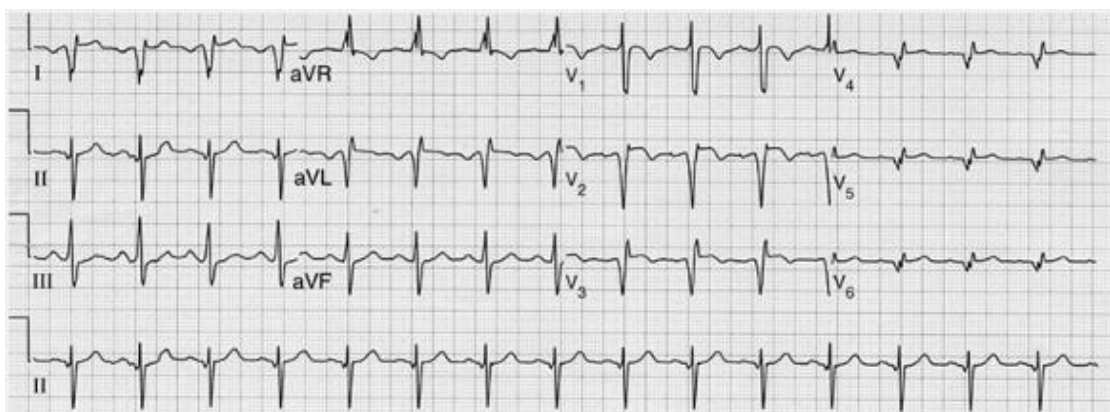
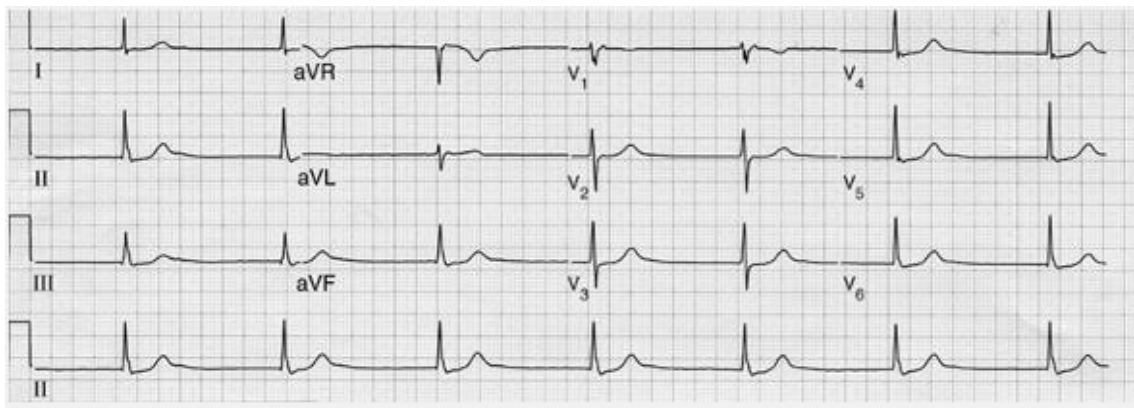


Figure 5: Left atrial rhythm



The rhythm is functional if there is no P wave in front of the QRS and if the QRS is narrow (<80 msecond; two small boxes) (Figure 6). Usually, functional rhythm is slower than the expected sinus rate. Intermittent functional rhythm can be normal, especially during sleep. The treatment for functional rhythm in the absence of any sinus rhythm may involve insertion of a pacemaker. However, it is difficult to identify patients who require a pacemaker. When functional rhythm is a complication of cardiac surgery, most experts recommend insertion of a pacemaker. If functional rhythm is particularly slow or is associated with symptoms of lightheadedness or syncope, insertion of a pacemaker is indicated.

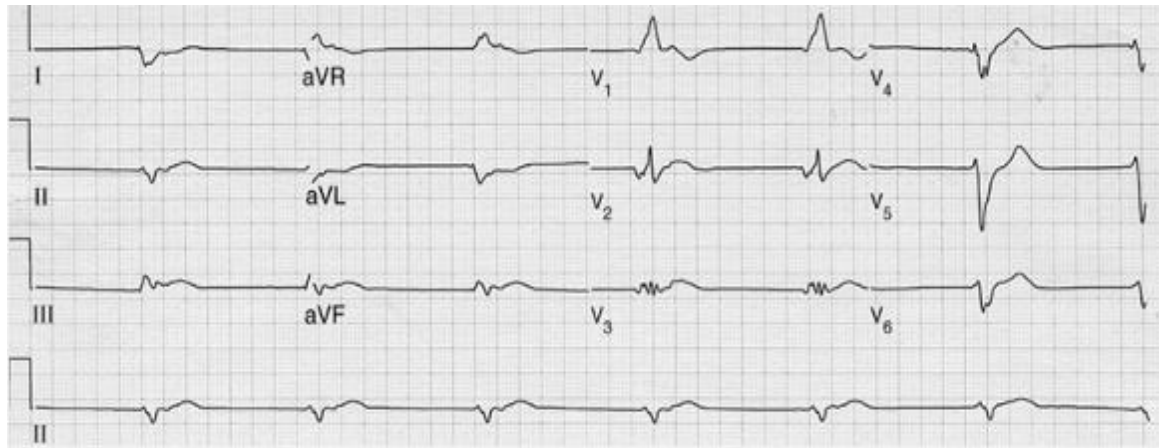
Figure 6: Functional rhythm



If there is no P wave in front of the QRS and if the QRS is wide (>120 msecond), the rhythm likely is originating distal to the His bundle (Figure 7). The rhythm most likely is ventricular in origin. Alternatively, the rhythm could be originating from the junction if there is bundle branch block. The treatment of this condition depends upon many factors. Firstly, one must determine whether the rhythm is functional with aberrant conduction or is ventricular or fascicular in origin. If a previous ECG is available when the patient was in sinus rhythm and if the morphology of the QRS complex in sinus rhythm is identical to that when there is no sinus rhythm, then the rhythm is functional and treated accordingly (see preceding text). Secondly, if the rhythm is ventricular or fascicular, its cause must be determined. The causes of ventricular or fascicular rhythms include myocarditis, electrolyte imbalance, long QT-interval syndrome, Brugada syndrome, and myocardial ischemia, among others. The treatment will depend upon the underlying cause but might include correction of metabolic abnormalities causing the

arrhythmia, drugs to suppress the rhythm, and/or an implantable cardiac defibrillator (ICD). There is a condition of benign ventricular tachycardia (VT) of childhood that requires no treatment. However, before arriving at this diagnosis, all other causes of ventricular rhythms must be excluded.

Figure 11.7: Rhythm likely originating distal to the His bundle



Abnormal ST-segment changes

In orthodox ECG language, injury implies abnormal ST-segment changes, necrosis implies abnormal Q waves, and ischemia implies symmetric T-wave inversion (or elevation). Following conventional ECG theory, several authors consider that ECG "injury" occurs because the affected cells are unable to maintain their normal polarization during diastole. Various hypotheses have been postulated to explain how this diastolic hypopolarization or generalized diastolic depolarization is manifested as abnormal ST-segment shifts in the surface ECG. One hypothesis is based on the existence of a diastolic current of "injury." During the control (diastolic) period, both membrane resting potential and surface ECG baseline are at their normal level. At the onset of injury, the resting intracellular potential decreases (e.g., from 90 to 70 mV), and the ECG baseline shifts below its preinjury level. Because the injured cells leak negative ions, their exterior becomes relatively negative (or less positive) than that of the normal cells.

Thus, a "current of injury" flows between the negative ("injured") zone and the positive ("normal") region. This produces a negative displacement of the surface ECG baseline in the leads facing the injured region. In the surface ECG, depolarization (by virtue of the electrical negativization of the nonaffected area)

practically reduces the potential difference between noninjured and injured regions. Therefore, the ST segment remains at the preinjury level, which is relatively elevated in reference to the injury baseline.

Consequently, the ST segment appears to be abnormally displaced above the latter. Note that the apparent presence of a systolic current of injury actually reflects disappearance of the diastolic current of injury. Finally, after the end of repolarization, the current of injury between injured and noninjured regions is reestablished, and the ECG baseline is again depressed (as it was immediately before depolarization). Since the precise moment at which injury starts is not recorded in the usual alternating-current (ac) electrocardiographic recordings, the baseline that is almost invariably recorded is the postinjury baseline. It also has been shown that the abnormal ST-segment elevation in leads facing the affected zone does not merely represent the (passive) return of the baseline to its preinjury level but reflects a true, active, positive displacement.

Thus, when depolarization of both normal and injured regions has occurred, the surface of the normal cells will (on account of their greater initial polarization) be able to accumulate more negative ions. Hence the normal regions become more negative than the injured regions, which are relatively more positive.

In consequence, the ST segment becomes actively elevated above and beyond the preinjury baseline because of the relative potential difference existing at the end of depolarization. Most likely, injury reflects both disappearance of diastolic baseline shifts and active ST-segment elevation.

According to the current-of-injury theory, this process results in ST-segment elevation when the injured muscle is located between normal muscle and the corresponding unipolar electrode. On the other hand, ST-segment depression occurs when normal muscle is located between the injured tissue and the corresponding electrode. The mechanism of abnormal ST-segment elevation in anatomically defined ventricular aneurysms has not been fully established. Some authors consider that it results from the earlier repolarization of a ring of persistently viable (but nevertheless affected) tissue surrounding the aneurysm. For other investigators, chronic ST-

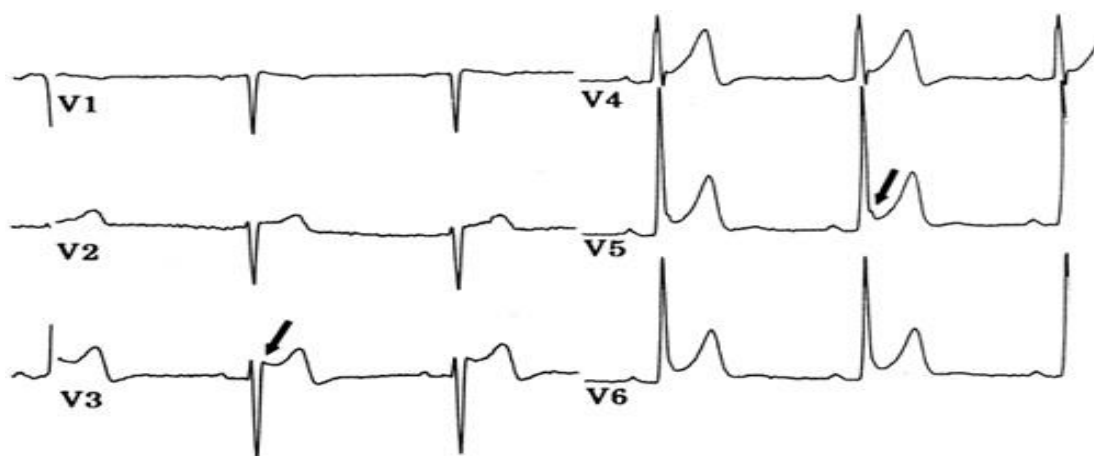
segment elevation reflects functional (echocardiographic) dyskinesia, thus not necessarily being due to a pathologic ventricular aneurysm.

Coronary artery disease is the most frequent cause of abnormal ST-segment elevation. The latter, when generalized, also can be due to epicardial injury due to pericarditis. Both should be differentiated from the benign "early repolarization" pattern, a normal variant. In its classic form, there is J-point elevation (of no more than 3 mm) with an upwardly concave ST segment.

Early repolarization phenomenon

R waves may be tall and at times have a distinct notch and slur on the downstroke (Figure 8). ST-segment elevation is more frequent in chest leads but can occur in leads I and II. These dynamic ECG changes may be affected by exercise and hyperventilation. Isoproterenol reduces and propranolol increases ST-segment elevation. Although the mechanism of early repolarization has not been fully elucidated, it has been related to enhanced activity of the right sympathetic nerves.

Figure 8: Early repolarization phenomenon



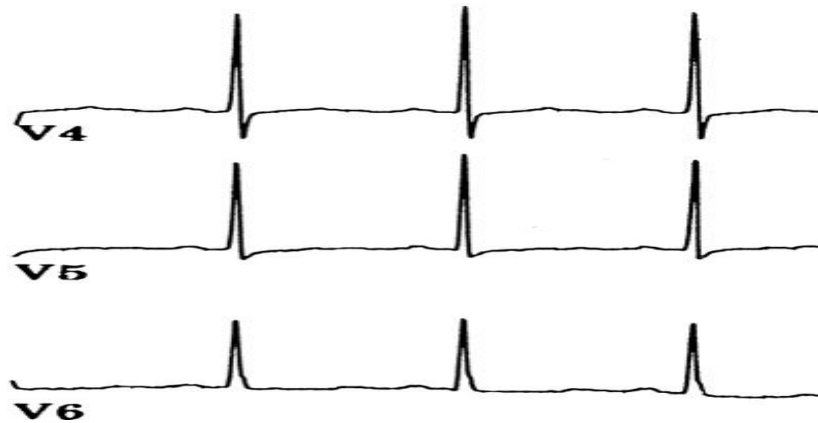
Note: This normal variant is characterized by narrow QRS complexes with J-point and ST-segment elevation in the chest leads. Left chest leads often show tall R waves with a distinct notch or slur in their downstroke (arrow in V5), while the right chest leads may display ST segments having a "saddleback" or "humpback" shape (arrow in V3).

Nonspecific ST-segment-T-wave changes

While it seems more appropriate to discuss ST-segment and T-wave changes separately, they will be dealt with together because of their often coexistence. While

nonspecific (or rather, nondiagnostic) ST-segment-T-wave changes are the most commonly diagnosed ECG abnormalities, they have not been categorized adequately and represent different findings for various interpreters (Figure 10).

Figure 10: Nonspecific (nondiagnostic) ST-segment-T-wave changes, the most common abnormalities in ECG interpretation



Depth of ST-segment depression and T-wave inversion as well as their contour. When analyzed without clinical information, this diagnosis was made in 40 percent of 410 abnormal ECGs. The number was reduced to 10 percent, however, when clinical data became available. In the absence of structural heart disease, these changes can be due to a variety of physiologic (i.e., hyperventilation, anxiety, body position, food, neurogenic influences, and temperature), pharmacologic (i.e., antiarrhythmic and psychotropic drugs, digoxin), and extracardiac (i.e., electrolyte abnormalities, upper gastrointestinal processes, allergic reactions, etc.) factors.

U wave

A number of hypotheses have been advanced to explain the genesis of the U wave. Foremost among them is the relationship to late repolarization of the Purkinje system. A criticism of this hypothesis is that the conducting system does not have sufficient mass to generate a large deflection at the body surface. The recent identification of another population of (M) cells between epicardium and endocardium may provide the necessary mass to produce not only U waves but also the J (or Osborn) wave characteristic of hypothermia. What sometimes appears to be a U wave merging with a T wave simple may be a notched T wave whose ascending or descending limbs are interrupted by differences in the end of the composite action

potential of epicardial and M cells. The normal U wave, most prominent in leads V2 and V3, has the same polarity as the T wave and is approximately 10 percent of its amplitude. A large positive U wave may be due to hypokalemia and multiple antiarrhythmic drugs. In orthodox ECG interpretation, merging of T and U is still considered a stage in hypokalemia but can result from such drugs as quinidine and sotalol. Repolarization of the His-Purkinje system was first suggested by Watanabe as the most likely cause of the "real" U wave. Causes of negative U waves are ischemia, hypertension, and occasionally, right ventricular enlargement.

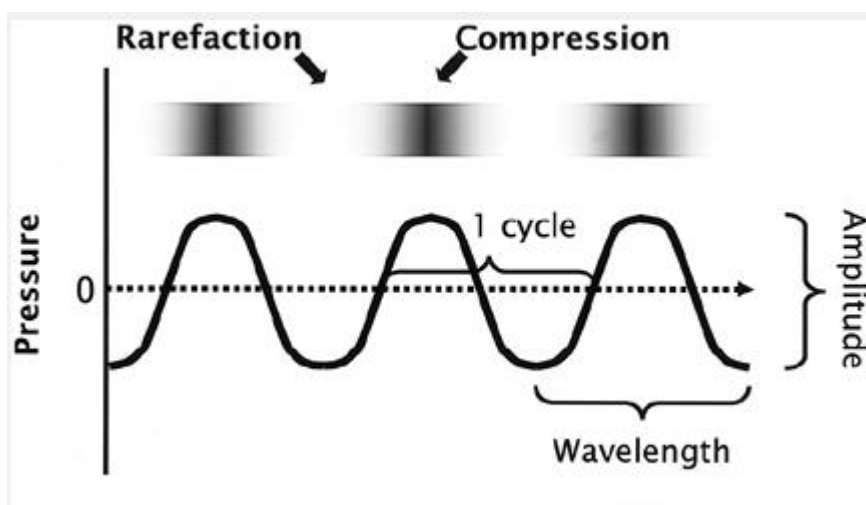
1.2. Mastering the skills of echocardiogramms' interpretation in the field of the topic.

Ultrasound (in contrast to lower, i.e., audible, frequency sound) has several characteristics that contribute to its diagnostic utility. First, ultrasound can be directed as a beam and focused. Second, as ultrasound passes through a medium, it obeys the laws of reflection and refraction. Finally, targets of relatively small size reflect ultrasound and can therefore be detected and characterized. A major disadvantage of ultrasound is that it is poorly transmitted through a gaseous medium and attenuation occurs rapidly, especially at higher frequencies. As a wave of ultrasound propagates through a medium, the particles of the medium vibrate parallel to the line of propagation, producing longitudinal waves. Thus, a sound wave is characterized by areas of more densely packed particles within the medium (an area of compression) alternating with regions of less densely packed particles (an area of rarefaction). The amount of reflection, refraction, and attenuation depends on the acoustic properties of the various media through which an ultrasound beam passes. Tissues composed of solid material interfaced with gas will reflect most of the ultrasound energy, resulting in poor penetration. Very dense media also reflect a high percentage of the ultrasound energy. Soft tissues and blood allow relatively more ultrasound energy to be propagated, thereby increasing penetration and improving diagnostic utility. Bone also reflects most ultrasound energy, not because it is dense but because it contains so many interfaces.

The ultrasound wave is often graphically depicted as a sine wave in which the peaks and troughs represent the areas of compression and rarefaction, respectively. Microscopic pressure changes occur within the medium, corresponding to these areas, and result in tiny oscillations of particles, although no actual particle motion occurs. Depicting ultrasound in the form of a sine wave has some limitations but allows the demonstration of several fundamental principles. The sum of one compression and one rarefaction represents one cycle, and the distance between two similar points along the wave corresponds to wavelength. Over the range of diagnostic ultrasound, wavelength varies from approximately 0.15 to 1.5 mm in soft tissue.

Figure 11 schematic illustrates how sound can be depicted as a sine wave whose peaks and troughs correspond to areas of compression and rarefaction, respectively. As sound energy propagates through tissue, the wave has a fixed wavelength that is determined by the frequency and amplitude that is a measure of the magnitude of pressure changes.

Figure 11: The physical principles of ultrasound



Velocity through a given medium depends on the density and elastic properties or stiffness of that medium. Velocity is directly related to stiffness and inversely related to density. Ultrasound travels faster through a stiff medium, such as bone. Velocity also varies with temperature, but because body temperature is maintained within a relatively narrow range, this phenomenon is of little significance in medical imaging.

If an ultrasound wave encounters an area of higher stiffness, for example, velocity will increase. Because frequency does not change, wavelength will also

increase. As is discussed later, wavelength is a determinant of resolution: the shorter the wavelength is, the smaller the target that is able to reflect the ultrasound wave and thus the greater the resolution.

Another fundamental property of sound is amplitude, which is a measure of the strength of the sound wave. It is defined as the difference between the peak pressure within the medium and the average value, depicted as the height of the sine wave above and below the baseline. Amplitude is measured in decibels, a logarithmic unit that relates acoustic pressure to some reference value. The primary advantage of using a logarithmic scale to display amplitude is that a very wide range of values can be accommodated and weak signals can be displayed along side much stronger signals. Of practical use, an increase of 6 dB is equal to a doubling of signal amplitude, and 60 dB represents a 1,000-fold change in amplitude or loudness. A parameter closely related to amplitude is power, which is defined as the rate of energy transfer to the medium, measured in watts. For clinical purposes, power is usually represented over a given area (often the beam area) and referred to as intensity (watts per centimeter squared or W/cm²). This is analogous to loudness. Intensity diminishes rapidly with propagation distance and has important implications with respect to the biologic effects of ultrasound.

These basic characteristics of ultrasound have practical implications for the interaction between ultrasound and tissue. For example, the higher the frequency of the ultrasound wave (and the shorter the wavelength), the smaller the structures that can be accurately resolved. Because precise identification of small structures is a goal of imaging, the use of high frequencies would seem desirable. However, higher frequency ultrasound has less penetration compared with lower frequency ultrasound. The loss of ultrasound as it propagates through a medium is referred to as attenuation. This is a measure of the rate at which the intensity of the ultrasound beam diminishes as it penetrates the tissue. Attenuation has three components: absorption, scattering, and reflection. Attenuation always increases with depth and is also affected by the frequency of the transmitted beam and the type of tissue through which the ultrasound passes. The higher the frequency is, the more rapidly it will attenuate. Attenuation may be expressed as the α -half-value layer or the α -half-power

distance, α which is a measure of the distance that ultrasound travels before its amplitude is attenuated to one half its original value. Representative half-power distances are listed in Table 2.3. As a rule of thumb, the attenuation of ultrasound in tissue is between 0.5 and 1.0 dB/cm/MHz. This approximation describes the expected loss of energy (in decibels) that would occur over the round-trip distance that a beam would travel after being emitted by a given transducer. For example, if a 3-MHz transducer is used to image an object at a depth of 12 cm (24-cm round trip), the returning signal could be attenuated as much as 72 dB (or nearly 4,000-fold). As expected, attenuation is greater in soft tissue compared with blood and is even greater in muscle, lung, and bone.

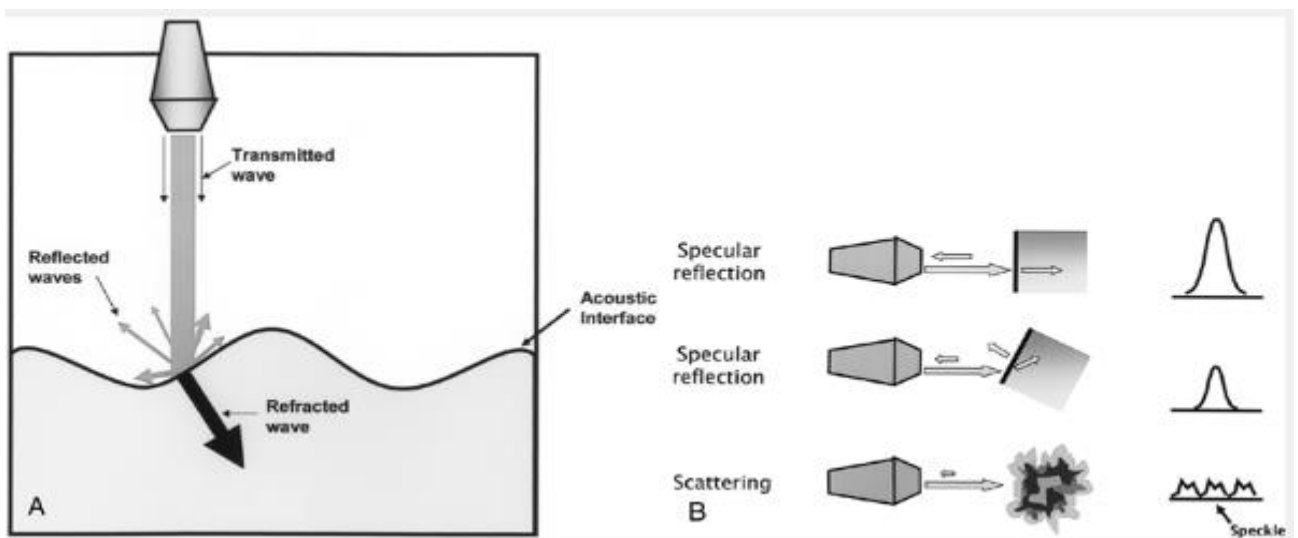
The velocity and direction of the ultrasound beam as it passes through a medium are a function of the acoustic impedance of that medium. Acoustic impedance (Z , measured in rayls) is simply the product of velocity (in meters per second) and physical density (in kilograms per cubic meter). As impedance increases, a greater acoustic mismatch is created and relatively more ultrasound energy will be reflected rather than transmitted. Within a homogeneous structure, the density of the medium primarily determines these parameters. In such a structure, sound would travel in a straight line at a constant velocity, depending on the density and stiffness. Within the body, the tissues through which an ultrasound beam passes have different acoustic impedances.

When the beam crosses a boundary between two media, a portion of the energy is reflected, a portion is refracted, and a portion continues in a relatively straight line. These interactions between the ultrasound beam with acoustic interfaces form the basis for ultrasound imaging. The phenomena of reflection and refraction obey the laws of optics and depend on the angle of incidence between the transmitted beam and the acoustic interface as well as the acoustic mismatch, i.e., the magnitude of the difference in acoustic impedance. Small differences in velocity also determine refraction. These properties explain the importance of using an acoustic coupling gel during transthoracic imaging. Without the gel, the air-tissue interface at the skin surface results in more than 99% of the ultrasonic energy being reflected at this level. This is primarily due to the very high acoustic impedance of air. The use of gel

between the transducer and the skin surface greatly increases the percentage of energy that is transmitted into and out of the body, thereby allowing imaging to occur.

Figure 12 is reported a transmitted wave interacts with an acoustic interface in a predictable way. Some of the ultrasound energy is reflected at the interface and some is transmitted through the interface. The transmitted portion of the energy is refracted, or bent, depending on the angle of incidence and differences in impedance between the tissues. B: The interaction between an ultrasound wave and its target depends on several factors. A specular reflection occurs when ultrasound encounters a target that is large relative to the transmitted wavelength. The amount of ultrasound energy that is reflected to the transducer by a specular target depends on the angle and the impedance of the tissue. Targets that are small relative to the transmitted wavelength produce a scattering of ultrasound energy, resulting in a small portion of energy being returned to the transducer. This type of interaction results in speckle-tracing that produces the texture within tissues.

Figure 12: The interactions between the ultrasound beam with acoustic interfaces



As the ultrasound beam is transmitted through tissue, it encounters a complex array of large and small interfaces and targets, each of which affect the transmission of the ultrasound energy. These interactions can be broadly categorized as specular echoes and scattered echoes. Specular echoes are produced by reflectors that are large relative to ultrasound wavelength, such as the endocardial surface of the left ventricle. Such targets reflect a relatively greater proportion of the ultrasound energy

in an angle-dependent fashion. The spatial orientation and the shape of the reflector determine the angles of specular echoes. Examples of specular reflectors include endocardial and epicardial surfaces, valves, and pericardium.

Targets that are small relative to the wavelength of the transmitted ultrasound produce scattering, and such objects are sometimes referred to as Rayleigh scatterers. The resultant echoes are diffracted or bent and scattered in all directions. Because the percentage of energy returning to the transducer from scattered echoes is considerably less than that resulting from specular interactions, the amplitude of the signals produced by scattered echoes is very low. Despite this fact, scattering has important clinical significance (and forms the basis for Doppler imaging). Scattered echoes contribute to the visualization of surfaces that are parallel to the ultrasonic beam and also provide the substrate for visualizing the texture of gray-scale images. The term speckle is used to describe the tissue-ultrasound interactions that result from a large number of small reflectors within a resolution cell. Without the ability to record scattered echoes, the left ventricular wall, for example, would appear as two bright linear structures, the endocardial and the epicardial surfaces, with nothing in between.

From the above discussion, it is evident that the interaction between an ultrasound beam and a reflector depends on the relative size of the targets and the wavelength of the beam. If a solid object is submerged in water, for example, whether reflection of ultrasound occurs depends on the size of the object with respect to the wavelength of the transmitted ultrasound. Specifically, the thickness or profile of the object relative to the ultrasound beam must be at least one-fourth the wavelength of the ultrasound. Thus, as the size of the target decreases, the wavelength of the ultrasound must decrease proportionately to produce a reflection and permit the object to be recorded. This explains why higher frequency ultrasound allows smaller objects to be visualized. In clinical practice, echocardiography typically employs ultrasound with a range of 2,000,000 to 8,000,000 cycles per second

At a frequency of 2 MHz, it is generally possible to record distinct echoes from interfaces separated by approximately 1 mm. However, because high-frequency ultrasound is reflected by many small interfaces within tissue, resulting in scattering,

much of the ultrasonic energy becomes attenuated and less energy is available to penetrate deeper into the body. Thus, penetration is reduced as frequency increases. Similarly, as the medium becomes less homogeneous, the degree of reflection and refraction increases, resulting in less penetration of the ultrasound energy.

The use of ultrasound for imaging became practical with the development of piezoelectric transducers. The principles of piezoelectricity are illustrated in Figure 2.3. Piezoelectric substances or crystals rapidly change shape or vibrate when an alternating electric current is applied. It is the rapidly alternating expansion and contraction of the crystal material that produces the sound waves. Equally important is the fact that a piezoelectric crystal will produce an electric impulse when it is deformed by reflected sound energy. Such piezoelectric crystals form the critical component of ultrasound transducers. Although a variety of piezoelectric materials exist, most commercial transducers employ ceramics, such as ferroelectrics, barium titanate, and lead zirconate titanate. The creation of an ultrasound pulse thus requires that an alternating electric current be applied to a piezoelectric element. This results in the emission of sound energy from the transducer, followed by a period of quiescence during which the transducer listens for some of the transmitted ultrasound energy to be reflected back (known as dead time). The amount of acoustic energy that returns to the transducer is a measure of the strength and depth of the reflector. The time required for the ultrasound pulse to make the round-trip from transducer to target and back again allows calculation of the distance between the transducer and reflector.

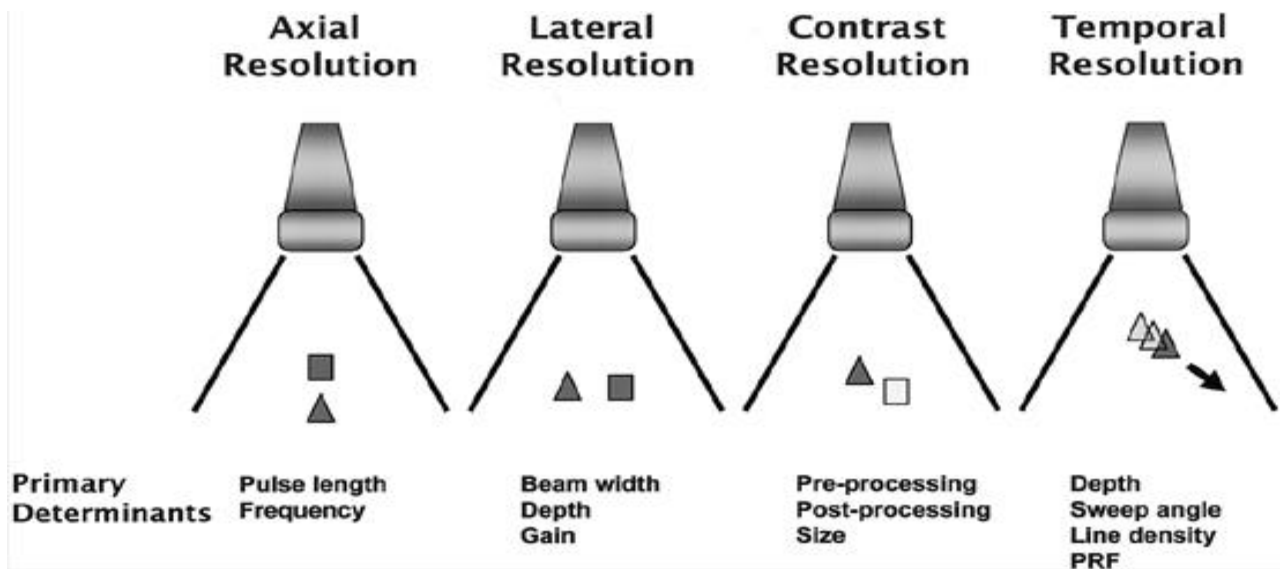
An ultrasound transducer consists of many small, carefully arranged piezoelectric elements that are interconnected electronically. The frequency of the transducer is determined by the thickness of these elements. Each element is coupled to electrodes, which transmit current to the crystals, and then record the voltage generated by the returning signals. An important component of transducer design is the dampening (or backing) material, which shortens the ringing response of the piezoelectric material after the brief excitation pulse. An excessive ringing response lengthens the ultrasonic pulse and decreases range resolution. Thus, the dampening material both shortens the ringdown and provides absorption of backward and

laterally transmitted acoustic energy. At the surface of the transducer, matching layers are applied to provide acoustic impedance matching between the piezoelectric elements and the body. This increases the efficiency of transmitted energy by minimizing the reflection of the ultrasonic wave as it exits the transducer surface.

Transducer design is critically important to optimal image creation. An important feature of ultrasound is the ability to direct or focus the beam as it leaves the transducer. This results in a parallel and cylindrically shaped beam. Eventually, however, the beam diverges and becomes cone shaped. The proximal or cylindrical portion of the beam is referred to as the near field or Fresnel zone. When it begins to diverge, it is called the far field or Fraunhofer zone. For a variety of reasons, imaging is optimal within the near field. Thus, maximizing the length of the near field is an important goal of echocardiography.

Resolution is the ability to distinguish between two objects in close proximity. Because echocardiography depends on its ability to image small structures and provide detailed anatomic information, resolution is one of its most important variables. Furthermore, because echocardiography is a dynamic imaging technique, resolution has at least two components: spatial and temporal. Spatial resolution is defined as the smallest distance that two targets can be separated for the system to distinguish between them. It, too, has two components: Axial resolution refers to the ability to differentiate two structures lying along the axis of the ultrasound beam (i.e., one behind the other) and lateral resolution refers to the ability to distinguish two reflectors that lie side by side relative to the beam (Figure 12).

Figure 12: The different types of resolution are demonstrated in this schematic



The primary determinants of axial resolution are the frequency of the transmitted wave and, more importantly, its effect on pulse length. Higher frequency is associated with shorter wavelength, and the size of the wave relative to the size of the object determines resolution. In addition to frequency, pulse length or duration also affects axial resolution. The shorter the train of cycles is, the greater the likelihood that two closely positioned targets can be resolved. Because a higher frequency and/or broad bandwidth transducer delivers a shorter pulse, it is also associated with higher resolution.

Lateral resolution varies throughout the field of imaging and is affected by several factors. The width or thickness of the interrogating beam, at a given depth, is the most important determinant. Ideally, the ultrasonic beam should be very narrow to provide a thin slice of the heart. Recall that the beam has finite width, even in the near field, and tends to diverge as it propagates. The importance of beam width stems from the fact that the system will display all targets within the path of the beam along a single line represented by the central axis of the beam. In other words, the echograph displays structures within the image as if the beam were infinitely narrow. Thus, lateral resolution diminishes as beam width (and depth) increases. The distribution of intensity across the beam profile will also affect lateral resolution. Both strong and weak reflectors can be resolved within the central portion of the beam, where intensity is greatest. At the edge of the beam, however, only relatively strong reflectors may produce a signal. Furthermore, the true size and position of such objects may be distorted by the width of the beam, resulting in significant beam

width artifacts. This observation also explains the importance of overall system gain and its effect on lateral resolution. Gain is the amplitude, or the degree of amplification, of the received signal. When gain is low, weaker echoes from the edge of the beam may not be recorded and the beam appears relatively narrow. If system gain is increased, weaker and more peripheral targets are recorded and beam width appears greater.

A third component of resolution is called contrast resolution. Contrast resolution refers to the ability to distinguish and to display different shades of gray within the image. This is important both for the accurate identification of borders and for the ability to display texture or detail within the tissues. To convert the returning radio frequency (RF) information into a gray-scale image, pre- and post-processing of the data are performed. These steps in image formation rely heavily on contrast resolution. From a practical standpoint, contrast resolution is necessary to differentiate tissue signals from background noise. Contrast resolution is also dependent on target size. A higher degree of contrast is needed to detect small structures compared with larger targets.

Creating the image

The instrument used to create an ultrasound image is called an echograph. It contains the electronics and circuitry needed to transmit, receive, amplify, filter, process, and display the ultrasound information. As a first step, the returning energy is converted from sound waves to voltage signals. These are very low amplitude, high-frequency signals that must be amplified and, because they arrive slightly out of phase, realigned in time. In modern instrumentation, this realignment is accomplished using a digital beam former to allow proper summation and phasing of all the channels. Because the signals are still very high frequency at this point, the scan lines are referred to as RF data. The complexity of the information at this stage is in part due to the wide range of amplitudes and the inclusion of background noise. Logarithmic compression and filtering are performed to render the RF data more suitable for processing.

The polar scan line data at this point consist of sinusoidal waves, and each ultrasound target is represented as a group of these high-frequency spikes. Each

group of high-frequency RF data is consolidated into a single envelope through a curve-fitting process called envelope detection. The resulting signal is then referred to as the polar video signal. This is sometimes called R-theta, indicating that each point in a polar map can be defined by its distance (R) and angle (theta) from a reference point. The next very important step involves digital scan conversion and refers to the complex task of converting polar video data into a cartesian or rectangular format. The image formed at this stage can be either stored in digital format or converted to analog data for videotape storage and display.

Transmitting ultrasound energy

For most clinical applications, ultrasound is emitted from the transducer as a brief pulse of energy. A fundamental control feature is power output, which is simply the amount of ultrasound energy within each emitted pulse. In general, the higher the power output, the higher the amplitude of the returning signal. The pulse, which is a collection of cycles traveling together, is emitted at fixed intervals. The time between pulsing is referred to as the dead time and is largely a function of depth. The duration of the ultrasound pulse is sometimes referred to as pulse length, and the pulse repetition period represents the total of one pulse length plus one dead time. To image at a greater depth, the dead time is lengthened, allowing the ultrasound system to listen for reflections arising from greater depths before returning to the transducer. Duty factor, or the percentage of time that the transducer is pulsing, is simply the pulse duration divided by the pulse repetition period.

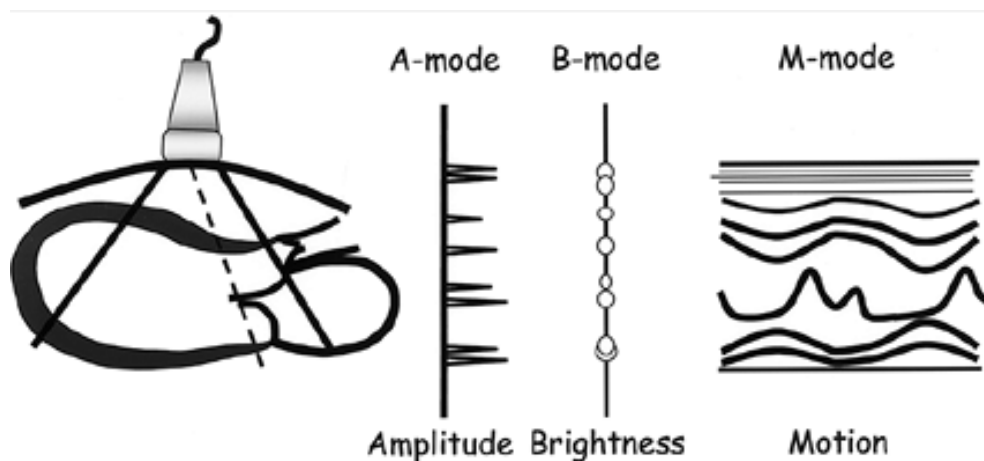
Pulsing in ultrasound is necessary to obtain range resolution, that is, to localize reflectors accurately along the axis of the beam. In theory, an emitted pulse must travel to the target and be reflected back to the transducer before a second pulse can be emitted to prevent interference and range ambiguity. Pulses are typically quite short, usually less than 5 microseconds. Unlike continuous-wave ultrasound, pulsed ultrasound results in a relatively broad frequency spectrum. This means that the distribution of frequencies occurs over predictable range that is centered on a central frequency. This is referred to as bandwidth, and such a transducer is said to deliver a band of frequencies. Bandwidth has important effects on the texture of the image and

the resolution. Transducers that deliver a wider bandwidth will provide higher axial resolution, primarily because the pulse length is shorter.

To obtain an image, ultrasound must be transmitted, reflected, and received. A brief current of electricity intermittently excites the piezoelectric elements. This results in a pulse or burst of ultrasound that travels into the body while the transducer waits for the returning signal. Commercial echographs have repetition rates between 200 and 5,000 per second. To perform M-mode examinations, pulse repetition rates of between 1,000 and 2,000 per second are used. For two-dimensional imaging, repetition rates of 3,000 to 5,000 per second are necessary to create the 90-degree sector scan. This does not mean, however, that temporal resolution is higher for two-dimensional imaging. In fact, the opposite is true. Although the pulse repetition rate is lower for M-mode, because all the pulses are devoted to a single raster line, the temporal resolution is actually much higher for M-mode compared with two-dimensional echocardiography.

Echocardiography provides several display options that are reported on the Figure 14.

Figure 14: Representation of the echocardiography options



Left: A transducer is applied to the chest wall, and an ultrasound beam is directed through the heart at the level of the mitral valve. The returning ultrasound information can be displayed in amplitude mode (A-mode) in which the amplitude of the spikes corresponds to the strength of the returning signal. Amplitude can be converted to brightness (B-mode), in which the strength of the echoes at various

depths is depicted as relative brightness. Motion can be introduced by plotting the B-mode display against time. This is the basis of M-mode echocardiography.

Tissue harmonic imaging

In the course of propagation of the ultrasound wave, the transmitted, or fundamental, frequency of the signal may be altered due to nonlinear interactions with the tissue. The net effect of such interactions is the generation of frequencies not present in the original signal. These new frequencies are integer multiples of the original frequency and are referred to as harmonics. The returning signal contains both fundamental and harmonic frequencies. By suppressing or eliminating the fundamental component, an image is created primarily from the harmonic energy. Unlike the harmonic technique that is so important to contrast echocardiography, in which the interaction of the ultrasound energy and the microbubbles produces vibrations that occur at multiple (harmonic) frequencies, tissue harmonics are generated during propagation by gradual conversion of energy from one frequency to another. The development of tissue harmonics can be compared with an ocean wave that changes shape and speed as it approaches the beach. Thus, the strength of the harmonic frequency actually increases as the wave penetrates the body. This is profoundly different from the fate of the fundamental frequency wave that attenuates constantly during propagation (Fig. 2.28A). This difference in behavior has important and practical implications for imaging. Close to the chest wall, where many of the troublesome imaging artifacts are generated, there is very little harmonic signal. For this reason, imaging that exploits the harmonic frequency avoids many of the near field artifacts that affect fundamental imaging. At depths of 4 to 8 cm, the relative strength of the harmonic signal is near its maximum, whereas the fundamental frequency has diminished considerably. Thus, the harmonic signal is strongest at distances that are most relevant to transthoracic imaging.

A second feature of tissue harmonic imaging, again the result of nonlinear interactions, relies on the fact that strong fundamental signals produce intense harmonics and weak fundamental signals produce almost no harmonic energy. This phenomenon further reduces the artifact generation during harmonic imaging because most such artifacts result from weak fundamental signals. By producing images from

the harmonic frequency reflections, the weak signals that cause many artifacts are disproportionately suppressed. The net result is that harmonic imaging reduces near field clutter and many of the other sources of imaging artifact that plague fundamental frequency imaging. The signal-to-noise ratio is improved and image quality is enhanced, especially in patients with poor fundamental frequency images. A consistent finding in most studies has been improved endocardial border definition. However, an important side effect of tissue harmonic imaging is that strong specular echoes, such as those arising from valves. This is particularly true in the far field and can lead to false-positive interpretations. To avoid such pitfalls but to take advantage of the benefits of harmonic imaging, most clinical studies should include both fundamental and harmonic imaging in the course of the examination.

A recent application of harmonic imaging involves pulse inversion technology. Unlike tissue harmonic imaging, in which the fundamental signal is filtered, pulse inversion harmonic imaging takes a different approach to eliminating the fundamental frequency. In the pulse inversion mode, the transducer sequentially emits two pulses with similar amplitude but with inverted phase. When backscattered from a linear reflector such as tissue, and then summed, these pulses cancel each other, resulting in almost complete elimination of the fundamental frequency signal, called destructive interference. The remaining harmonic energy can then be selectively amplified, producing a relatively pure harmonic frequency spectrum. The result is an image with many of the potential advantages previously attributed to tissue harmonic imaging. How much additional benefit can be ascribed to pulse inversion technology remains to be determined.

Doppler echocardiography

Despite being clinically adopted more recently than two-dimensional imaging, Doppler imaging is an integral and indispensable part of the echocardiographic examination. Knowledge of basic Doppler imaging principles is essential to fully understand the value and limitations of these techniques. Although Doppler imaging can be regarded as being complementary to two-dimensional imaging, the principles and instrumentation underlying this technique are substantially different. Used primarily to examine the flow of blood, Doppler imaging is concerned with the

direction, velocity, and then pattern of blood flow through the heart and great vessels. The differences between B-mode or imaging echocardiography and Doppler imaging are fundamental. The primary targets of the anatomic echocardiographic examination are the myocardium and valves of the heart. For Doppler imaging, the primary target is the red blood cells. Whereas echocardiography provides information on structure, Doppler imaging provides information on function. Thus, echocardiography can be regarded as an imaging technique that focuses on anatomy, whereas Doppler imaging focuses on physiology and hemodynamics. Finally, whereas echocardiography functions optimally when the beam and the target are at right angles, the Doppler equations rely on a more parallel alignment between the beam and the flow of blood. Thus, echocardiography and Doppler imaging provide diagnostic data that are largely complementary.

Color Flow Imaging

Color flow imaging is a form of pulsed wave Doppler imaging that uses multiple sample volumes along multiple raster lines to record the Doppler shift, based on principles described earlier for pulsed wave and high PRF Doppler imaging. By overlaying this information on a two-dimensional or M-mode template, the color flow image is created. Constructing the color flow image is complex. Each pixel represents a region of interest in which the flow characteristics must be measured. Rather than analyzing the entire velocity spectrum within one of these small regions (which would require several seconds for each image if a complete Fourier transform were performed), some compromises are necessary and only mean frequencies and frequency spreads (variance) are calculated.

Tissue Doppler Imaging

A unique and relatively recent application of the Doppler principle is tissue Doppler imaging. By adjusting gain and reject settings, the Doppler technique can be used to record the motion of the myocardium rather than the blood within it. To apply Doppler imaging to tissue, two important differences must be recognized. First, because the velocity of the tissue is much lower than blood flow, the machine must be adjusted to record a much lower range of velocities. Second, because the tissue is a much stronger reflector of the Doppler signal compared with blood, additional

adjustments are required to avoid oversaturation. When these factors are taken into account, a semiquantitative approach to myocardial velocity analysis is possible.

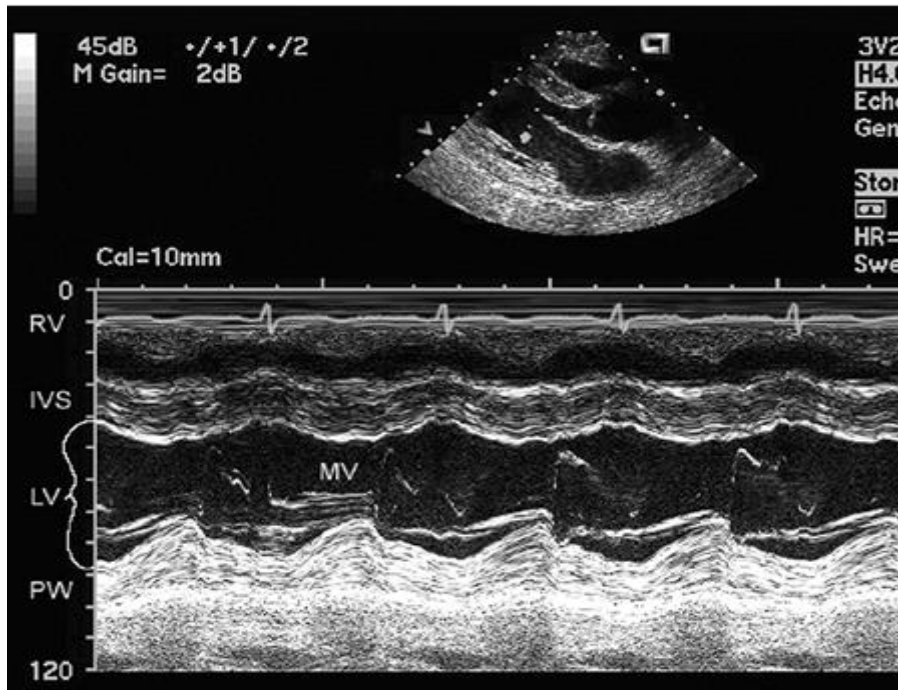
Note how this early systolic frame displays the direction and relative velocity of the different myocardial segments. One obvious limitation is that the incident angle between the beam and the direction of target motion varies from region to region. This limits the ability of the technique to provide absolute velocity information, although direction and relative changes in tissue velocity are displayed.

One potentially important derivation of this technique involves strain rate imaging. Strain is a measure of the deformation that occurs when force is applied to tissue. Strain rate is simply its temporal derivative. By measuring instantaneous velocity at two closely positioned points within the myocardium and knowing the initial distance between two points, both strain and strain rate can be determined. The Doppler tissue imaging technique has been used successfully to derive the velocity information needed to calculate strain.

M-Mode Echocardiography

The earliest ultrasound image was obtained using a single interrogation beam from a dedicated transducer. Basically, ultrasound energy is sent out from the transducer as an ultrasound packet that is then reflected back to the transducer. Transmission of ultrasound from the transducer is not continuous but rather interrupted, with the nontransmit time being used to receive the signal. When used in this method and directed into the thorax, the ultrasound along the single line of interrogation is reflected from cardiac structures and registered as a series of reflective interfaces. If the location and strength of these interfaces are then plotted over time, typically by recording the continuous returning signal on a strip-chart recorder or scrolling video screen, then an M-mode echocardiogram is recorded (Fig. 16).

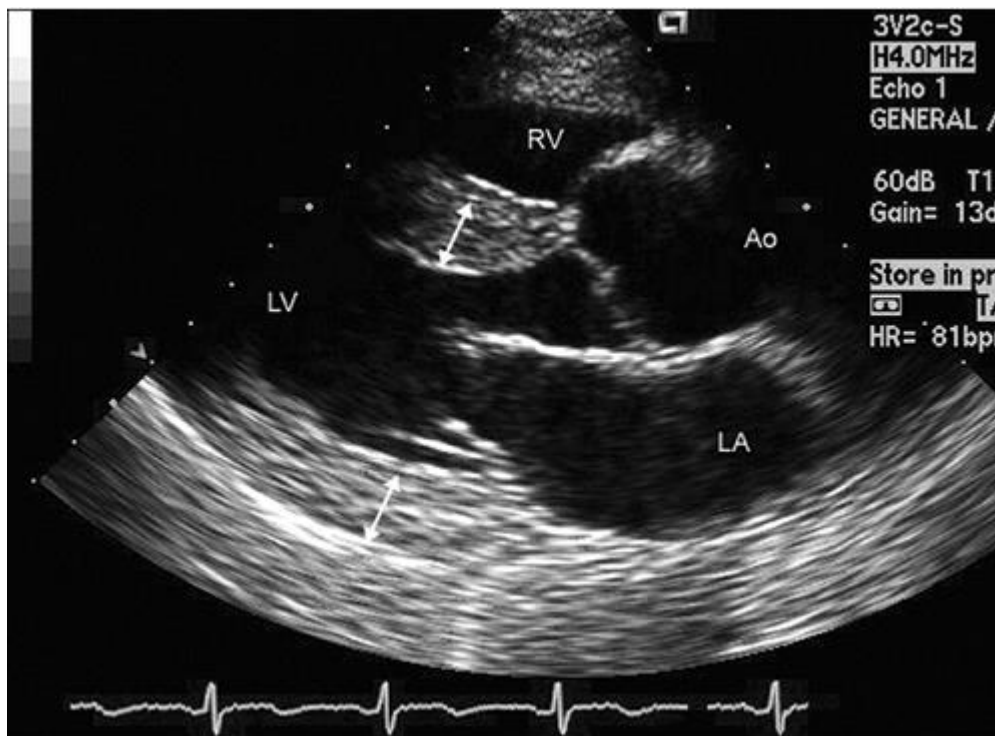
Figure 16: M-mode echocardiogram recorded through the left ventricle at the level of the mitral valve tips



Two-Dimensional Echocardiography

Two-dimensional echocardiography provides an expanded view of cardiac anatomy by imaging not along a single line of interrogation but along a series of lines typically spanning a 90-degree arc (Fig. 17). In modern scanners, any of the additional domains of imaging such as M-mode and Doppler can be simultaneously performed and superimposed on the two-dimensional image or otherwise simultaneously displayed.

Figure 17: Transthoracic two-dimensional echocardiogram recorded in a parasternal long-axis view revealing the right ventricle, left ventricle, left atrium, and proximal aorta as well as septal and posterior wall thickness (double-headed arrows).



Doppler interrogation

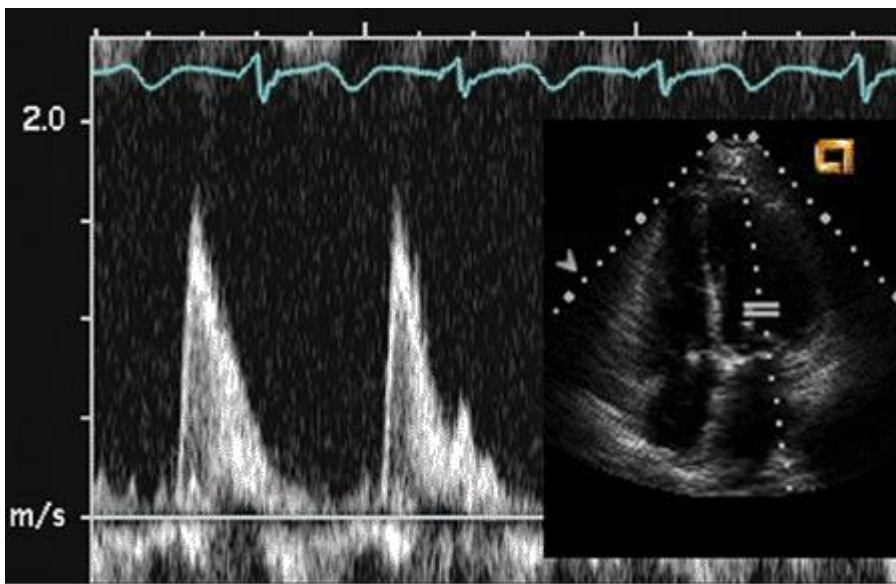
Whereas two-dimensional structural imaging relies on analysis of the time of transit and intensity of a returning ultrasound signal to identify an anatomic structure, Doppler interrogation relies on analysis of a change in the frequency of the transmitted ultrasound. Initially, this was displayed as the actual frequency shift. The magnitude of frequency shift is in the kilohertz range. This frequency shift can be converted to velocity of the interrogated target by the Doppler equation. Virtually all modern instrumentation provides this computation online, and it is the actual velocities that are displayed rather than frequency shifts. Doppler is used in multiple different formats.

The first Doppler format to be clinically used was a spectral display of the returning frequency shifts, which, as noted previously, is converted to velocity on all modern clinical scanners. This is typically displayed with reference to a zero crossing line. Any signal above that line represents motion toward the transducer, and any signal below the line represents motion away from the transducer. The magnitude of the frequency shift is directly related to velocity by the Doppler equation.

Any of the Doppler methodologies can be simultaneously performed with anatomic two-dimensional imaging by sharing the computational resources of the ultrasound instrument. The spectral Doppler display can then be displayed

simultaneously with the two-dimensional image. Early instrumentation did not have the computational power to perform both of these analyses simultaneously, and often anatomic imaging was suspended during Doppler interrogation. Modern instrumentation overcomes this shortcoming and can simultaneously display real-time, two-dimensional imaging and Doppler interrogation (Fig. 18).

Figure 18: Pulsed Doppler of the mitral valve inflow derived from an apical four-chamber view. The small inset is the simultaneously obtained apical four-chamber view showing the location of the sample volume at the tips of the mitral valve.



Spectral Doppler imaging is acquired through two different methods, continuous and pulsed wave. As the name implies, continuous wave Doppler imaging continuously transmits and receives the ultrasound signal. Because it is continuously transmitting and receiving, the ability to determine the time of transit is lost and only the frequency shift of the returning signal is calculated. This results in a phenomenon known as range ambiguity, in which the precise velocity of motion can be calculated but not the precise location at which that velocity occurred.

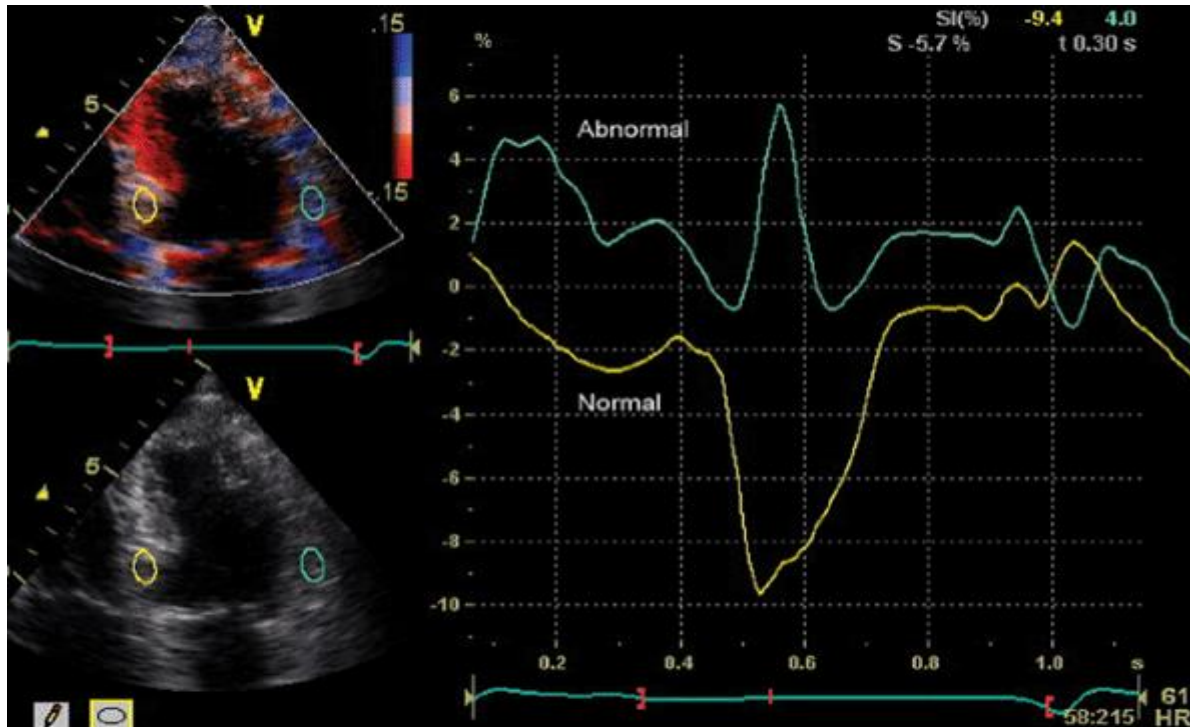
In contrast, pulsed wave Doppler imaging interrogates velocity of motion by way of discrete ultrasound packets sent out at a predefined rate, the pulse repetition frequency. Transmit and receipt timing are employed so that the location from which the frequency shift arises can be calculated from the time of transit. This allows the sample volume to be steered along both its longitudinal and lateral axes. Because sampling is not continuous, there are limitations on the maximal velocity that can be

determined, which is related to the pulse repetition frequency. The maximal obtainable velocity is known as the Nyquist limit. Using pulsed wave Doppler imaging, one can obtain a recording of velocity at any specific point within the cardiac anatomy, but the maximal velocity that can be displayed will be limited by the Nyquist limit and defines the total velocity range that can be measured, i.e., is the sum of velocity in both directions.

Tissue characterization

Tissue characterization refers to the ultrasound determination of myocardial texture. It has been employed for investigational purposes for more than 20 years, initially using dedicated, specifically designed ultrasound units that evaluated the complete returning radio frequency signal for cyclical changes in image intensity (backscatter) and tissue signature. This was necessary because the generation of clinically used ultrasound equipment at that time did not have the dynamic range to allow a similar analysis to be undertaken from the clinically used image. In the normally contracting myocardium, there is a cyclic variation in the intensity of the signal being reflected from the myocardium such that reflected intensities are lower in systole and greater in diastole. With ischemia, the normal pattern of systolic thickening is lost and with it the magnitude of cyclic variation in backscatter is diminished. This technique was demonstrated to be a sensitive indicator of both myocardial infarction and ischemia. Subsequent to its initial development, advances in routine ultrasound instrumentation have made available a tremendous increase in dynamic range and availability of the radio frequency signal on some commercially available clinical instruments. Many of these instruments also contain algorithms for determining image intensity from digitally captured loops and can be used to determine the cyclic variation of myocardial image intensity and texture (Fig.19). As with the earlier dedicated investigational instruments, several investigators have demonstrated a lack of cyclic variation in integrated backscatter in the presence of myocardial ischemia and myocardial infarction. Some studies have suggested that the tissue signature obtained in this way may also be an accurate marker of reperfused myocardium, which has not yet recovered function.

Figure 19: Myocardial strain image recorded in a normal and abnormal segment of the left ventricle from an apical four-chamber view. The two regions of interest are noted by ovals superimposed on the myocardium. For the normal segment, note the negative strain during systole, and for the abnormal segment, the systolic expansion is noted by a positive wave form.

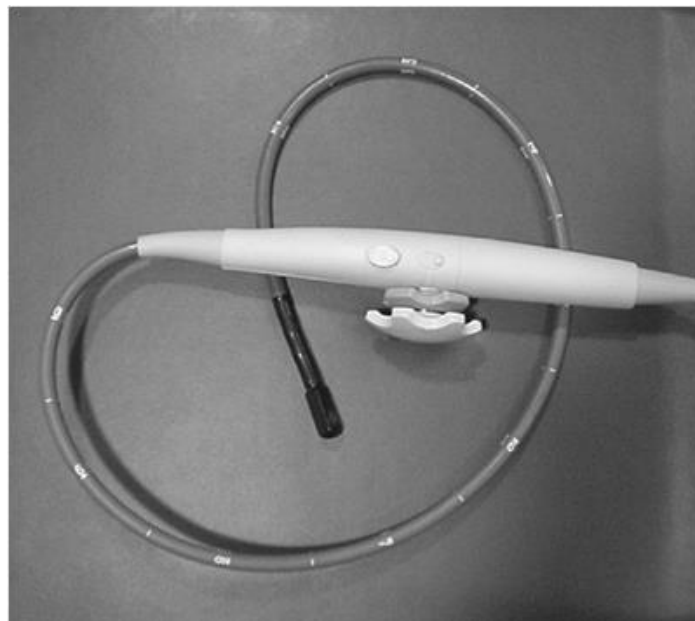


Transesophageal Echocardiography

The techniques for transesophageal echocardiography involve incorporating an ultrasound transducer on the tip of a gastroscope-like device. The early transesophageal echocardiographic probes were actually modified gastroscopes. Current transesophageal probes have been specifically manufactured for echocardiographic purposes. The method by which ultrasound is propagated from the transducer and returning signals processed is identical to that for transthoracic echocardiography. The transducer face is obviously smaller than a transthoracic probe, and hence there are fewer channels available for transmission. There have been four generations of transesophageal echocardiographic probes. The first was a single dedicated M-mode transducer that saw brief use in the early 1970s. The first functional transesophageal probes were single-plane devices typically using phased-array methodology, although several early devices used a rotating mechanical scanner. These monoplane probes were rapidly replaced by biplane devices that had

two separate ultrasound transducers with perpendicular orientation of the two imaging planes. These devices use an array of ultrasound crystals either in a square or circular configuration and phased-array technology to steer the ultrasound examining plane through a 180-degree arc (Figure 20).

Figure 20: A commercially available standard multiplane transesophageal probe. The knobs on the handle allow lateral flexion in both directions and anteflexion and retroflexion of the probe. The button on the handle controls the rotation of the imaging plane from 0 to 180 degrees.



All the modalities discussed including M-mode, spectral, color flow Doppler imaging, and color M-mode typically can be obtained using a modern multiplane transesophageal scanner. Doppler tissue imaging and second harmonic imaging are also provided on some of the most recent-generation instrumentation. Transesophageal probes operate at multiple frequencies, typically 3.5 to 7.0 MHz. In view of the unobstructed window for interrogation and the intrinsically high frequencies, the potential benefit of tissue harmonic imaging is probably less than that of transthoracic imaging. Pediatric transesophageal probes are smaller in diameter (5 to 7 mm), often limited to biplane imaging, and provide higher frequency (5 to 10 MHz) imaging. Their smaller size is more appropriate for children and infants. The greater flexibility of the probe may reduce control over imaging planes. For these reasons, they are not typically used in adult patients. As for transthoracic

echocardiography, the transesophageal echocardiogram provides a family of related views of cardiac anatomy

Three-Dimensional Echocardiography

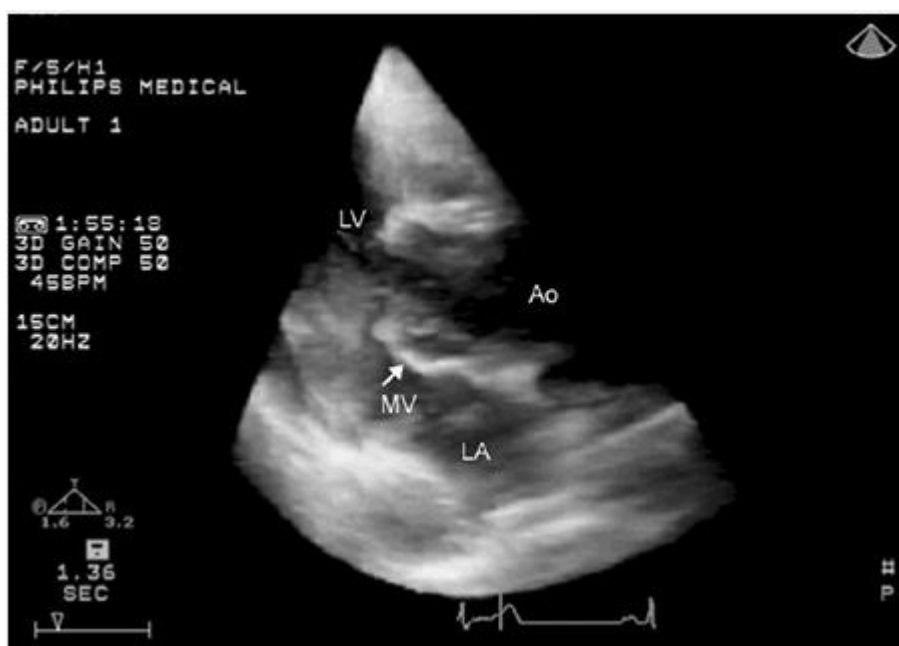
Three-dimensional echocardiography is a technique currently in evolution. The eventual goal is a real-time, three-dimensional display of cardiac anatomy including all the modalities mentioned above including Doppler flow imaging, M-mode echocardiography, and Doppler tissue imaging. Several approaches have been taken to acquire and display three-dimensional information. The basic problems with three-dimensional echocardiography can be divided into those of acquisition of the three-dimensional data set and subsequent display of the three-dimensional images. A limitation has been that the information either acquired or reconstructed into a three-dimensional data set must subsequently be displayed as a two-dimensional video image.

There have been two basic approaches to the acquisition of a three-dimensional data set. The first has been to acquire a series of two-dimensional images that are then stored, typically encoded with registration of the precise angle at which the heart is interrogated as well as electrocardiographic and respiratory gating information. An entire sequence of images is thus obtained, through either a transthoracic or transesophageal route, that is stored and then reconstructed into a three-dimensional data set.

From a transthoracic approach, this has required some mechanism for determining the precise location of the transducer and hence the location of the ultrasound beam within the thorax. In the past, this was accomplished either by attachment of a mechanical arm to the transducer, which then through either a series of position sensors or a spark gap or magnetic location device determines the exact position and orientation of the transducer. The localization device provides triangulation information that is encoded simultaneously with the echocardiographic images into a three-dimensional data set. Because of the cumbersome nature of this localization method and the complex nature of reconstruction, there has been little enthusiasm for this approach in clinical practice and it is currently not used.

Three-dimensional echocardiography from a transesophageal approach capitalizes on the rotational ability of the multiplane transducer. From the transesophageal approach, the transducer position remains fixed, and the multiplane rotational ultrasound beam is automatically rotated at 2- to 5-degree increments, creating a 360-degree panoramic view of the cardiac structures. It is obviously important that the transducer position and orientation within the esophagus remain absolutely stable. Even slight motion of the transducer, due either to patient or operator motion results in marked deterioration in image quality. A three-dimensional data set is then obtained from the series of rotational images (Figure 21). Typically, 3 to 7 minutes are required to obtain a complete three-dimensional data set with this approach. More recently, a similar approach has been undertaken by mounting the rotational transesophageal imaging probe on a handheld transthoracic device that can be used to acquire a three-dimensional data set in exactly the same manner as that for transesophageal echocardiography.

Figure 21: Real-time, three-dimensional image recorded in a parasternal long-axis view.

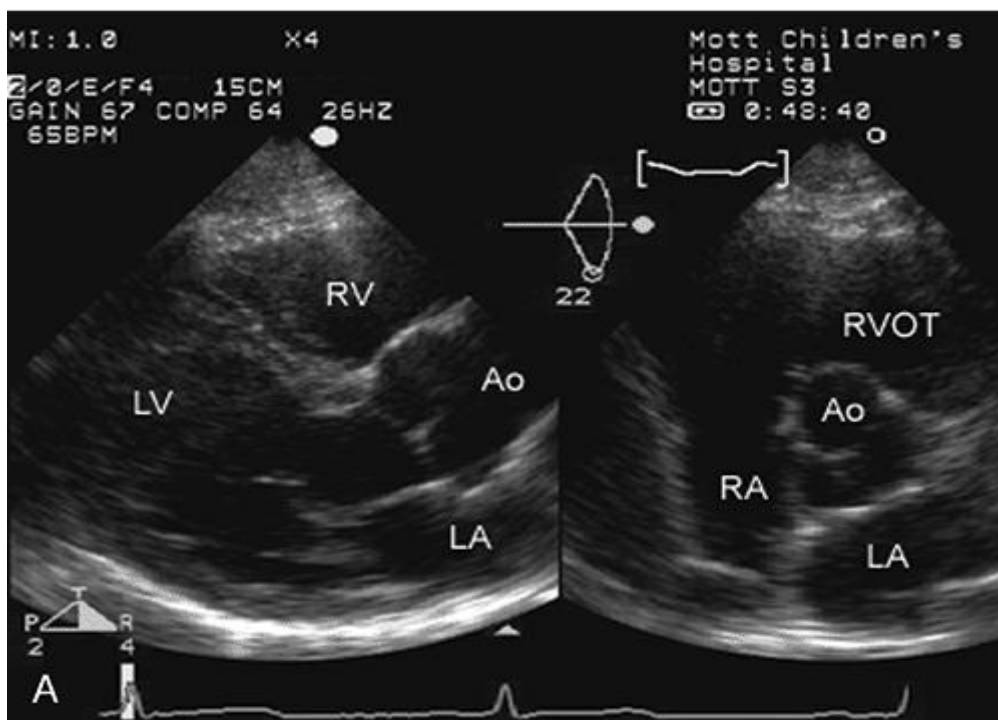


With this method, the volumetric scan is set to incorporate an approximate 90-degree sector that is approximately 20 degrees in elevation. This provides real-time, three-dimensional visualization of the cardiac structures as noted. Although in theory, only providing a different two-dimensional plane, three-dimensional echocardiography has the advantage of ensuring precise alignment of a two-

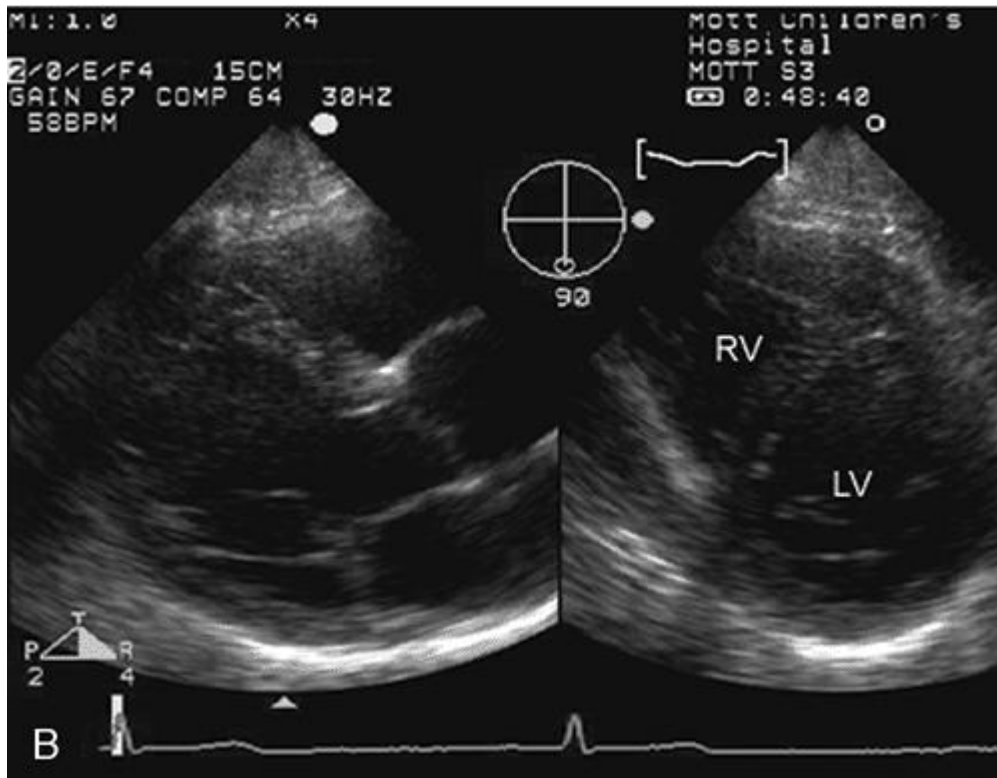
dimensional interrogation plane in atypical orientations. It also provides a more complete spatial orientation. This may be very useful for identification of small ventricular septal defects, assessment of the size of an atrial septal defect, and creating imaging planes that are not feasible using a single two-dimensional plane such as an en face view of the atrial septum for visualization of the fossa ovalis or an atrial septal defect. A major advantage is in the evaluation of complex congenital abnormalities. Three-dimensional echocardiography has also shown promise in assessing the mechanism of mitral regurgitation and in precise identification of flail leaflets.

Another area in which reconstructed three-dimensional echocardiography has shown substantial promise is in evaluating prosthetic valves for paravalvular regurgitation. It is frequently difficult to precisely identify the location and determine the size of a paravalvular leak, even with transesophageal echocardiography. Three-dimensional reconstruction of the face of the anulus frequently provides superb visualization of the entire circumference of the anulus and localization of multiple paravalvular leaks (Figure 22).

Figure 22: Real-time biplane imaging using a three-dimensional probe. Both images were recorded from the parasternal transducer position.



Finally, quantitative accuracy for chamber volume determination is greater for three-dimensional than for two-dimensional echocardiography. This advantage is most obvious when dealing with irregularly shaped chambers such as the right ventricle or abnormal left ventricles.



Note the ability to simultaneously visualize any two planes:

A: Parasternal long- and short-axis views at the base of the heart, revealing the proximal aorta, are demonstrated.

B: The second plane has been adjusted to intersect the left ventricle at the level of the mitral valve. In each image set, both images are simultaneously visualized in real time.

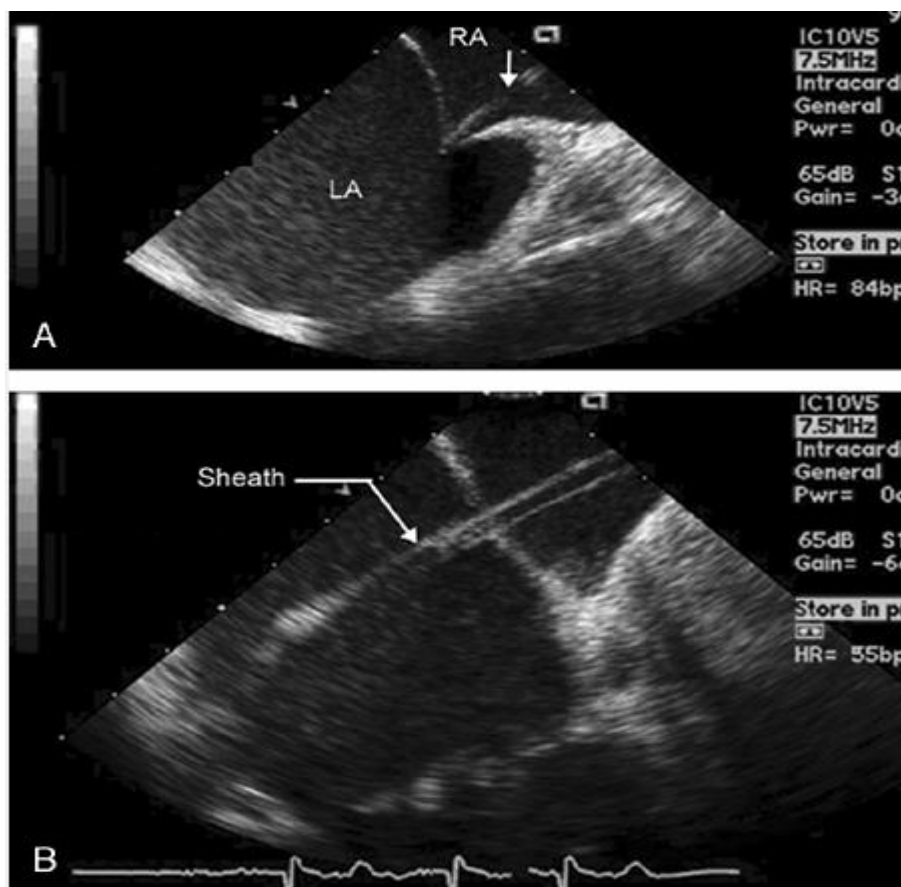
Additional imaging formats have been proposed for three-dimensional echocardiography including real-time, three-dimensional holographic displays of the three-dimensional data set. The feasibility of this approach has been demonstrated; however, the clinical availability of equipment to produce these images is limited. A final approach has been to create physical three-dimensional models from the ultrasound data set. This relies on the technology used in plastics manufacturing and can provide a solid or hollow model of a three-dimensional data set from cardiac images.

Intracardiac Echocardiography

Catheter-based transducers for intracardiac (vs. intracoronary) echocardiography have recently been developed (Figure 23).

This technology involves a single-plane, high-frequency transducer (typically 10 MHz) on the tip of a steerable intravascular catheter, typically 9 to 13 French in size. The catheter can be steered in both directions laterally and can be retroflexed and anteflexed. There is a 64-element, single-plane ultrasound transducer mounted at the tip that provides high-resolution, two-dimensional imaging as well as color flow imaging and Doppler spectral imaging. This technique is obviously applicable only in the cardiac catheterization laboratory and requires large-bore intravascular access. To date, it has been used predominantly in the venous circuit and provides remarkably high-resolution views of the right atrium including the fossa ovalis area.

Figure 23: Images from an intracardiac two-dimensional imaging device recorded at the time of atrial septal puncture for performance of an electrophysiologic procedure. Top: The transseptal needle (arrow) as it is puncturing the atrial septum near the foramen ovale. Bottom: Recorded after passing a sheath from the right to the left atrium for subsequent passage of electrophysiologic catheters



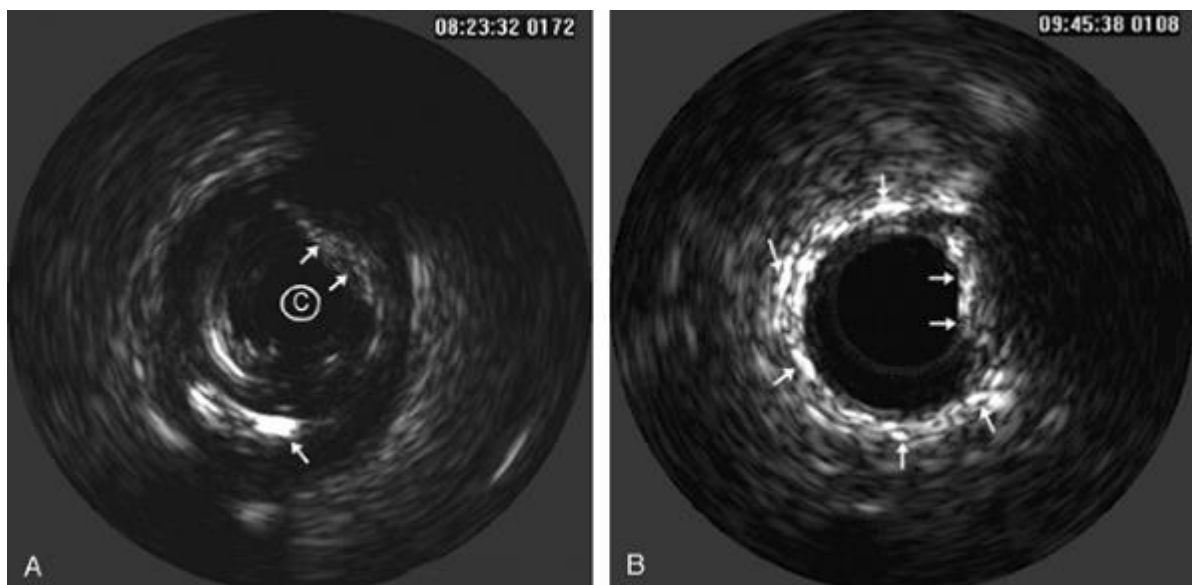
The depth of penetration is such that visualization of the left atrium and the base of the heart is likewise available as is visualization of left ventricular function. This technique has seen greatest use for monitoring complex interventional

procedures such as percutaneous atrial septal defect closure, atrial septostomy, and pulmonary vein isolation for treatment of atrial fibrillation.

Intravascular Ultrasound

Intracoronary ultrasound (IVUS) was developed before the intracardiac probes noted previously. Typically, these are ultraminiaturized ultrasound transducers mounted on modified intracoronary catheters. Both phased-array and mechanical rotational devices have been developed. These devices operate at frequencies of 10 to 30 MHz and provide circumferential 360-degree imaging. Because of the high frequencies, the depth of penetration is relatively low and the field of depth is limited to usually less than 1 cm. Most devices provide only anatomic imaging and do not provide Doppler information. Intracoronary ultrasound is by definition performed in the cardiac catheterization laboratory and in the majority of instances is performed by an invasive cardiologist rather than a dedicated echocardiographer. The technique provides high-resolution images of the proximal coronary arteries and can identify calcification and plaque and further characterize plaque (Figure 24).

Figure 24: Intracoronary ultrasound recorded in two patients. The catheter (C) is the dark circle in the center of the image.



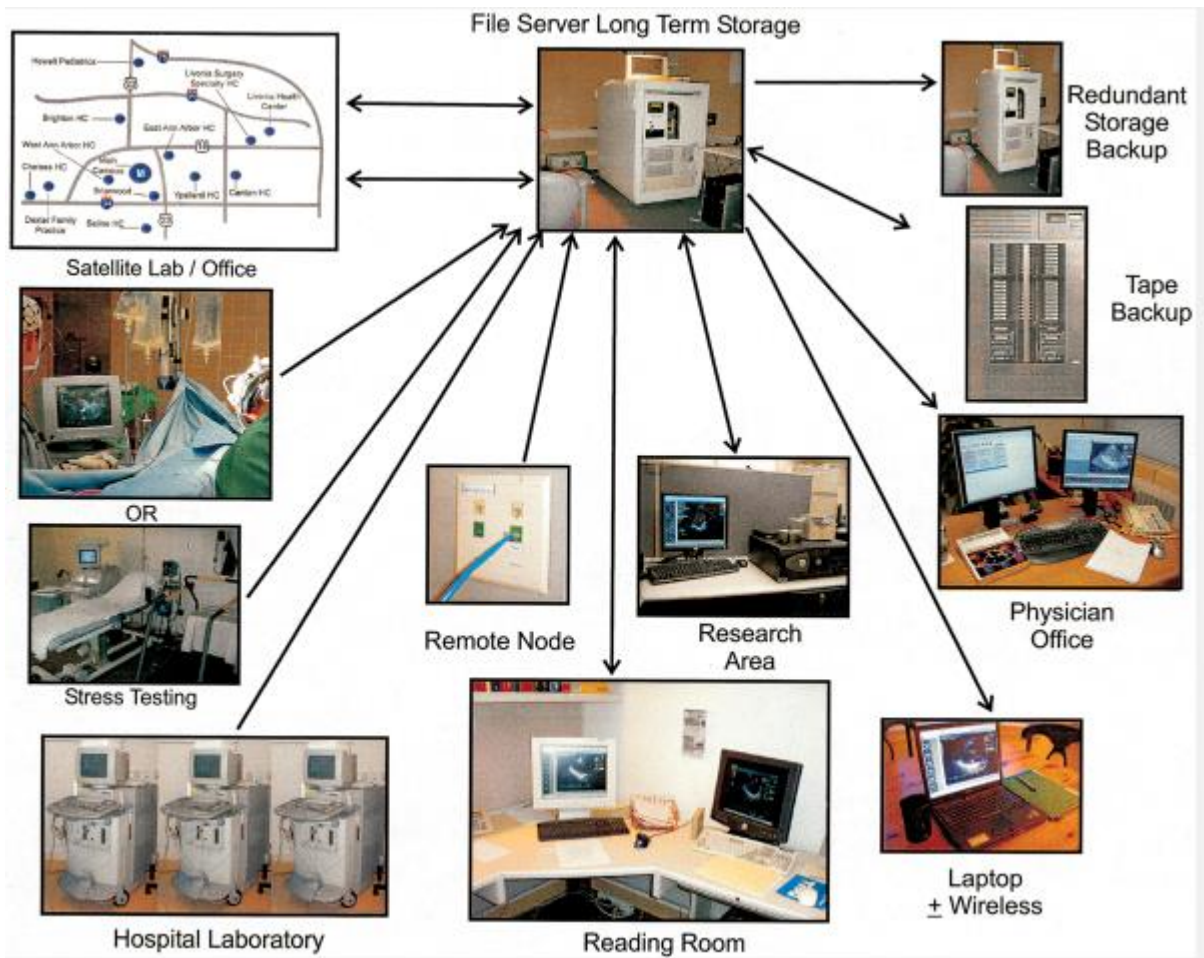
Left: Recorded in a patient with moderate intraluminal atheroma (arrows) and also calcific atheroma creating a bright echo and shadow (lower arrow). Right: Recorded in a patient who had undergone coronary stenting. The individual wire mesh of the stent is clearly seen as a sequence of bright echoes at the periphery of the

artery. From roughly 1 o'clock to 5 o'clock, there is nonobstructive intimal hyperplasia/recurrent atheroma within the lumen of the artery.

The digital echo laboratory

Cardiac ultrasound examinations generate a tremendous amount of information consisting of moving gray-scale images, color images, and static images. There has been a rapid evolution of the manner in which these images are acquired, stored, and analyzed. During the early days of echocardiography, only M-mode tracings were available, and these were typically recorded on a strip-chart recorder and stored as light-sensitive paper output. With the advent of two-dimensional echocardiography, the need arose to store moving video images. For approximately two decades, these images were stored using standard video technology and reviewed from videotape. Although this provides digital registration and review of all available information, it is an inefficient method for reviewing studies, results in the need for substantial storage and archiving space, and has the disadvantage of the degradation of video information over time. In the early 1980s, high-speed digitizing devices became available that allowed analog data to be converted to a digital format and stored as such. The limitation of these early attempts was the relatively slow speed of computer processors and the limitations in both speed and cost of computer memory. Over time, there has been a dramatic reduction in cost and improvement in speed and reliability, so that storage of large amounts of digital information is now within the reach of virtually all echocardiography laboratories. The information collected from the transducer face is done so in a digital format, processed as digital information, and displayed by a computer processor as digital information. It is converted to analog format only for purposes of recording on videotape. As such, the original, nondegraded digital images are available for both review and storage if the appropriate offline systems are made available (Figure 25).

Figure 25: Diagrammatic representation of a modern digital echocardiography laboratory denoting the multiple components for image analysis and storage as well as the diversity of sites from which images can be transferred or viewed.



Digital archiving systems are now available from a number of ultrasound and third-party vendors, all of which are capable of providing transfer from current-generation ultrasound platforms to a file server (and subsequently to bulk storage devices) and retrievable to standard computer workstations. A major breakthrough in digital medical imaging came with the advent of the DICOM standard (digital imaging and communication in medicine). The DICOM standard was negotiated among major medical manufacturers, regulatory bodies, and professional organizations in an effort to ensure that medical imaging information would be available in a standardized nonproprietary format so that it could be easily transferred from institution to institution and platform to platform for storage and analysis. Virtually all current-generation ultrasound platforms provide output of echocardiographic images in a DICOM-compatible format that can be archived to and retrieved from offline analysis systems.

The DICOM committee has also standardized image formats and recommended standards for image compression. Because a complete ultrasound examination may include 30 to 100 image clips and static images, it represents a

substantial file size. In an effort to reduce file size, image clips are typically compressed. Compression can be either lossless (no information lost) or lossy, with the potential for image degradation. The DICOM committee has recommended motion JPEG, which provides as much as 20:1 compression as the accepted compression method of video images.

In a typical installation, ultrasound platforms are connected to a file server by either a local area network (LAN) or Internet connection. In either instance, the ultrasound platform can be configured to either automatically or on command transmit the DICOM format ultrasound images to the file server for storage. Reading stations typically are desktop personal computers that can retrieve images for analysis and report generation. Because all information is digital and communicated over a computer network, echocardiograms recorded in remote sites can be transmitted almost instantaneously to the file server for review at the interpreting laboratory. Additionally, physicians can retrieve images at any appropriately equipped desktop computer, including physician offices, hospital ward stations, and catheterization laboratories.

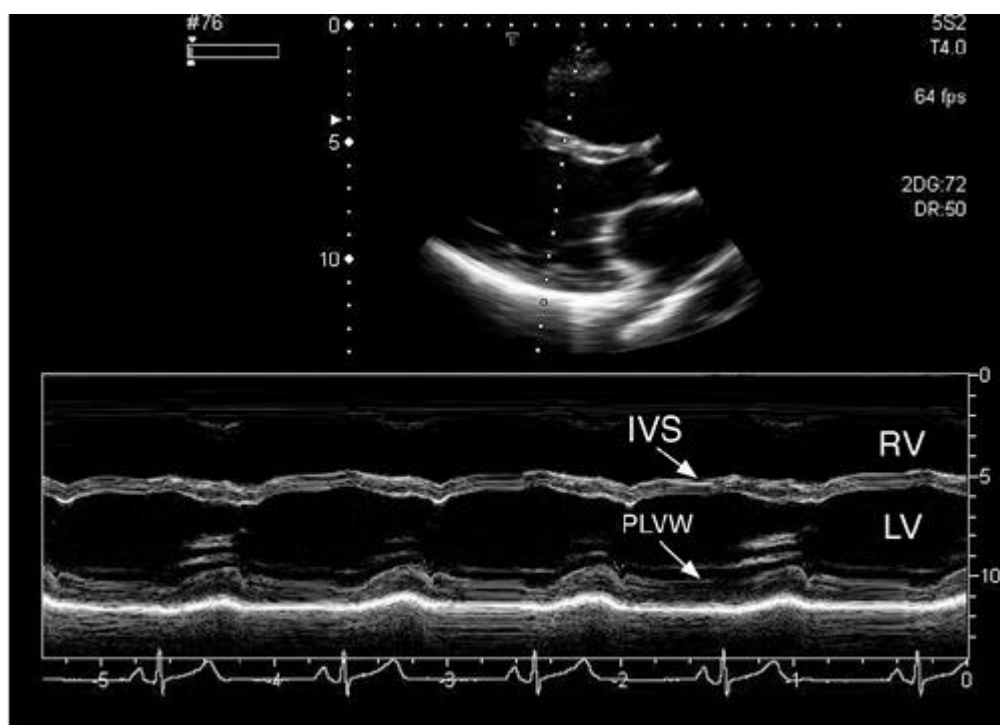
The method for long-term storage of digital information is currently in evolution and can result in substantially more expense than the initial outlay for a basic digital echocardiography laboratory. Most hospital and regulatory agency stipulations require that medical information be stored with several layers of redundancy, and, as such, an ultrasound laboratory must be prepared to provide storage at a minimum of two separate sites along with tape backup to ensure guaranteed access to medical information, even in the event of catastrophic failure at one site. In view of this, many laboratories that rely heavily on digital imaging still record standard analog videotape as a means of long-term archiving for regulatory purposes.

An approach to the transthoracic examination

A comprehensive transthoracic echocardiographic examination will include two-dimensional imaging, Doppler imaging, and M-mode imaging. It is customary to start with the two-dimensional examination, which provides orientation and a frame of reference for the other components. In most laboratories, the parasternal window

serves as a starting point for the study. Beginning at the third left intercostal space, the transducer is applied and rotated to record the parasternal long-axis view. To optimize the image, it may be necessary to move up or down one or two intercostal spaces and to rotate the patient into a left lateral decubitus position. When properly recorded, this view depicts the mid portion and base of the left ventricle, both leaflets of the mitral valve, the aortic valve and aortic root, the left atrium, and the right ventricle (Figure 26). The left ventricular apex is rarely visualized from this window. The transducer position should be adjusted so that the scanning plane is parallel to the major axis of the left ventricle and passes through the center of the left ventricular chamber.

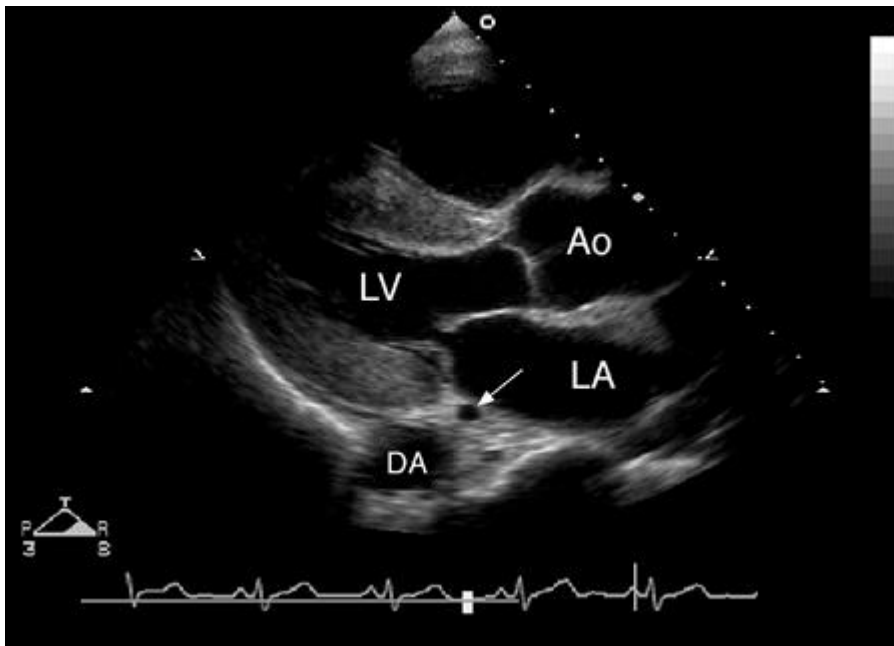
Figure 26: From the two-dimensional image, an M-mode display at the mid ventricular level is derived.



Abbreviations: IVS, interventricular septum; LV, left ventricle; PLVW, posterior left ventricular wall; RV, right ventricle

This is the point where the minor-axis diameter is maximal and the mitral valve leaflet excursion is greatest. This is best accomplished by gradual medial to lateral angulation until left ventricular size is at its maximum. From this view, an M-mode cursor can be placed to record minor-axis dimensions (Figure 27).

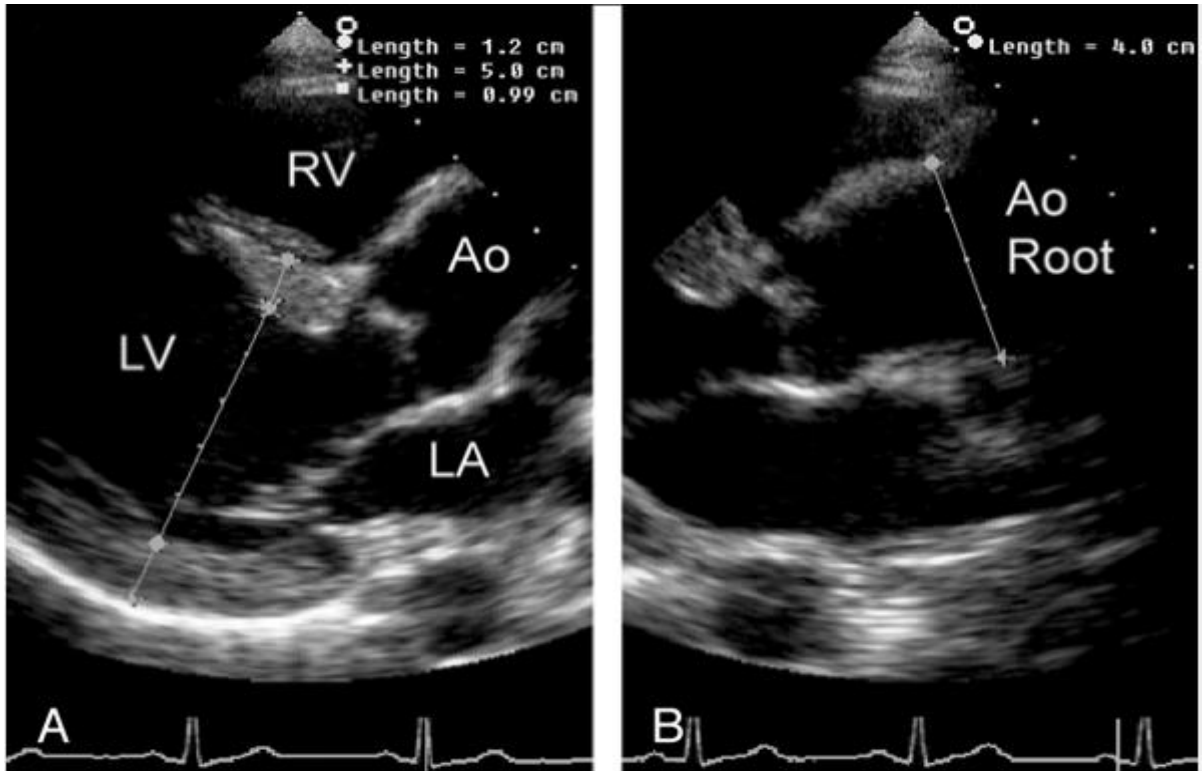
Figure 27: This parasternal long-axis view illustrates the relationship between the coronary sinus (arrow) and the descending aorta (DA).



Abbreviations: Ao, aorta; LA, left atrium; LV, left ventricle

This orientation will record the full excursion of the mitral valve, aortic valve opening and closing, right ventricular free wall motion, and the left ventricular septal and posterior wall motion. The coronary sinus will be visualized in the posterior atrioventricular groove, just below the base of the posterior mitral leaflet. An example of this is shown in Figure 28, which demonstrates the normal relationship between the coronary sinus, the atrioventricular groove, and the descending aorta. Behind the left atrium, a portion of the descending aorta will often be recorded. This view is also ideal to confirm the presence or absence of a pericardial effusion. A narrow, echo-free space behind the posterior left ventricular wall, but anterior to the descending aorta is strongly suggestive of pericardial fluid.

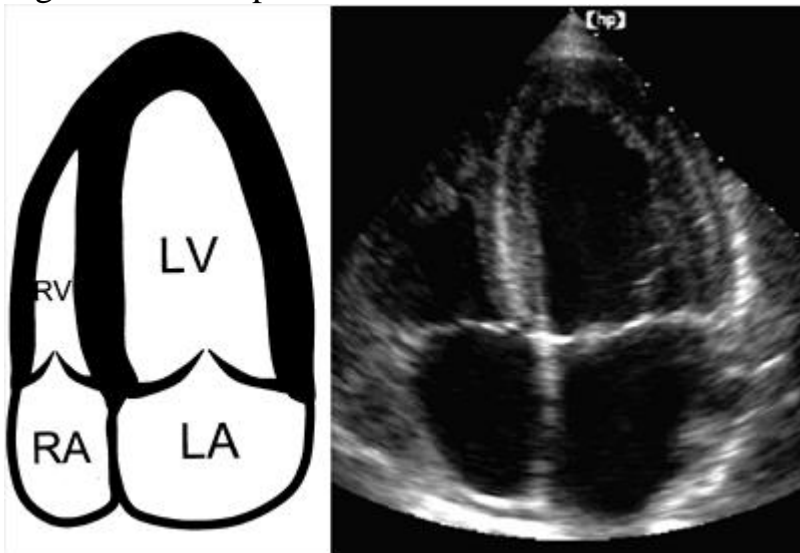
Figure 28: The parasternal long-axis view is adjusted so that the scan plane is parallel to the long-axis of the left ventricle (LV).



Notes: In this plane, the proximal aorta (Ao) appears normal. B: The plane is rotated slightly counterclockwise to better align with the long axis of the ascending aorta. By doing so, the true dimension of the aortic root is apparent. LA, left atrium; RV, right ventricle.

With the patient rotated to the left and the transducer placed at the cardiac apex, a family of long-axis images is available. A useful starting point for this part of the examination is the apical four-chamber view, illustrated in Figure 29.

Figure 29: The apical four-chamber view.



Abbreviations: LA, left atrium; LV, left ventricle; RA, right atrium; RV, right ventricle

This occurs when the full excursion of both mitral and tricuspid valves is recorded and the apex of the left ventricle lies in the near field. The normal true apex can be identified by its relatively thin walls and lack of motion. Incorrect transducer position will lead to foreshortening of the left ventricle and failure to visualize the true apex.

Such structures are benign anomalies but must be differentiated from pathologic findings, including a thrombus or tumor. When properly adjusted, this image includes the four chambers, both atrioventricular valves, and the interventricular and interatrial septa. Examining the crux of the heart, it should be noted that the insertion of the septal leaflet of the tricuspid valve is several millimeters more apical than the insertion of the mitral leaflet. In a properly oriented four-chamber view, the anterior mitral leaflet is recorded medially and the smaller posterior leaflet is seen as it arises from the lateral margin of the atrioventricular ring. On the right side, the septal leaflet of the tricuspid valve inserts medially and the larger anterior leaflet arises laterally.

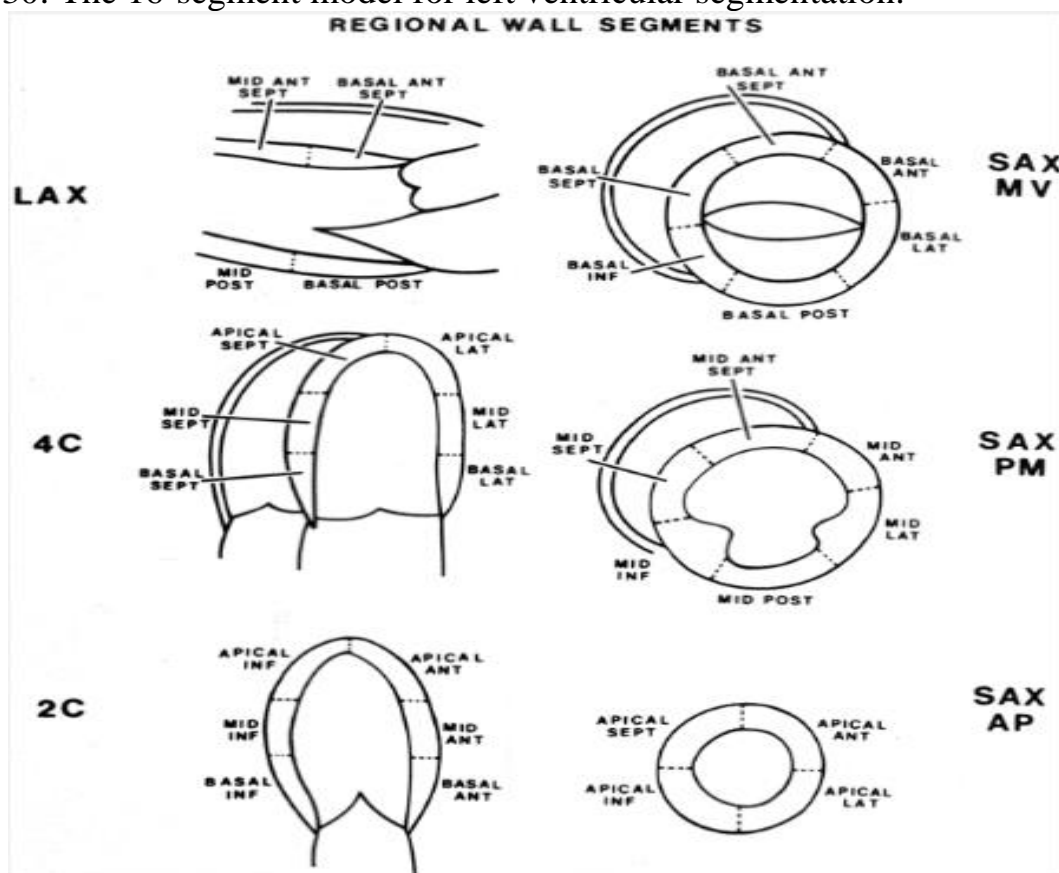
In most patients, placement of the transducer in the subcostal location provides an opportunity to record a four-chamber and a series of short-axis planes. The subcostal four-chamber view is similar to the corresponding apical view with two exceptions. First, the ultrasound beam is oriented perpendicular to the long axis of the left ventricle and thus often provides better endocardial definition of the ventricular walls. Second, because of the position of the transducer relative to the cardiac apex, foreshortening or inability to visualize the left ventricular apex is more likely from the subcostal position.

The primary use of the suprasternal views is to examine the great vessels. Extending and rotating the patient's head can position the transducer so that the aortic arch is readily recorded. Orientation of the scan plane is based on the position of the arch relative to the ultrasound beam. Although a variety of terms have been used to define the various transducer positions, describing the imaging plane as either parallel or perpendicular to the arch is most intuitive.

Using three short-axis planes (one corresponding to each of the thirds of the left ventricle) and the three longitudinal projections, a total of six basal, six mid, and

four apical segments are recorded. Thus, whether one assesses the left ventricular segments from a series of three short-axis planes or three longitudinal projections, the total number of segments and their interrelationships are preserved. This occurs because the parasternal long-axis view does not visualize the apex, thereby accounting for the fact that there are only four segments in the apical short-axis projection. Even so, the apex is relatively overrepresented in this scheme. This is commonly referred to as the 16-segment model and has become the standard approach for assessing regional left ventricular function and wall motion analysis. Finally, the standard 16-segment model for left ventricular segmentation is demonstrated on Figure 30.

Figure 30: The 16-segment model for left ventricular segmentation.



Abbreviations: LAX, parasternal long-axis; 4C, apical four chamber; 2C, apical two chamber; SAX MV, parasternal short-axis view at the level of the mitral valve; SAX PM, parasternal short-axis view at the papillary muscle level; SAX AP, apical short-axis view

References:

1. Feigenbaum's Echocardiography, 9th Edition / Feigenbaum H., Armstrong W.F., Ryan Th. Lippincott Williams & Wilkins, 2017.
2. Lang RM, Bierig M, Devereux RB, Flachskampf FA, et al. Chamber Quantification Writing Group. American Society of Echocardiography's Guidelines and Standards Committee. European Association of Echocardiography Recommendations for chamber quantification: a report from the American Society of Echocardiography's Guidelines and Standards Committee and the Chamber Quantification Writing Group, developed in conjunction with the European Association of Echocardiography, a branch of the European Society of Cardiology. *J Am Soc Echocardiogr.* 2005; 18(12):1440–1463.
3. Marriott H.J.L. *Practical Electrocardiography*, 8th ed. Baltimore: Williams & Wilkins; 2008
4. Nagueh SF, Appleton CP, Gillebert TC, Marino PN, Oh JK, Smiseth OA, et al. Recommendations for the evaluation of left ventricular diastolic function by echocardiography. *J Am Soc Echocardiogr.* 2009; 22(2):107–133.
5. Rosen M.R., Janse M.J., Wit A.L., eds. *Cardiac Electrophysiology: A Textbook*. Mount Kisco, NY: Futura; 2007.

2. Topic 2. Practical skills for the topics №2, №3 and №4 «Primary arterial hypertension. Secondary arterial hypetension. Neurocirculatory dystonia».

Hypertension is the most common disease-specific reason for a physician. It is currently among the leading causes of morbidity and mortality in the world and is expected to have an even greater impact on the health of the public as more of the world becomes developed. In addition to the morbidity and mortality directly attributable to hypertension, high blood pressure (BP) is a powerful risk factor (a condition or characteristic of an individual or a population) that in this case increases the likelihood that an individual or population will develop a wide variety of cardiovascular (CV) diseases. Hypertension even has been associated with an increased risk of certain cancers. Some authors have failed to appreciate this relationship when attributing certain cancers to particular antihypertensive treatments. All health care providers routinely encounter patients whose BP is elevated. In patients with definite hypertension, the paramount consideration is the choice of treatment, but in an increasing number of individuals, lowering BP may be beneficial even if definite hypertension cannot be diagnosed. In the next decade, it is expected that more and more patients will become candidates for antihypertensive therapy, especially as trials demonstrate the benefits of treatment and pharmacologic approaches become safer and more effective. Furthermore, many citizens, perhaps of the majority of those over 40 years of age, who do not yet meet the criteria for pharmacologic treatment for hypertension will benefit from lifestyle modification, a presumably safe and cost-effective public health approach to reducing BP. Many of the lifestyle habits that lower BP or slow the rate of rise of BP probably should be incorporated into everyone's lifestyle very early

2.1. Acquiring methodology of blood pressure measure.

Estimation of the pressure generated by the heart during its normal con-tractile cycle has been measured for more than 100 years. The value of such readings in predicting prognosis was recognized in the early 1930s by insurance companies, which probably have the best data correlating causal BP measurements and the risk of future disability and death. Since the second half of the 1800s, palpation of the pulse and appreciation of the contour and pressure within a peripheral artery were skills

learned only through extensive experience. Such subjective observations were supplanted by objective (albeit indirect) measurements after the introduction of the Riva-Rocci sphygmomanometer in the late nineteenth century. This instrument was refined by Janeway and Korotkoff, who characterized the sounds heard when using a stethoscope placed over the compressed artery in 1906. Even today, the terminology introduced by Korotkoff is still used: Systolic BP is recognized when clear and repetitive tapping sounds are heard; diastolic BP is recorded when the sounds disappear. Exceptions to these general rules are still recognized among patients who have audible sounds even down to zero mmHg and in obstetric patients: In both situations, the "muffling" of the sounds (Korotkoff phase IV) is recorded either in addition to the phase V measurement or as the diastolic BP, respectively.

Blood pressure measurement

Blood pressure is characterized by large spontaneous variations both during the day and between days, months and seasons.

Therefore the diagnosis of hypertension should be based on multiple blood pressure measurements, taken on separate occasions over a period of time. If blood pressure is only slightly elevated, repeated measurements should be obtained over a period of several months to define the patients 'usual' blood pressure as accurately as possible. On the other hand, if the patient has a more marked blood pressure elevation, evidence of hypertension-related organ damage or a high or very high cardiovascular risk profile, repeated measurements should be obtained over shorter periods of time (weeks or days).

In general, the diagnosis of hypertension should be based on at least 2 blood pressure measurements per visit and at least 2 to 3 visits, although in particularly severe cases the diagnosis can be based on measurements taken at a single visit. Blood pressures can be measured by the doctor or the nurse in the office or in the clinic (office or clinic blood pressure), by the patient or a relative at home, or automatically over 24 h.

Methodological aspects

A number of methodological aspects have been addressed by the ESH Working Group on Blood Pressure Monitoring. ABPM is performed with the patient wearing a

portable BP measuring device, usually on the nondominant arm, for a 24–25 h period, so that it gives information on BP during daily activities and at night during sleep. At the time of fitting of the portable device, the difference between the initial values and those from BP measurement by the operator should not be greater than 5mmHg. In the event of a larger difference, the ABPM cuff should be removed and fitted again. The patient is instructed to engage in normal activities but to refrain from strenuous exercise and, at the time of cuff inflation, to stop moving and talking and keep the arm still with the cuff at heart level. The patient is asked to provide information in a diary on symptoms and events that may influence BP, in addition to the times of drug ingestion, meals and going to- and rising from bed. In clinical practice, measurements are often made at 15 min intervals during the day and every 30 min overnight; excessive intervals between BP readings should be avoided because they reduce the accuracy of 24-h BP estimates [69]. It may be recommended that measurements be made at the same frequency during the day and night - for example every 20 min throughout. The measurements are downloaded to a computer and a range of analyses can be performed. At least 70% of BPs during daytime and night-time periods should be satisfactory, or else the monitoring should be repeated. The detection of artifactual readings and the handling of outlying values have been subject to debate but, if there are sufficient measurements, editing is not considered necessary and only grossly incorrect readings should be deleted. It is noteworthy that readings may not be accurate when the cardiac rhythm is markedly irregular.

Based on specific recommendations of the European Society of Hypertension, these procedures can be summarized as follows:

Office or clinic blood pressure

Blood pressure can be measured by a mercury sphygmomanometer the various parts of which (rubber tubes, valves, quantity of mercury, etc.) should be kept in proper working order. Other non-invasive devices (auscultatory or oscillometric semiautomatic devices) can also be used and will indeed become increasingly important because of the progressive banning of the medical use of mercury.

Ambulatory blood pressure

Several devices (mostly oscillometric) are available for automatic blood pressure measurements in patients allowed to conduct a near normal life. They provide information on 24-hour average blood pressure as well as on mean values over more restricted periods such as the day, night or morning. This information should not be regarded as a substitute for information derived from conventional blood pressure measurements.

In addition to the visual plot, average daytime, night-time and 24-h BP are the most commonly used variables in clinical practice. Average daytime and night-time BP can be calculated from the diary on the basis of the times of getting up and going to bed. An alternative method is to use short, fixed time periods, in which the rising and retiring periods - which differ from patient to patient - are eliminated. It has, for example, been shown that average BPs from 10 am to 8 pm and from midnight to 6 am correspond well with the actual waking and sleeping BPs, but other short, fixed time periods have been proposed, such as from 9 am to 9 pm and from 1 am to 6 am. In the event of different measurement intervals during the day and the night, and to account for missing values, it is recommended that average 24-h BP be weighted for the intervals between successive readings or to calculate the mean of the 24 hourly averages to avoid overestimation of average 24-h BP. The night-to-day BP ratio represents the ratio between average night-time and daytime BP. BP normally decreases during the night - defined as 'dipping'. Although the degree of night-time dipping has a normal distribution in a population setting, it is generally agreed that the finding of a nocturnal BP fall of >10% of daytime values (night-day BP ratio <0.9) will be accepted as an arbitrary cut-off to define subjects as 'dippers'. Recently, more dipping categories have been proposed: absence of dipping, i.e. nocturnal BP increase (ratio >1.0); mild dipping (0.9 <ratio <1.0); dipping (0.8 < ratio <0.9); and extreme dipping (ratio <0.8). One should bear in mind that the reproducibility of the dipping pattern is limited. Possible reasons for absence of dipping are sleep disturbance, obstructive sleep apnoea, obesity, high salt intake in salt-sensitive subjects, orthostatic hypotension, autonomic dysfunction, chronic kidney disease (CKD), diabetic neuropathy and old age.

A number of additional indices may be derived from ABPM recordings. They include: BP variability, morning BP surge, blood pressure load, and the ambulatory arterial stiffness index. However, their added predictive value is not yet clear and they should thus be regarded as experimental, with no routine clinical use.

When measuring 24-hour blood pressure care should be taken to:

- Use only devices validated by international standardized protocols.
- Use cuffs of appropriate size and compare the initial values with those from a sphygmomanometer to check that the differences are not greater than 5 mmHg.
- Set the automatic readings at no more than 30 min intervals to obtain an adequate number of values and have most hours represented if some readings are rejected because of artefact.
- Automatic deflation of the equipment should be at a rate of no more than 2 mmHg/s.
- Instruct the patients to engage in normal activities but to refrain from strenuous exercise, and to keep the arm extended and still at the time of cuff inflations.
- Ask the patient to provide information in a diary on unusual events and on duration and quality of night sleep.
- Obtain another ambulatory blood pressure if the first examination has less than 70% of the expected number of valid values because of frequent artefacts. Ensure that the proportion of valid values is similar for the day and night periods.
- Remember that ambulatory blood pressure is usually several mmHg lower than office blood pressure. A different population studies indicate that office values of 140/90 mmHg correspond to average 24-h values of either 125–130 mmHg systolic and 80 mmHg diastolic, the corresponding average daytime and nighttime values being 130–135/85 and 120/70 mmHg. These values may be regarded as approximate threshold values for diagnosing hypertension by ambulatory blood pressure.
- Clinical judgement should be mainly based on average 24-hour, day and/or night values.

Predictive value of 24-h BP measure

Several studies have shown that hypertensive patients' left ventricular hypertrophy (LVH), increased carotid intima-media thickness (IMT) and other markers of OD correlate with ambulatory BP more closely than with office BP.

Furthermore, 24-h average BP has been consistently shown to have a stronger relationship with morbid or fatal events than office BP.

There are studies in which accurately measured office BP had a predictive value similar to ambulatory BP. Evidence from meta-analyses of published observational studies and pooled individual data, however, has shown that ambulatory BP in general is a more sensitive risk predictor of clinical CV outcomes, such as coronary morbid or fatal events and stroke, than office BP. The superiority of ambulatory BP has been shown in the general population, in young and old, in men and women, in untreated and treated hypertensive patients, in patients at high risk and in patients with CV or renal disease.

It has found that night-time BP is a stronger predictor than daytime BP. The night-day ratio is a significant predictor of clinical CV outcomes but adds little prognostic information over and above 24-h BP. With regard to the dipping pattern, the most consistent finding is that the incidence of CV events is higher in patients with a lesser drop in nocturnal BP than in those with greater drop, although the limited reproducibility of this phenomenon limits the reliability of the results for small between-group differences in nocturnal hypotension. Extreme dippers may have an increased risk for stroke. However, data on the increased CV risk in extreme dippers are inconsistent and thus the clinical significance of this phenomenon is uncertain

Home blood pressure

Self-measurement of blood pressure at home cannot provide the extensive information on daily life blood pressure values provided by ambulatory blood pressure monitoring. The Definitions of hypertension by office and out-of-office blood pressure levels is represented in Table 2.1.

Table 2.1: Definitions of hypertension by office and out-of-office blood pressure levels

Category	Systolic BP, mm Hg		Diastolic BP, mm Hg
Office BP	≥140	And / or	≥90
Ambulatory BP			
Daytime (or awake)	≥135	And / or	≥85
Nighttime (or asleep)	≥120	And / or	≥70
24h	≥130	And / or	≥80
Home BP	≥135	And / or	≥85

The ESH Working Group on Blood Pressure Monitoring has proposed a number of recommendations for HBPM. The technique usually involves self-measurement of BP but, in some patients, the support of a trained healthprovider or family member may be needed. Devices worn on the wrist are currently not recommended but their use might be justified in obese subjects with an extremely large arm circumference. For diagnostic evaluation, BP should be measured daily on at least 3–4 days and preferably on 7 consecutive days in the mornings as well as in the evenings. BP is measured in a quiet room, with the patient in the seated position, back and arm supported, after 5 min of rest and with two measurements per occasion taken 1–2 min apart: the results are reported in a standardized logbook immediately after each measurement. However, BP values reported by the patient may not always be reliable, which can be overcome by storage in a memory-equipped device. Home BP is the average of these readings, with exclusion of the first monitoring day. Use of telemonitoring and smartphone applications for HBPM may be of further advantage. Interpretation of the results should always be under the close guidance of the physician. When compared with office BP, HBPM yields multiple measurements over several days, or even longer periods, taken in the individual's usual environment. Compared with ambulatory BP, it provides measurements over extended periods and day-to-day BP variability, is cheaper, more widely available and more easily repeatable. However, unlike ABPM, it does not provide BP data during routine, day-to-day activities and during sleep, or the quantification of short-term BP variability.

Home BP is more closely related to hypertension-induced organ damage than office BP, particularly LVH, and recent meta-analyses of the few prospective studies in the general population, in primary care and in hypertensive patients, indicate that the prediction of CV morbidity and mortality is significantly better with home BP than with office BP. Studies in which both ABPM and HBPM were performed show that home BP is at least as well correlated with organ damage as is the ambulatory BP, and that the prognostic significance of home BP is similar to that of ambulatory BP after adjustment for age and gender

White-coat (or isolated office) hypertension and masked (or isolated ambulatory) hypertension

Office BP is usually higher than BP measured out of the office, which has been ascribed to the alerting response, anxiety and/or a conditional response to the unusual situation, and in which regression to the mean may play a role. Although several factors involved in office or out-of-office BP modulation may be involved, the difference between the two is usually referred to- although somewhat improperly - as the ‘white-coat effect’, whereas ‘white-coat-’ or ‘isolated office-’ or ‘isolated clinic hypertesion’ refers to the condition in which BP is elevated in the office at repeated visits and normal out of the office, either on ABPM or HBPM. Conversely, BP may be normal in the office and abnormally high out of the medical environment, which is termed ‘masked-’ or ‘isolated ambulatory hypertension’. The terms ‘true-’ or ‘consistent normotension’ and ‘sustained hypertension’ are used when both types of BP measurement are, respectively, normal or abnormal. Whereas the cut-off value for office BP is the conventional 140/90 mmHg, most studies in whitecoat or masked hypertension have used a cut-off value of 135/85 mmHg for out-of-office daytime or home BP and 130/80 mmHg for 24-h BP. Notably, there is only moderate agreement between the definition of white-coat or masked hypertension diagnosed by ABPM or HBPM. It is recommended that the terms ‘white-coat hypertension’ and ‘masked hypertension’ be reserved to define untreated individuals.

2.2.Mastering the skills of risk stratification in patients with arterial hypertension.

For a long time, hypertension guidelines focused on blood pressure values as the only or main variables determining the need and the type of treatment. New concept is based on the fact that only a small fraction of the hypertensive population has an elevation of blood pressure alone, with the great majority exhibiting additional cardiovascular risk factors, with a relationship between the severity of the blood pressure elevation and that of alterations in glucose and lipid metabolism. Furthermore, when concomitantly present, blood pressure and metabolic risk factors potentiate each other, leading to a total cardiovascular risk (CV) which is greater than the sum of its individual components. Finally, evidence is available that in high risk

individuals thresholds and goals for antihypertensive treatment, as well as other treatment strategies, should be different from those to be implemented in lower risk individuals. In order diabetes, and individuals with severely elevated single risk factors. In all these conditions the total cardiovascular risk is high, calling for the intense cardiovascular risk reducing measures that will be outlined in the following sections. However, a large number of hypertensive patients do not belong to one of the above categories and identification of those at high risk requires the use of models to estimate total cardiovascular risk so as to be able to adjust the intensity of the therapeutic approach accordingly (Figure 31).

In SCORE, total CV risk is expressed as the absolute risk of dying from CVD within 10 years. Because of its heavy dependence on age, in young patients, absolute total CV risk can be low even in the presence of high BP with additional risk factors. If insufficiently treated, however, this condition may lead to a partly irreversible high-risk condition years later. In younger subjects, treatment decisions should better be guided by quantification of relative risk or by estimating heart and vascular age. A relative-risk chart is available in the Joint European Societies' Guidelines on CVD Prevention in Clinical Practice, which is helpful when advising young persons.

Figure 31: Stratification of CV Risk in four categories

Other risk factors, asymptomatic organ damage or disease	Blood pressure (mmHg)			
	High normal SBP 130–139 or DBP 85–89	Grade 1 HT SBP 140–159 or DBP 90–99	Grade 2 HT SBP 160–179 or DBP 100–109	Grade 3 HT SBP ≥180 or DBP ≥110
No other RF		Low risk	Moderate risk	High risk
1–2 RF	Low risk	Moderate risk	Moderate to high risk	High risk
≥3 RF	Low to moderate risk	Moderate to high risk	High risk	High risk
OD, CKD stage 3 or diabetes	Moderate to high risk	High risk	High risk	High to very high risk
Symptomatic CVD, CKD stage ≥ 4 or diabetes with OD/RFs	Very high risk	Very high risk	Very high risk	Very high risk

Notes: Stratification of total CV risk in categories of low, moderate, high and very high risk according to SBP and DBP and prevalence of RFs, asymptomatic organ damages, diabetes, CKD stage or symptomatic CVD. Subjects with a high normal office but a raised out-of-office BP (masked hypertension) have a CV risk in the hypertension range. Subjects with a high office BP but normal out-of-office BP (white-coat hypertension), particularly if there is no diabetes, organ damages, CVD or CKD, have lower risk than sustained hypertension for the same office BP

Several computerized methods have been developed for estimating total cardiovascular risk, i.e. the absolute chance of having a cardiovascular event usually over 10 years. However, some of them are based on Framingham data which are only applicable to some European populations due to important differences in the incidence of coronary and stroke events. More recently, a European model has become available based on the large data-base provided by the SCORE project. SCORE charts are available for high and low risk countries in Europe. They estimate the risk of dying from cardiovascular (not just coronary) disease over 10 years and allow calibration of the charts for individual countries provided that national mortality statistics and estimates of the prevalence of major cardiovascular risk factors are known.

The charts and their electronic versions can assist in CV risk assessment and management but must be interpreted in the light of the physician's knowledge and experience, especially with regard to local conditions. Furthermore, the implication that total CV risk estimation is associated with improved clinical outcomes when compared with other strategies has not been adequately tested. Because of its heavy dependence on age, in young patients, absolute total CV risk can be low even in the presence of high BP with additional risk factors. If insufficiently treated, however, this condition may lead to a partly irreversible high-risk condition years later. In younger subjects, treatment decisions should better be guided by quantification of relative risk or by estimating heart and vascular age. A relative-risk chart is available in the Joint European Societies' Guidelines on CVD Prevention in Clinical Practice, which is helpful when advising young persons.

The distinction between high and very high risk categories has been maintained in the present guidelines, thereby preserving a separate place for secondary prevention, i.e. prevention in patients with established cardiovascular disease. In these patients, compared with the high risk category, not only can total risk be much higher, but multidrug treatment may be necessary throughout the blood pressure range from normal to high. The dashed line drawn in Figure 31 illustrates how total cardiovascular risk evaluation influences the definition of hypertension when this is

correctly considered as the blood pressure value above which treatment does more good than harm.

All currently available models for CV risk assessment have limitations that must be appreciated. The significance of organ damage in determining calculation of overall risk is dependent on how carefully the damage is assessed, based on available facilities. Conceptual limitations should also be mentioned.

One should never forget that the rationale of estimating total CV risk is to govern the best use of limited resources to prevent CVD; that is, to grade preventive measures in relation to the increased risk. Yet, stratification of absolute risk is often used by private or public healthcare providers to establish a barrier, below which treatment is discouraged. It should be kept in mind that any threshold used to define high total CV risk is arbitrary, as well as the use of a cut-off value leading to intensive interventions above this threshold and no action at all below.

It is so strong that younger adults (particularly women) are unlikely to reach high-risk levels even when they have more than one major risk factor and a clear increase in relative risk. By contrast, many elderly men (e.g. >70 years) reach a high total risk level whilst being at very little increased risk relative to their peers. The consequences are that most resources are concentrated in older subjects, whose potential lifespan is relatively short despite intervention, and little attention is given to young subjects at high relative risk despite the fact that, in the absence of intervention, their long-term exposure to an increased risk may lead to a high and partly irreversible risk situation in middle age, with potential shortening of their otherwise longer life expectancy.

The most common clinical variables that should be used to stratify the risk are follow:

1. The metabolic syndrome has been mentioned because it represents a cluster of risk factors often associated with high blood pressure which markedly increases cardiovascular risk. No implication is made that it represents a pathogenetic entity.

2. Further emphasis has been given to identification of target organ damage, since hypertension-related subclinical alterations in several organs indicate progression in the cardiovascular disease continuum which markedly increases the risk beyond that caused by the simple presence of risk factors.

3. The list of renal markers of organ damage has been expanded, to include estimates of creatinine clearance by the EPI-CKD formula or of glomerular filtration rate by the MDRD formula, because of the evidence that these estimated values are a more precise index of the cardiovascular risk accompanying renal dysfunction.

4. Microalbuminuria has now been considered as an essential component in the assessment of organ damage because its detection is easy and relatively inexpensive.

5. Concentric left ventricular hypertrophy has been identified as the cardiac structural parameter that more markedly increases cardiovascular risk.

6. Whenever possible the recommendation is made to measure organ damage in different tissues (e.g. heart, blood vessels, kidney and brain) because multiorgan damage is associated with a worse prognosis.

7. Increased pulse wave velocity is added to the list of factors influencing prognosis as an early index of large artery stiffening, although with the caveat that it has a limited availability in the clinical practice.

8. A low ankle to brachial blood pressure ratio (<0.9) is listed as a relatively easy to obtain marker of atherosclerotic disease and increased total cardio-vascular risk.

9. Not only is assessment of organ damage recommended pre-treatment (in order to stratify risk) but also during therapy because of the evidence that regression of left ventricular hypertrophy (LVH) and reduction of proteinuria indicate treatment-induced cardiovascular protection.

10. There may be reasons to include an elevated heart rate as a risk factor because of a growing body of evidence that elevated heart rate values relate to the risk of cardiovascular morbidity and mortality as well as to all cause mortality. Also, there is evidence that an elevated heart rate increases the risk of new onset hypertension and is frequently associated with metabolic disturbances and the metabolic syndrome.

2.3. Mastering the skills of ECGs' interpretation in the field of the topic.

A 12-lead electrocardiogram (ECG) should be part of the routine assessment of all hypertensive patients. Its sensitivity in detecting LVH is low but, nonetheless, LVH detected by the Sokolow-Lyon index ($SV1 + RV5 >3.5$ mV), the modified Sokolow-Lyon index (largest S-wave + largest R-wave >3.5 mV), $RaVL >1.1$ mV, or Cornell voltage QRS duration product (>244 mV ms) has been found in observational studies and clinical trials to be an independent predictor of CV events. Accordingly, the ECG is valuable, at least in patients over 55 years of age. Electrocardiography can

also be used to detect patterns of ventricular overload or ‘strain’, which indicates more severe risk, ischaemia, conduction abnormalities, left atrial dilatation and arrhythmias, including atrial fibrillation.

Holter ECG monitoring is indicated when arrhythmias and possible ischaemic episodes are suspected. Atrial fibrillation is a very frequent and common cause of CV complications, especially stroke, in hypertensive patients. Early detection of atrial fibrillation would facilitate the prevention of strokes by initiating appropriate anticoagulant therapy if indicated.

References:

1. 2013 ESH/ESC Guidelines for the management of arterial hypertension. // Journal of Hypertension. – Vol. 31. - N 7. - 2013. – p. 1281-1357.
2. Omboni S, Guarda A. Impact of home blood pressure telemonitoring and blood pressure control: a meta-analysis of randomized controlled studies. Am J Hypertens 2011; 24:989–998
3. Greenland P, Alpert JS, Beller GA, Benjamin EJ, Budoff MJ, Fayad ZA, et al. 2010 ACCF/AHA guideline for assessment of cardiovascular risk in asymptomatic adults: a report of the American College of Cardiology Foundation/American Heart Association Task Force on Practice Guidelines. Circulation 2010; 122:e584–e636.

3. Topic 3. Practical skills for the topics №5, №6 and № 7 «Atherosclerosis. Chronic coronary artery disease. Acute coronary syndrome (unstable angina, acute myocardial infarction)».

Cardiovascular disease (CVD) due to atherosclerosis of the arterial vessel wall and to thrombosis is the foremost cause of premature mortality and of disability-adjusted life years. The main clinical entities are coronary artery disease (CAD), ischaemic stroke, and peripheral arterial disease (PAD). The causes of these CVDs are multifactorial. Some of these factors relate to lifestyles, such as tobacco smoking, lack of physical activity, and dietary habits, and are thus modifiable. Other risk factors are also modifiable, such as elevated blood pressure, type 2 diabetes, and dyslipidaemias, or non-modifiable, such as age and male gender.

3.1. Mastering the skills of cardiovascular risk stratification.

A basic principle of prevention is that the intensity of risk-reduction therapy should be adjusted to a person's absolute risk. Hence, the first step in selection of LDL-lowering therapy is to assess a person's risk status. Risk assessment requires measurement of LDL cholesterol as part of lipoprotein analysis and identification of accompanying risk determinants. In all adults aged 20 years or older, a fasting lipoprotein profile (total cholesterol, LDL cholesterol, high-density lipoprotein [HDL] cholesterol, and triglyceride) should be obtained once every 5 years. If the testing opportunity is nonfasting, only the values for total cholesterol and HDL cholesterol will be usable. In such a case, if total cholesterol is >200 mg/dL or HDL is <40 mg/dL, a follow-up lipoprotein profile is needed for appropriate management based on LDL. The relationship between LDL cholesterol levels and CHD risk is continuous over a broad range of LDL levels from low to high. Therefore, ATP III adopts the classification of LDL cholesterol levels shown in Table 3.1, which also shows the classification of total and HDL cholesterol levels.

Risk determinants in addition to LDL cholesterol include the presence or absence of CHD, other clinical forms of atherosclerotic disease, and the major risk factors other than LDL (Table 3.2). LDL is not counted among the risk factors in Table 3.2 because the purpose of counting those risk factors is to modify the treatment of LDL.

Table 3.1: ATP III Classification of LDL, Total, and HDL Cholesterol (mg/dL)

Parameters	Value (mg/dL)	Risk
LDL cholesterol	<100	Optimal
	100-129	Near or above optimal
	130-159	Borderline high
	160-189	High
	≥190	Very high
Total cholesterol	<200	Desirable
	200-239	Borderline high
	≥240	High
HDL cholesterol	<40	Low
	≤60	High

Table 3.2: Major Risk Factors (Exclusive of LDL Cholesterol) That Modify LDL Goals

• Cigarette smoking
• Hypertension (blood pressure ≥140/90mmHg or on antihypertensive medication)
• Low HDL cholesterol (<40 mg/dL)
• Family history of premature CHD (CHD in male first-degree relative <55 years; CHD in female first-degree relative <65 years)
• Age (men ≥45 years; women ≥55 years)

Based on these other risk determinants, ATP III identifies 3 categories of risk that modify the goals and modalities of LDL-lowering therapy. Table 3 defines these categories of risk and shows corresponding LDL cholesterol goals. The category of highest risk consists of CHD and CHD risk equivalents. The latter carry a risk for major coronary events equal to that of established CHD, ie., 20% per 10 years (ie, more than 20 of 100 such individuals will develop CHD or have a recurrent CHD event within 10 years).

CHD risk equivalents comprise:

- Other clinical forms of atherosclerotic disease (peripheral arterial disease, abdominal aortic aneurysm, and symptomatic carotid artery disease)
- Diabetes
- Multiple risk factors that confer a 10-year risk for CHD >20%.

Diabetes counts as a CHD risk equivalent because it confers a high risk of new CHD within 10 years, in part because of its frequent association with multiple risk factors. Furthermore, because persons with diabetes who experience a myocardial infarction have an unusually high death rate either immediately or in the long term, a

more intensive prevention strategy is warranted. Persons with CHD or CHD risk equivalents have the lowest LDL cholesterol goal (<100 mg/dL). The second category consists of persons with multiple (2+) risk factors in whom 10-year risk for CHD is $\leq 20\%$. Risk is estimated from Framingham risk scores. The major risk factors, exclusive of elevated LDL cholesterol, are used to define the presence of multiple risk factors that modify the goals and cut-points for LDL lowering treatment, and these are listed in Table 3.3. The LDL cholesterol goal for persons with multiple (2+) risk factors is <130 mg/dL. The third category consists of persons having 0-1 risk factor; with few exceptions, persons in this category have a 10-year risk <10%. Their LDL cholesterol goal is <160 mg/dL.

Table 3.3: Three Categories of Risk That Modify LDL Cholesterol Goals

Risk Category	LDL Goal (mg/dL)
CHD and CHD risk equivalents	<100
Multiple (2+) risk factors	<130
0-1 risk factor	<160

Method of Risk Assessment: Counting Major Risk Factors and Estimating 10-Year CHD Risk

In USA a risk status in persons without clinically manifest CHD or other clinical forms of atherosclerotic disease is determined by a 2-step procedure. First, the number of risk factors is counted (Table 3.3). Second, for persons with multiple (2+) risk factors, 10-year risk assessment is carried out with Framingham scoring to identify individuals whose short-term (10- year) risk warrants consideration of intensive treatment.

Estimation of the 10-year CHD risk adds a step to risk assessment beyond risk factor counting, but this step is warranted because it allows better targeting of intensive treatment to people who will benefit from it. When 0-1 risk factor is present, Framingham scoring is not necessary because 10-year risk rarely reaches levels for intensive intervention; a very high LDL level in such a person may nevertheless warrant consideration of drug therapy to reduce long-term risk. Risk factors used in Framingham scoring include age, total cholesterol, HDL cholesterol, blood pressure, and cigarette smoking. Total cholesterol is used for 10-year risk assessment because of a larger and more robust Framingham database for total than

for LDL cholesterol, but LDL cholesterol is the primary target of therapy. Framingham scoring divides persons with multiple risk factors into those with 10-year risk for CHD of .20%, 10%-20%, and 10%. It should be noted that this 2-step sequence can be reversed with essentially the same results. (If Framingham scoring is carried out before risk factor counting, persons with 10% risk are then divided into those with 2+ risk factors and 0-1 risk factor by risk factor counting to determine the appropriate LDL goal) Initial risk assessment in ATP III uses the major risk factors to define the core risk status. Only after the core risk status has been determined should any other risk modifiers be taken into consideration for adjusting the therapeutic approach.

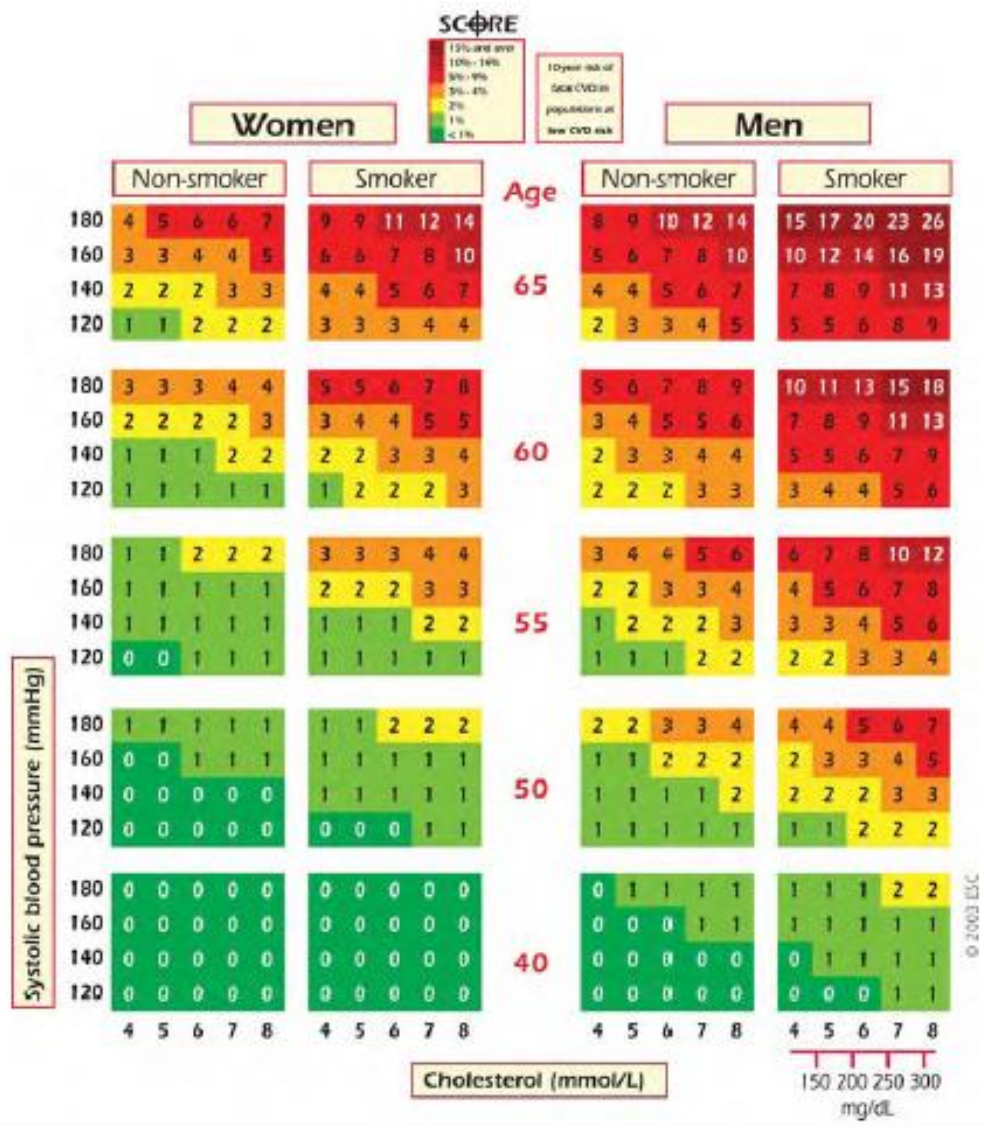
Role of Other Risk Factors in Risk Assessment

ATP III recognizes that risk for CHD is influenced by other factors not included among the major, independent risk factors (Table 3.3). Among these are life-habit risk factors and emerging risk factors. The former include obesity, physical inactivity, and atherogenic diet; the latter consist of lipoprotein -LP(a), homocysteine, prothrombotic and proinflammatory factors, impaired fasting glucose, and evidence of subclinical atherosclerotic disease. The lifehabit risk factors are direct targets for clinical intervention but are not used to set a lower LDL cholesterol goal of therapy. The emerging risk factors do not categorically modify LDL cholesterol goals; however, they appear to contribute to CHD risk to varying degrees and can have utility in selected persons to guide intensity of riskreduction therapy. Their presence can modulate clinical judgment when making therapeutic decisions.

In EU as well as in Ukraine a total CV risk estimate is part of a continuum using SCORE (Figure 32).

Figure 32: SCORE chart: 10 year risk of fatal cardiovascular disease (CVD) in populations at low CVD risk based on the following risk factors: age, gender, smoking, systolic blood pressure, and total cholesterol. To convert the risk of fatal CVD to risk of total (fatal + non-fatal) hard CVD, multiply by 3 in men and 4 in women, and slightly less in old people. Note: the SCORE chart is for use in people without overt CVD, diabetes, chronic kidney disease, or very high levels of

individual risk factors because such people are already at high risk and need intensive risk factor advice.



The cut-off points that are used to define high risk are in part arbitrary and based on the risk levels at which benefit is evident in clinical trials. In clinical practice, consideration should be given to practical issues in relation to the local healthcare and health insurance systems. Not only should those at high risk be identified and managed; those at moderate risk should also receive professional advice regarding lifestyle changes, and in some cases drug therapy will be needed to control their plasma lipids.

In these subjects we should do all we realistically can to:

- prevent further increase in total CV risk,
- increase awareness of the danger of CV risk,

- improve risk communication, and
- promote primary prevention efforts.

Low risk people should be given advice to help them maintain this status. Thus, the intensity of preventive actions should be tailored to the patient's total CV risk. With these considerations one can propose the following levels of total CV risk:

Very high CV risk

Subjects with any of the following:

- Documented CVD by invasive or non-invasive testing (such as coronary angiography, nuclear imaging, stress echocardiography, carotid plaque on ultrasound), previous myocardial infarction (MI), ACS, coronary revascularization [percutaneous coronary intervention (PCI), coronary artery bypass graft (CABG)] and other arterial revascularization procedures, ischaemic stroke, PAD.
- Patients with type 2 diabetes, patients with type 1 diabetes with target organ damage (such as microalbuminuria).
- Patients with moderate to severe CKD [glomerular filtration rate (GFR) <60 mL/min/1.73 m²).
- A calculated 10 year risk SCORE $\geq 10\%$.

High CV risk

- Subjects with any of the following:
- Markedly elevated single risk factors such as familial dyslipidaemias and severe hypertension.
- A calculated SCORE $\geq 5\%$ and <10% for 10 year risk of fatal CVD.

Moderate CV risk

Subjects are considered to be at moderate risk when their SCORE is $\geq 1\%$ and <5% at 10 years. Many middle-aged subjects belong to this risk category. This risk is further modulated by a family history of premature CAD, abdominal obesity, physical activity pattern, HDL-C, TG, hs-CRP, Lp(a), fibrinogen, homocysteine, apo B, and social class.

The low CV risk

The low risk category applies to individuals with SCORE <1%. In Table 3.4 different intervention strategies are presented as a function of the total CV risk and the LDL-C level.

Table 3.4: Intervention strategies as a function of total CV risk and LDL-C level

Total CV risk (SCORE) %	LDL-C levels				
	<70 mg/dL <1.8 mmol/L	70 to <100 mg/dL 1.8 to <2.5 mmol/L	100 to <155 mg/dL 2.5 to <4.0 mmol/L	155 to <190 mg/dL 4.0 to <4.9 mmol/L	>190 mg/dL >4.9 mmol/L
<1	No lipid intervention	No lipid intervention	Lifestyle intervention	Lifestyle intervention	Lifestyle intervention, consider drug if uncontrolled
Class ^a /Level ^b	I/C	I/C	I/C	I/C	IIa/A
≥1 to <5	Lifestyle intervention	Lifestyle intervention	Lifestyle intervention, consider drug if uncontrolled	Lifestyle intervention, consider drug if uncontrolled	Lifestyle intervention, consider drug if uncontrolled
Class ^a /Level ^b	I/C	I/C	IIa/A	IIa/A	I/A
>5 to <10, or high risk	Lifestyle intervention, consider drug*	Lifestyle intervention, consider drug*	Lifestyle intervention and immediate drug intervention	Lifestyle intervention and immediate drug intervention	Lifestyle intervention and immediate drug intervention
Class ^a /Level ^b	IIa/A	IIa/A	IIa/A	I/A	I/A
≥10 or very high risk	Lifestyle intervention, consider drug*	Lifestyle intervention and immediate drug intervention	Lifestyle intervention and immediate drug intervention	Lifestyle intervention and immediate drug intervention	Lifestyle intervention and immediate drug intervention
Class ^a /Level ^b	IIa/A	IIa/A	I/A	I/A	I/A

Risk intervention in older people.

The strongest driver of CVD risk is age, which may be regarded as ‘exposure time’ to risk factors. This raises the issue that Table 4.3 might suggest that most older men in high risk countries who smoke would be candidates for drug treatment, even if they have satisfactory blood pressure and lipid levels. To date, this is not supported by trial evidence, and the clinician is strongly recommended to use clinical judgement in making therapeutic decisions in older people, with a firm commitment to lifestyle measures such as smoking cessation in the first instance.

3.2. Mastering the skills of lipid profile interpretation.

Lipid metabolism can be disturbed in different ways, leading to changes in plasma lipoprotein function and/or levels. This by itself and through interaction with other CV risk factors may affect the development of atherosclerosis. Therefore, dyslipidaemias cover a broad spectrum of lipid abnormalities, some of which are of great importance in CVD prevention. Dyslipidaemias may be related to other diseases

(secondary dyslipidaemias) or to the interaction between genetic predisposition and environmental factors.

Elevation of total cholesterol (TC) and low-density lipoprotein-cholesterol (LDL-C) has received most attention, particularly because it can be modified by lifestyle changes and drug therapies. The evidence showing that reducing TC and LDL-C can prevent CVD is strong and compelling, based on results from multiple randomized controlled trials (RCTs). TC and LDL-C levels continue therefore to constitute the primary targets of therapy. Besides an elevation of TC and LDL-C levels, several other types of dyslipidaemias appear to predispose to premature CVD. A particular pattern, termed the atherogenic lipid triad, is more common than others, and consists of the co-existence of increased very low density lipoprotein (VLDL) remnants manifested as mildly elevated triglycerides (TG), increased small dense low-density lipoprotein (LDL) particles, and reduced highdensity lipoprotein-cholesterol (HDL-C) levels. However, clinical trial evidence is limited on the effectiveness and safety of intervening in this pattern to reduce CVD risk; therefore, this pattern or its components must be regarded as optional targets of CVD prevention. Lp(a) measurement should be considered at least once in each adult person's lifetime to identify those with very high inherited. Lp(a) levels >180 mg/dL (>430 nmol/L) who may have a lifetime risk of ASCVD equivalent to the risk associated with heterozygous familial hypercholesterolaemia

Dyslipidaemias may also have a different meaning in certain subgroups of patients which may relate to genetic predisposition and/or co-morbidities. This requires particular attention complementary to the management of the total CV risk.

Risk factor screening, including the lipid profile, may be considered in adult men ≥ 40 years of age, and in women ≥ 50 years of age or post-menopausal, particularly in the presence of other risk factors. In addition, all subjects with evidence of atherosclerosis in any vascular bed or with type 2 diabetes, irrespective of age, are regarded as being at high risk; it is recommended to assess their lipid profile. Individuals with a family history of premature CVD also deserve early screening. Several other medical conditions are associated with premature CVD.

Patients with arterial hypertension should be carefully assessed for concomitant metabolic disorders and dyslipidaemias.

Patients with central obesity, as defined for Europeans by an increased waist circumference of ≥ 94 cm for men (90 cm for Asian males) and ≥ 80 cm for women, or with a BMI ≥ 25 kg/m² but < 30 kg/m² (overweight), or ≥ 30 kg/m² (obesity), should also be screened—although one should recognize that the risk for CVD increases more rapidly as the BMI increases, becoming almost exponential from 27 kg/m² upwards.

Autoimmune chronic inflammatory conditions such as rheumatoid arthritis, systemic lupus erythematosus (SLE), and psoriasis are associated with increased CV risk. Patients with CKD (GFR < 60 mL/min/1.73 m²) are also at increased risk for CVD events and should be screened for dyslipidaemias. Clinical manifestations of genetic dyslipidaemias, including xanthomas, xanthelasmas, and premature arcus cornealis, should be sought because they may signal the presence of a severe lipoprotein disorder, especially FH, the most frequent monogenic disorder associated with premature CVD. Antiretroviral therapies may be associated with accelerated atherosclerosis. It is also indicated to screen for dyslipidaemias in patients with PAD or in the presence of increased CIMT or carotid plaques.

Finally, it is indicated to screen offspring of patients with severe dyslipidaemia [FH, familial combined hyperlipidaemia (FCH) or chylomicronaemia] and to follow them in specialized clinics if affected. Similarly, screening for significant lipoprotein disorders of family members of patients with premature CVD is recommended.

The recommendations for lipid profiling in order to assess total CV risk are presented in Table 3.4. The baseline lipid evaluation suggested is: TC, TG, HDL-C, and LDL-C, calculated with the Friedewald formula unless TG are elevated (> 4.5 mmol/L or greater than 400 mg/dL) or with a direct method, non-HDL-C and the TC/HDL-C ratio. Friedewald formula, in mmol/L: LDL-C $\frac{1}{4}$ TC - HDL-C - TG/2.2; in mg/dL: LDL-C $\frac{1}{4}$ TC - HDL-C - TG/5. Alternatively apo B and the apo B/apo A1 ratio can be used, which have been found to be at least as good risk markers compared with traditional lipid parameters. For these analyses, most commercially available methods are well standardized. Methodological developments may cause

shifts in values, especially in patients with highly abnormal lipid levels or in the presence of interacting proteins. Recent progression in dry chemistry has made possible analysis of lipids on site in clinical practice. Among such available methods, only certified and well standardized products should be used whenever possible.

Lipid and lipoprotein analyses

Throughout this section it should be noted that most risk estimation systems and virtually all drug trials are based on TC and LDL-C, and that clinical benefit from using other measures including apo B, non-HDL-C, and various ratios, while sometimes logical, has not been proven. While their role is being established, traditional measures of risk such as TC and LDL-C remain robust and supported by a major evidence base. Furthermore, multiple clinical trials have established beyond all reasonable doubt that, at least in high risk subjects, reduction of TC or LDL-C is associated with a statistically and clinically significant reduction in cardiovascular mortality.

Lipoprotein particle size

Lipoproteins are heterogeneous classes of particles, and a lot of evidence suggests that the different subclasses of LDL and HDL may bear different risks for atherosclerosis. Determination of small dense LDL may be regarded as an emerging risk factor that may be used in the future but is not currently recommended for risk estimation.

Genotyping

Several genes have been associated with CVD. At present the use of genotyping for risk estimation is not recommended. However, studies suggest that in the future a panel of genotypes may be used for identification of high risk subjects. For the diagnosis of specific genetic hyperlipidaemias, genotyping of apolipoprotein E (apo E) and of genes associated with FH may be considered. Apo E is present in three isoforms (apo E2, apo E3, and apo E4). Apo E genotyping is primarily used for the diagnosis of dysbetalipoproteinaemia (apo E2 homozygosity) and is indicated in cases with severe combined hyperlipidaemia.

Treatment targets

Treatment targets of dyslipidaemia are primarily based on results from clinical trials. In nearly all lipid-lowering trials the LDL-C level has been used as an indicator of response to therapy. Therefore, LDL-C remains the primary target of therapy in most strategies of dyslipidaemia management. Every 1.0 mmol/L (40 mg/dL) reduction in LDL-C is associated with a corresponding 22% reduction in CVD mortality and morbidity.

Extrapolating from the available data, an absolute reduction to an LDL-C level <1.4 mmol/L (less than 55 mg/dL) or at least a 50% relative reduction in LDL-C provides the best benefit in terms of CVD reduction. In the majority of patients, this is achievable with statin monotherapy. Therefore, for patients with high CV risk, the treatment target for LDL-C is <1.8 mmol/L (less than 70 mg/dL) or a $\geq 50\%$ reduction from baseline LDL-C. Target levels for subjects at moderate risk are extrapolated from several clinical trials. An LDL-C level of <2.5 mmol/L (less than 100 mg/dL) should be considered for them.

In patients with T2DM at very-high risk, an LDL-C reduction of >50% from baseline and an LDL-C goal of <1.4 mmol/L (<55mg/dL) is recommended. In patients with T2DM at high risk, an LDL-C reduction of >50% from baseline and an LDL-C goal of <1.8 mmol/L (<70 mg/dL) is recommended. Statins are recommended in patients with T1DM who are at high or very-high risk.

Secondary targets of therapy in the high risk category are based on data extrapolation; therefore, clinical judgement is required before a final treatment plan is implemented. Clinicians again should exercise judgement to avoid premature or unnecessary implementation of lipid-lowering therapy. Lifestyle interventions will have an important long-term impact on health, and the long-term effects of pharmacotherapy must be weighed against potential side effects. For subjects at moderate risk, an LDL-C target of <3 mmol/L (less than 115 mg/dL) should be considered.

Because apo B levels have also been measured in outcome studies in parallel with LDL-C, apo B can be substituted for LDL-C. Based on the available evidence, apo B appears to be a risk factor at least as good as LDL-C and a better index of the adequacy of LDL-lowering therapy than LDL-C. Also, there now appears to be less

laboratory error in the determination of apo B than of LDL-C, particularly in patients with HTG. However, apo B is not presently being measured in all clinical laboratories. Clinicians who are using apo B in their practice can do so; the apo B treatment targets for subjects at very high or high total CV risk are 80 mg/dL and 100 mg/dL, respectively. The specific target for non-HDL-C should be 0.8 mmol/L (30 mg/dL) higher than the corresponding LDL-C target; this corresponds to the LDL-C level augmented by the cholesterol fraction which is contained in 1.7 mmol/L (150 mg/dL) of TG, which is the upper limit of what is recommended. Adjusting lipid-lowering therapy to optimize one or more of the secondary and optional targets may be considered in patients at very high CV risk after achieving a target LDL-C (or apo B), but the clinical advantages of this approach, with respect to patient outcomes, remain to be addressed.

For secondary prevention, patients at very-high risk not achieving their goal on a maximum tolerated dose of statin and ezetimibe, a combination with a PCSK9 inhibitor is recommended. For very-high-risk FH patients (that is, with ASCVD or with another major risk factor) who do not achieve their goals on a maximum tolerated dose of statin and ezetimibe, a combination with a PCSK9 inhibitor is recommended. Statin treatment is recommended as the first drug of choice for reducing CVD risk in high-risk individuals with hypertriglyceridaemia [TG >2.3 mmol/L (200 mg/dL)]. For FH patients with ASCVD who are at very-high risk, treatment to achieve at least a 50% reduction from baseline and an LDL-C <1.4 mmol/L (<55 mg/dL) is recommended. If goals cannot be achieved, a drug combination is recommended.

3.3. Mastering the skills of biochemistry data interpretation (biomarkers of myocardial necrosis).

In the past, a general consensus existed for the clinical syndrome designated as myocardial infarction. In studies of disease prevalence, the World Health Organization (WHO) defined myocardial infarction from symptoms, ECG abnormalities, and enzymes. However, the development of more sensitive and specific serological biomarkers and precise imaging techniques allows detection of ever smaller amounts of myocardial necrosis. Accordingly, current clinical practice,

health care delivery systems, as well as epidemiology and clinical trials all require a more precise definition of myocardial infarction and a re-evaluation of previous definitions of this condition.

It should be appreciated that over the years, while more specific bio-markers of myocardial necrosis became available, the accuracy of detecting myocardial infarction has changed. Such changes occurred when glutamine-oxaloacetic transaminase (GOT) was replaced by lactate dehydrogenase (LDH) and later by creatine kinase (CK) and the MB fraction of CK, i.e. CKMB activity and CKMB mass. Current, more specific, and sensitive biomarkers and imaging methods to detect myocardial infarction are further refinements in this evolution.

In response to the issues posed by an alteration in our ability to identify myocardial infarction, the European Society of Cardiology (ESC) and the American College of Cardiology (ACC) convened a consensus conference in 1999 in order to re-examine jointly the definition of myocardial infarction (published in the year 2010 in the *European Heart Journal* and *Journal of the American College of Cardiology*). The scientific and societal implications of an altered definition for myocardial infarction were examined from seven points of view: pathological, biochemical, electrocardiographic, imaging, clinical trials, epidemiological, and public policy. It became apparent from the deliberations of the former consensus committee that the term myocardial infarction should not be used without further qualifications, whether in clinical practice, in the description of patient cohorts, or in population studies. Such qualifications should refer to the amount of myocardial cell loss (infarct size), to the circumstances leading to the infarct (e.g. spontaneous or procedure related), and to the timing of the myocardial necrosis relative to the time of the observation (evolving, healing, or healed myocardial infarction).

Following the 2009 ESC/ACC consensus conference, a group of cardiovascular epidemiologists met to address the specific needs of population surveillance. This international meeting, representing several national and international organizations. These recommendations addressed the needs of researchers engaged in long-term population trend analysis in the context of changing diagnostic tools using retrospective medical record abstraction. Also considered was surveillance in

developing countries and out-of-hospital death, both situations with limited and/or missing data. These recommendations continue to form the basis for epidemiological research.

Given the considerable advances in the diagnosis and management of myocardial infarction since the original document was published, the leadership of the ESC, the ACC, and the American Heart Association (AHA) convened, together with the World Heart Federation (WHF), a Global Task Force to update the 2012 consensus document. As with the previous consensus committee, the Global Task Force was composed of a number of working groups in order to refine the ESC/ACC criteria for the diagnosis of myocardial infarction from various perspectives. With this goal in mind, the working groups were composed of experts within the field of biomarkers, ECG, imaging, interventions, clinical investigations, global perspectives, and implications. During several Task Force meetings, the recommendations of the working groups were coordinated, resulting in the present updated consensus document.

Biomarker Evaluation

Myocardial cell death can be recognized by the appearance in the blood of different proteins released into the circulation from the damaged myocytes: myoglobin, cardiac troponin T and I, CK, LDH, as well as many others. Myocardial infarction is diagnosed when blood levels of sensitive and specific biomarkers such as cardiac troponin or CKMB are increased in the clinical setting of acute myocardial ischemia. Although elevations in these biomarkers reflect myocardial necrosis, they do not indicate its mechanism. Thus, an elevated value of cardiac troponin in the absence of clinical evidence of ischemia should prompt a search for other etiologies of myocardial necrosis, such as myocarditis, aortic dissection, pulmonary embolism, congestive heart failure, renal failure, and other examples indicated below:

- Cardiac contusion, or other trauma including surgery, ablation, pacing, etc.
- Acute and chronic heart failure
- Aortic dissection
- Aortic valve disease
- Hypertrophic cardiomyopathy
- Tachy- or bradyarrhythmias, or heart block

- Apical ballooning syndrome
- Rhabdomyolysis with cardiac injury
- Pulmonary embolism, severe pulmonary hypertension
- Renal failure
- Acute neurological disease, including stroke or subarachnoid haemorrhage
- Infiltrative diseases, e.g. amyloidosis, haemochromatosis, sarcoidosis, and scleroderma
- Inflammatory diseases, e.g. myocarditis or myocardial extension of endo-/pericarditis
- Drug toxicity or toxins
- Critically ill patients, especially with respiratory failure or sepsis
- Burns, especially if affecting >30% of body surface area
- Extreme exertion

The preferred biomarker for myocardial necrosis is cardiac troponin (I or T), which has nearly absolute myocardial tissue specificity as well as high clinical sensitivity, thereby reflecting even microscopic zones of myocardial necrosis. An increased value for cardiac troponin is defined as a measurement exceeding the 99th percentile of a normal reference population (URL = upper reference limit). Detection of a rise and/or fall of the measurements is essential to the diagnosis of acute myocardial infarction.

Blood samples for the measurement of troponin should be drawn on first assessment (often some hours after the onset of symptoms) and 6–9 h later. An occasional patient may require an additional sample between 12 and 24 h if the earlier measurements were not elevated and the clinical suspicion of myocardial infarction is high. To establish the diagnosis of myocardial infarction, one elevated value above the decision level is required. The demonstration of a rising and/or falling pattern is needed to distinguish background elevated troponin levels, e.g. patients with chronic renal failure, from elevations in the same patients which are indicative of myocardial infarction. However, this pattern is not absolutely required to make the diagnosis of myocardial infarction if the patient presents >24 h after the onset of symptoms. Troponin values may remain elevated for 7–14 days following the onset of infarction.

If troponin assays are not available, the best alternative is CKMB (measured by mass assay). As with troponin, an increased CKMB value is defined as a

measurement above the 99th percentile URL, which is designated as the decision level for the diagnosis of myocardial infarction. Gender-specific values should be employed. The CKMB measurements should be recorded at the time of the first assessment of the patient and 6–9 h later in order to demonstrate the rise and/or fall exceeding the 99th percentile URL for the diagnosis of myocardial infarction. An occasional patient may require an additional diagnostic sample between 12 and 24 h if the earlier CKMB measurements were not elevated and the clinical suspicion of myocardial infarction is high.

Measurement of total CK is not recommended for the diagnosis of myocardial infarction, because of the large skeletal muscle distribution and the lack of specificity of this enzyme.

Reinfarction

Traditionally, CKMB has been used to detect reinfarction. However, recent data suggest that troponin values provide similar information. In patients where recurrent myocardial infarction is suspected from clinical signs or symptoms following the initial infarction, an immediate measurement of the employed cardiac marker is recommended. A second sample should be obtained 3–6 h later. Recurrent infarction is diagnosed if there is a >20% increase of the value in the second sample. Analytical values are considered to be different if they are different by >3 SDs of the variance of the measures. For troponin, this value is 5–7% for most assays at the levels involved with reinfarction. Thus, a 20% change should be considered significant, i.e. over that expected from analytical variability itself.

Other biomarkers of necrosis

There is a large number of biomarkers of necrosis that are actively investigated (free fatty lipid-bound protein, pregnancy-associated protein etc.), but there are not incorporated into routine clinical practice.

3.4. Mastering the skills of ECG interpretation in the field of the topic

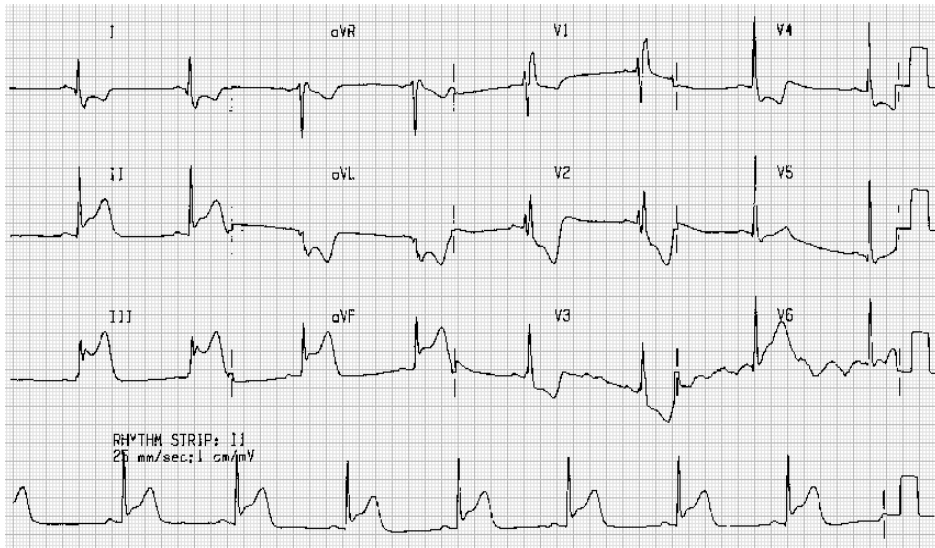
The ECG is an integral part of the diagnostic work-up of patients with suspected myocardial infarction. The acute or evolving changes in the ST-T waveforms and the Q-waves when present potentially allow the clinician to date the event, to suggest the infarct-related artery, and to estimate the amount of myocardium

at risk. Coronary artery dominance, size and distribution of arterial segments, collateral vessels, and location, extent, and severity of coronary stenoses can also impact ECG manifestations of myocardial ischemia. The ECG by itself is often insufficient to diagnose acute myocardial ischemia or infarction since ST deviation may be observed in other conditions such as acute pericarditis, LV hypertrophy, LBBB, Brugada syndrome, and early repolarization patterns. Also Q-waves may occur due to myocardial fibrosis in the absence of coronary artery disease, as in, for example, cardiomyopathy.

ECG abnormalities of myocardial ischemia or infarction may be inscribed in the PR segment, the QRS complex, and the ST segment or T-waves. The earliest manifestations of myocardial ischemia are typical T-waves and ST segment changes. Increased hyper-acute T-wave amplitude with prominent symmetrical T-waves in at least two contiguous leads is an early sign that may precede the elevation of the ST segment. Increased R-wave amplitude and width (giant R-wave with S-wave diminution) are often seen in leads exhibiting ST elevation, and tall T-waves reflecting conduction delay in the ischemic myocardium. Transient Q-waves may be observed during an episode of acute ischemia or rarely during acute myocardial infarction with successful reperfusion.

Although a recent article challenged this distinction, MIs are no longer classified as transmural and subendocardial but as Q-wave and non-Q-wave. In the thrombolytic era, the prevalence of the latter seems to be greater than that of the former, presumably due to a reduction in infarct size (Figure 33). The prethrombolytic "classic" evolution of acute MI has been transformed by pharmacologic therapy and interventional techniques. The succession of events in the course of a Q-wave MI is from hyperacute positive T waves (on occasion) to ST-segment elevation to abnormal Q waves to T-wave inversion. Commonly, two or more of these findings appear together, depending on the timing of the first recorded static ECG. Acceleration of these phases can occur with effective reperfusion. The time course of ST-segment elevation is a good predictor of reperfusion.

Figure 33: ECG in patient with acute inferior myocardial infarction



Sometimes, acute onset LBBB can mask acute MI (Figure 34).

Figure 34: Acute myocardial infarction in the presence of left bundle branch block

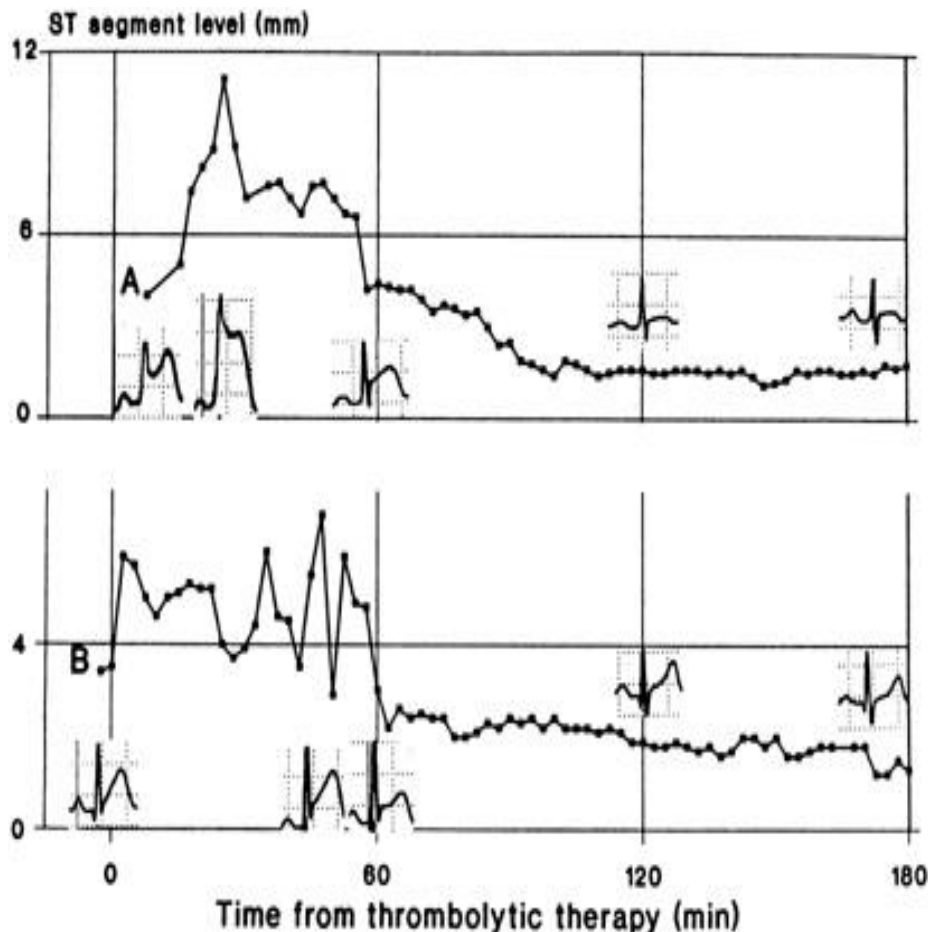


Because prethrombolytic 12-lead ECG studies on ST-segment evolutions were based on static recordings obtained at fixed time intervals, it became clear that continuous monitoring in the coronary care unit (which falls outside the realm of this chapter) was essential to adequately record the dynamics of ST-segment trends. Sensitivity increases as frequency of monitoring increases (Figure 35).

Continuous monitoring is thus essential to evaluate occurrence of reperfusion. Resolution of ST-segment elevation has been defined as a progressive decrease within 40 to 60 min to less than 50 percent of its maximally elevated value. It has been suggested that in patients treated with thrombolytics, the dichotomization for Q-wave and non-Q-wave MI should be made by the pre-discharge, rather than the 24-h, ECG due to possible crossover from one group to another. Aspects of the ECG other than ST-segment changes may be altered particularly during acute, anterior-wall MI.

In fact, the same degree of ST-segment elevation in V2 and V3 with disappearance of the S waves indicates a greater degree of affection than with preservation of this negative wave.

Figure 35: Plots of ST-segment levels versus time from therapy in two selected patients with patency of the infarct-related vessel at 60 min.



Note that a 50 percent decrease in ST-segment levels within 60 min occurred only when measurements were made from the peak ST-segment level (highest ST-segment level measurement within the first 60 min).

Clinical Value of the Electrocardiogram in Established Myocardial Infarction.

Autopsy, echocardiographic, and angiographic studies have shown that the 12-lead ECG has a limited capability to diagnose established myocardial infarction. The accuracy of the ECG depends on both the infarct location and size, and it may be hampered by the presence of intraventricular conduction defects, LAFB, Q-wave regression, multiple infarctions (e.g., an anterior infarct may reduce tall R waves in V1 to V2 from a previous posterior infarct), and LVH

Determination of the localization of myocardial infarction zone with ECG

I — anterior or lateral wall of left ventricle;
III, aVF — posterior wall (diaphragmal area);
aVL — higher-located anterior zone of left ventricle;
V₁, V₂ — interventricular septum;
V₃ — anterior wall;
V₄ — apical segment of left ventricle;
V₅, V₆ — lateral wall of left ventricle;
V₇, V₈, V₉ — basal segments of left ventricle;
V_{3R}, V_{4R} — right ventricle.

Infarct Location

The presence of abnormal Q waves in two or more leads of the same group has been classically associated to infarct areas that, anatomically, may not be accurately correlated. For example, in ventriculograms, abnormal Q waves in leads I, aVL, V₅, and V₆ are often associated with apical, rather than lateral, wall motion abnormalities. Anteroseptal infarct has classically been defined by the presence of Q waves in leads V₁ to V₃, yet in patients with ST-segment elevation in V₁ to V₃, echocardiographic and angiographic data have shown anteroapical infarcts and normal septa. Anatomically defined septal infarcts result instead in disappearance of septal Q waves in inferior leads and in I, V₅, and V₆. These changes are preceded by ST-segment depression in the same leads during the acute phase or, if the infarction was inferoseptal, by precordial ST-segment depression. Initial R waves may be reduced in V₁ to V₃.

Prominent right precordial R waves have been classically attributed to posterior infarct, but this may be a misnomer. The term posterior may apply better to the thoracic wall facing these areas of the LV than to the LV itself. Prominent R waves in V₁ (R/S >1) are highly specific and have a high positive predictive value for basal lateral asynergy of the LV. Specificity and positive predictive value drop slightly for prominent R waves in V₂. Abnormal R waves in V₁ in patients with chest pain are 96% specific for circumflex occlusion. In both posterior and inferoposterior infarcts, the culprit artery is usually the circumflex. In some patients, a taller R wave in V₁ and prominent R waves in V₂ to V₃ may develop after LAD occlusion. The R-wave amplitude and duration may also be used for the diagnosis of established infarction.

Because the electrical activation of the right ventricular free wall is insignificant in comparison with that of the LV myocardium, infarction of the right ventricle rarely alters the QRS complex beyond a slight voltage reduction. When present, Q waves in both V3R and V4R are highly specific markers for right ventricular infarction.

Table 3.5 shows an acceptable classification for the ECG location of MI according to leads showing abnormal Q waves.

Table 3.5: Electrocardiographic Location of Infarction Sites Based on the Presence of Abnormal Q Waves

Site	Leads	False Patterns
Inferior (diaphragmatic)	II, III, aVF	WPW (PSAP), HCM
Inferolateral	II, III, aVF, V ₄ -V ₆	-
'True' posterior (postero-basal)	V ₁	RVH, 'atypical' incomplete RBBB, Left AP
Inferoposterior	II, III, aVF, V ₁	WPW (left PSAP), HCM
Inferior-right ventricular	II, III, aVF plus V ₄ R-V ₆ R or V ₁ -V ₃	ASMI as defined from axis
Anteroseptal	V ₁ , V ₂ , V ₃	LVH, chronic lung disease, LBBB, chest electrode misplacement
Anterolateral	I, II, V ₄ -V ₆	HCM, ventricular septal defect
Extensive anterior	I, aVL, V ₁ -V ₆	-
High lateral	I, aVL	-
Anterior (apical)	V ₃ -V ₄	-
Posterolateral	V ₄ -V ₆ , V ₁ *	WPW (LFWAP)
Right ventricular	V ₄ R with V ₄ R-V ₆ R or V ₁ -V ₃	ASMI

Notes: ASMI - anteroseptal myocardial infarction; HCM - hypertrophic cardiomyopathy; LBBB - left bundle branch block; LFWAP - left free-wall accessory pathway; PSAP - posteroseptal accessory pathway; WPW - Wolff-Parkinson-White syndrome; RVH - right ventricular hypertrophy.

In addition, it depicts other processes that may result in false patterns of Q-wave MI. During the acute phase, ST-segment changes give a clue to the area at risk, but because of the normal variability in coronary anatomy and the presence of previous occlusions, there is sometimes more than one possible explanation for a specific ECG pattern.

Reciprocal ST-segment changes

In an inferior MI with abnormal ST-segment elevation limited to this wall, the reciprocal STsegment changes will occur in diametrically opposed leads located in the same plane. For example, "indicative" ST-segment elevation in leads III and aVF, which record the electrical activity of the inferior (posteroinferior or

diaphragmatic) wall, yields "reciprocal" ST-segment depression in leads I and aVL because they face the superior (anterolateral) wall. ST-segment depression in lead V2 may reflect injury in the anterior subendocardial wall as well as injury in the posterobasal (or true) posterior wall.

The ECG by itself cannot distinguish with absolute certainty between these two possibilities. The differential diagnosis perhaps can best be made by performing cardiac catheterization or radionuclear studies in the acute phase of the MI, when the ST-segment changes are still present. Another way is by analyzing ST-segment changes occurring during percutaneous transluminal coronary angioplasty in patients with proven single-vessel disease. This has shown that reciprocal ST-segment depression in leads V2 and V3 can occur during balloon occlusions of dominant right, as well as of dominant left, coronary arteries.

Right ventricular MI

An ST-segment elevation of at least 1 mm in lead V4R in patients with acute inferior MI had a sensitivity of 100 percent, a specificity of 87 percent, and a predictive accuracy of 92 percent for the diagnosis of right ventricular infarction in patients with ST-segment elevation in leads II, III, and aVF. These changes disappeared within 10 to 18 h after the onset of chest pain in 50 percent of their patients and after 72 h in the remaining patients. In addition to V4R, ST-segment elevation can be seen in leads V5 and V6R and in some cases (with decreasing amplitude) in V1, V2, and even V3. It is possible for ST-segment depression in V5 and V6 to be reciprocal to right ventricular involvement.

Atrial Infarction

Atrial infarction is rarely recognized in the ECG; however, it may occur in 1% to 17% of patients with acute myocardial infarction. The injury current affects atrial repolarization and results in elevation of the Ta wave with reciprocal changes in opposite leads. This produces displacement of the PR segment, better appreciated in patients with AV block.

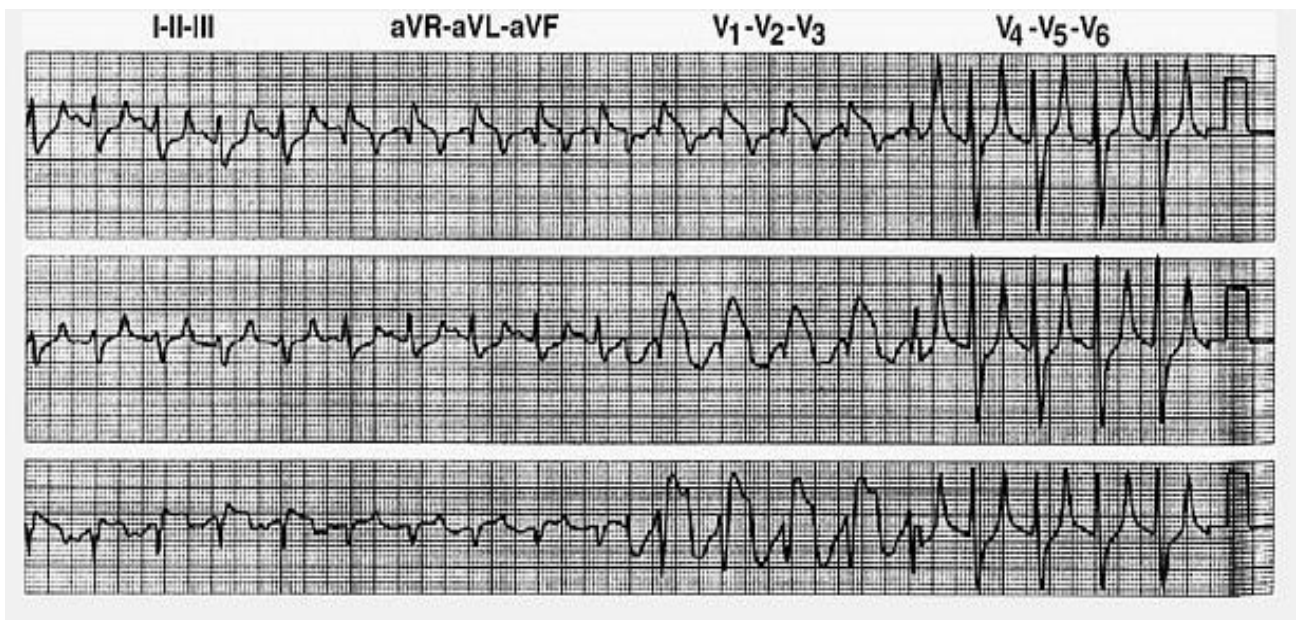
Pseudoinfarction Patterns

Aside from the setting of acute myocardial injury, in some conditions the ECG shows ST-segment elevation, usually with a concave pattern. These conditions

include severe hyperkalemia, pericarditis, uncomplicated LBBB, primary and secondary cardiac tumors, acute pulmonary embolism, early repolarization, ventricular aneurysm, and implantable defibrillator shocks.

Pathologic Q waves or decreased R-wave amplitude mimicking myocardial necrosis may occur in LVH, fascicular blocks, ventricular preexcitation, infiltrative heart disease, lead misplacement, acute pulmonary embolism, pulmonary emphysema, pleural effusion, and epicardial implantable defibrillator systems. LBBB and ventricular pacing may present the ECG appearance of acute or remote myocardial infarction. Figure 36 shows pseudoinfarction patterns mimicked by hyperkalemia.

Figure 36: Acute pseudoinfarction patterns mimicked by hyperkalemia



Pericarditis

The ECG pattern of acute (generalized) pericarditis not due to MI is produced by the associated epimyocarditis, which in turn results in diffuse epicardial "injury." The ST segments can be elevated in all leads except aVR and, rarely, in V1. Symmetric T-wave inversion (due to epicardial "ischemia") usually develops after the ST segments have returned to the baseline (but can appear during the injury stage).

Neither reciprocal ST-segment changes nor abnormal Q waves are seen. In most cases of acute pericarditis, the PR segment is depressed. Average ECG resolution occurs in close to 2 weeks. The ECG pattern of acute pericarditis has to be differentiated from the normal variant re-ferred to as early repolarization.

Myocardial Stunning from Sudden Emotional Stress (Stress Cardiomyopathy or Takotsubo Syndrome)

Emotional stress can induce clinical manifestations similar to those of an acute coronary event. This entity has been called stress cardiomyopathy, Takotsubo syndrome, and broken heart syndrome and now this phenomenon is considered as acute stress-induced heart failure. It affects mainly postmenopausal women. Patients present with chest pain, sometimes accompanied by ST-segment elevation, negative T waves, QT prolongation, pathologic Q waves, relatively minor elevation of cardiac enzyme and biomarker levels, and reversible LV dysfunction despite the absence of epicardial coronary disease. Plasma levels of catecholamines and stress-related neuropeptides are increased. Prognosis is good

References:

1. 2019 ESC/EAS Guidelines for the management of dyslipidaemias: lipid modification to reduce cardiovascular risk. The Task Force for the management of dyslipidaemias of the European Society of Cardiology (ESC) and European Atherosclerosis Society (EAS). *European Heart Journal* (2019) 00, 1-78.
2. 2019 ESC Guidelines for the diagnosis and management of acute pulmonary embolism developed in collaboration with the European Respiratory Society (ERS) The Task Force for the diagnosis and management of acute pulmonary embolism of the European Society of Cardiology (ESC). *European Heart Journal* (2019) 00, 1-61.
3. 2019 ESC Guidelines on diabetes, pre-diabetes, and cardiovascular diseases developed in collaboration with the EASD The Task Force for diabetes, pre-diabetes, and cardiovascular diseases of the European Society of Cardiology (ESC) and the European Association for the Study of Diabetes (EASD). *European Heart Journal* (2019) 00, 1-69.
4. 2019 ESC Guidelines for the management of patients with supraventricular tachycardia The Task Force for the management of patients with supraventricular tachycardia of the European Society of Cardiology (ESC) Developed in collaboration with the Association for European Paediatric and Congenital Cardiology (AEPC). *European Heart Journal* (2019) 00, 1-65
5. Catapano AL, Graham I, De Backer G, et al.; ESC Scientific Document Group. 2016 ESC/EAS Guidelines for the management of dyslipidaemias. *Eur Heart J*. 2016;37:2999-3058

6. Diercks DB, Peacock WF, Hiestand BC, et al. Frequency and consequences of recording an electrocardiogram >10 minutes after arrival in an emergency room in non-ST-segment elevation acute coronary syndromes (from the CRUSADE Initiative). *Am J Cardiol* 2006;97(4):437–442.
7. Ference BA, Ginsberg HN, Graham I, et al. Low-density lipoproteins cause atherosclerotic cardiovascular disease. 1. Evidence from genetic, epidemiologic, and clinical studies. A consensus statement from the European Atherosclerosis Society Consensus Panel. *Eur Heart J*. 2017; 38:2459-2472.
8. Perk J, De Backer G, Gohlke H, et al; European Association for Cardiovascular Prevention & Rehabilitation; ESC Committee for Practice Guidelines (CPG). European Guidelines on cardiovascular disease prevention in clinical practice (version 2012). The Fifth Joint Task Force of the European Society of Cardiology and Other Societies on Cardiovascular Disease Prevention in Clinical Practice (constituted by representatives of nine societies and by invited experts). *Eur Heart J* 2012; 33: 1635-1701.
9. Piepoli MF, Hoes AW, Agewall S, et al. 2016 European Guidelines on cardiovascular disease prevention in clinical practice: The Sixth Joint Task Force of the European Society of Cardiology and Other Societies on Cardiovascular Disease Prevention in Clinical Practice (constituted by representatives of 10 societies and by invited experts) Developed with the special contribution of the European Association for Cardiovascular Prevention & Rehabilitation (EACPR). *Eur Heart J*. 2016; 37:2315-2381.
10. Ponikowski P, Voors AA, Anker SD, et al. 2016 ESC Guidelines for the diagnosis and treatment of acute and chronic heart failure: The Task Force for the diagnosis and treatment of acute and chronic heart failure of the European Society of Cardiology (ESC). Developed with the special contribution of the Heart Failure Association (HFA) of the ESC. *Eur Heart J* 2016;37(27): 2129–2200.
11. Schiele F, Gale CP, Bonnefoy E, et al. Quality indicators for acute myocardial infarction: A position paper of the Acute Cardiovascular Care Association. *Eur Heart J Acute Cardiovasc Care* 2017; 6(1):34–59.
12. Thygesen K, Alpert JS, Jaffe AS, et al, Writing Group on the Joint ESC/ACCF/AHA/WHF Task Force for the Universal Definition of Myocardial Infarction, ESC Committee for Practice Guidelines. Third universal definition of myocardial infarction. *Eur Heart J* 2012; 33(20):2551–2567.
13. Emerging Risk Factors Collaboration, Di Angelantonio E, Gao P, Pennells L, et al. Lipid-related markers and cardiovascular disease prediction. *JAMA* 2012;307:2499-2506.

4. Topic 4. Practical skills for the topic №8 «Inherited heart diseases in adults. Acquired heart diseases».

Congenital heart disease (CHD) is defined as a gross structural abnormality of the heart, great arteries, or great veins that is present at birth. Congenital cardiac malformations are relatively uncommon. Multiple studies have demonstrated an incidence of 0.6% of live births for moderate to severe defects. The prevalence is higher in stillbirths and spontaneous abortions. There are approximately 32,000 new cases per year in the United States and greater than 1,000,000 new cases per year worldwide. Although the prevalence is low, the population of patients with CHD continues to expand. Because of the dramatic advances made in medical, surgical, and interventional device therapy, survival into adulthood is now the rule for the vast majority of patients with congenital cardiac defects.

Etiology

The etiology of CHD is multifactorial. Recurrence risks vary with the gender of the proband and the specific cardiac defect, with an overall recurrence risk of 3% to 5% in the offspring of patients with congenital heart disease. The exact proportion of patients with a specific genetic etiology is unknown. There are reports of familial defects following Mendelian patterns of inheritance. Certain chromosomal abnormalities are associated with congenital heart defects. The most common of these is trisomy 21 (Down syndrome). At least 50% of patients with Down syndrome have CHD (most commonly atrioventricular septal defects or ventricular septal defects), often associated with early pulmonary vascular obstructive disease. Despite the identification of many candidate genes on chromosome 21, the key genes contributing to the cardiac phenotype in Down syndrome have yet to be defined. Other syndromes associated with CHD include Turner syndrome, Noonan syndrome, Williams syndrome, Marfan syndrome, and trisomy 13, 14, 15, and 18.

Deletions of 22q11 are seen in DiGeorge syndrome (thymic aplasia, hypoparathyroidism, congenital heart defects involving the outflow tracts, and a dysmorphic appearance). From transgenic studies with a mouse model, TBX1 has been identified as the likely gene responsible for the cardiac and hypoparathyroid

phenotype. 22q11 deletions are now recognized as the cause of a broader group of defects and are seen in 50% of patients with conotruncal abnormalities. CATCH-22, a syndrome due to microdeletion at chromosome 22q11, consists of cardiac conotruncal abnormalities, abnormal facies, thymic abnormalities, cleft palate, and hypocalcemia. Some patients may have the gene deletion without accompanying syndromic features.

Mutations in a few specific genes have been identified in some cases of congenital heart defects. Mutations in *TBX5* are seen in the majority of patients with Holt-Oram syndrome, an autosomal disorder with cardiac septal defects and upper limb defects. Mutations in the elastin gene (*ELN*) have been identified as a cause of supravalvular aortic stenosis. Mutations in *NKX2.5* have been associated with the autosomal dominant phenotype of atrial septal defect or tetralogy of Fallot.

Fetal and Neonatal Circulation

In fetal life, the placenta is a low-resistance structure that acts as a respiratory organ and receives the largest amount of fetal blood flow. Blood from the placenta returns to the fetus through the ductus venosus, entering the inferior vena cava (IVC) to the right atrium (RA). A portion of the IVC blood flow is directed across the patent foramen ovale (PFO) to the left atrium (LA), bypassing the right heart. Blood from the superior vena cava (SVC) is directed into the right ventricle (RV) along with the remaining blood return from the IVC and is then pumped out into the pulmonary artery. Because of high pulmonary vascular resistance in the fetus, most pulmonary blood flow crosses the ductus arteriosus and enters the descending thoracic aorta. At birth, the relatively low resistance placental circulation is removed, and systemic vascular resistance increases within minutes. With respiration, the pulmonary vascular bed dilates in response to inspired oxygen, and pulmonary vascular resistance decreases while pulmonary blood flow increases. Pulmonary venous blood return increases, which increases systemic ventricular output and helps to close the foramen ovale. The ductus arteriosus is patent at birth, but begins to constrict shortly after birth and usually closes within hours to several days. Defects in which pulmonary blood flow depends on flow through the ductus are characterized as ductal dependent. With closure of the ductus in these patients, progressive hypoxemia,

acidosis, and death invariably occur. Prostaglandin E1 infusion to maintain patency of the ductus is used as a temporizing measure until more definitive therapy can be undertaken.

Diagnostic Tools

The physical exam is critical in the evaluation of patients with known or suspected CHD and includes elements that may not be routinely performed in patients with acquired forms of heart disease. In addition to precordial palpation, assessment of venous waveforms, and careful cardiac auscultation, it is also important to assess for cyanosis (including differential cyanosis), palpate pulses and measure blood pressure in both upper and lower extremities, and check oxygen saturation. Evidence of phenotypes associated with CHD (e.g., Down syndrome, William syndrome) should be sought. Although the electrocardiogram (ECG) and chest x-ray (CXR) are a routine part of the evaluation of patients with CHD, they are not specific enough for diagnostic purposes. Imaging studies by qualified personnel play a critical role in the evaluation of these patients. A careful review of prior data, including catheterization data, imaging, and operative reports, is essential as well.

Transthoracic echocardiography (TTE) is the most widely used diagnostic tool for establishing the initial diagnosis and following patients serially. Studies in these patients are complex and time-consuming and should be performed by sonographers and physicians with expertise in CHD. Transesophageal echocardiography (TEE) is particularly useful in adults with poor acoustic windows, providing excellent visualization of the atrial septum, pulmonary veins, interatrial baffles, and Fontan connections. Intraoperative TEE plays a critical role for patients undergoing surgical repair. TEE is also used to guide catheter interventions and device deployment. Increasingly, intracardiac echocardiography is being used for these procedures. Three-dimensional echocardiography is an evolving technology that may be helpful in evaluating patients with congenital heart disease.

Cardiac magnetic resonance imaging (MRI) is an extremely useful tool for the assessment of patients with congenital heart disease, providing high-quality images with a wide field of view in nearly all patients. MRI is particularly useful for assessment of extracardiac anatomy, including delineation of the great vessels,

branch pulmonary arteries, and surgical shunts, as well as systemic and pulmonary venous connections. MRI allows quantitation of ventricular mass, volumes, and ejection fraction and can be used to calculate shunt flow and regurgitant flow. Contrast is not required for routine imaging but may be particularly useful in assessing vascular structures. The role of cardiac computed tomography (CT) imaging is evolving. Cardiac CT provides excellent visualization of anatomy (particularly extracardiac anatomy) but does use ionizing radiation.

Cardiac catheterization plays a critical role in the management of patients with congenital heart disease, as both a diagnostic and a therapeutic tool. Due to the complex hemodynamic data and difficult anatomy in many of these patients, catheterization is best performed by experienced personnel. There is an expanding role for interventional catheterization procedures, including closure of shunts, pulmonary and aortic valvotomy, pulmonary artery stenting, stenting of conduits, and balloon aortoplasty for aortic coarctation.

In this section both skills of thoracic X-ray data interpretation and EchoCG interpretation are reported together to easily understand the principles of diagnosis of the diseases.

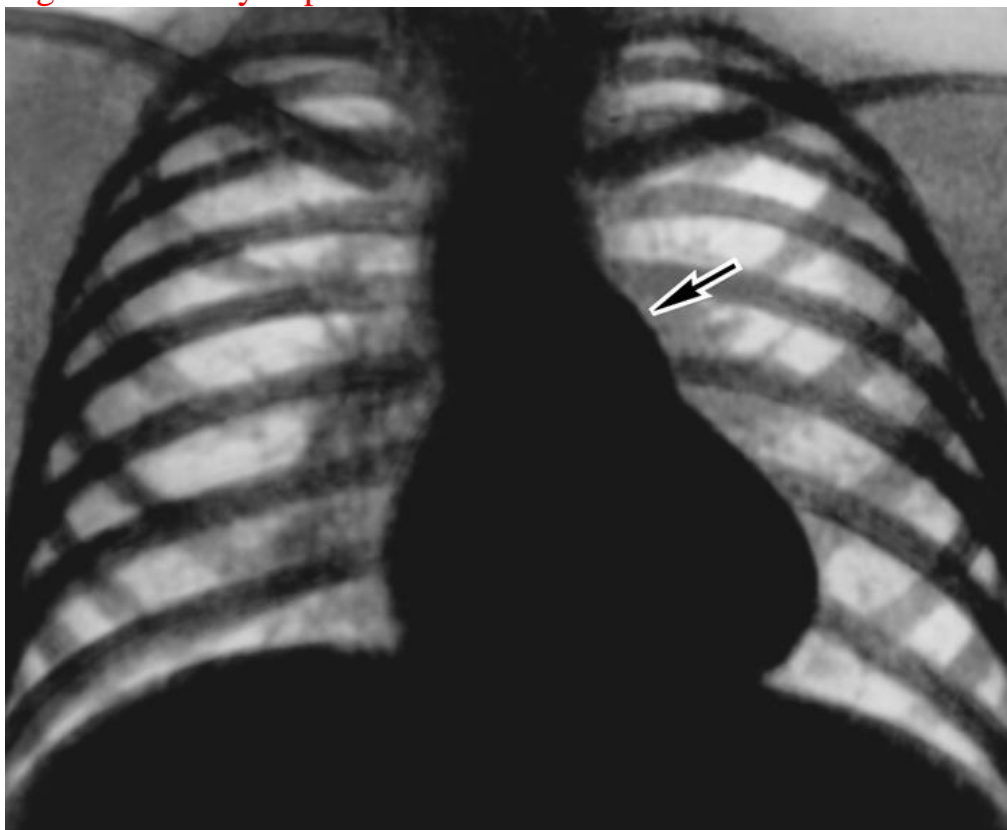
Specific Defects. Left-to-Right Shunts. Atrial Septal Defect

An atrial septal defect (ASD) is a direct communication between the atrial chambers. ASDs are common, accounting for 5% to 10% of all congenital heart defects and one third of all congenital defects diagnosed in adulthood. They are usually sporadic, but familial cases have been reported. They are more common in female than male individuals (2:1). An associated congenital defect may be seen in up to 30% of cases. ASDs are seen in association with skeletal deformities of the upper extremities, including Holt-Oram syndrome. Ostium secundum and primum defects are also associated with Down syndrome.

There are several morphologic types of ASDs. The most common is the ostium secundum defect (seen in 75% of cases). Secundum defect occurs in the region of the fossa ovalis, may extend in any direction, and may be multiple. Partial anomalous pulmonary venous connections are seen in 2% of patients with secundum defects. Ostium primum defects account for 15% of ASDs. Primum defects are part of the

spectrum of atrioventricular (AV) septal defects and are associated with a common AV junction. A common AV valve is usually present with fusion of the inferior and superior bridging leaflets, leading to separate mitral and tricuspid orifices. This results in a trileaflet appearance of the anterior mitral leaflet, sometimes referred to as cleft in the anterior leaflet. Mitral regurgitation may be associated with this abnormal valve. Sinus venosus defects account for 10% of ASDs. Sinus venosus defects occur in the superior portion of the septum near the insertion of the SVC and are frequently associated with anomalous pulmonary venous drainage of the right pulmonary veins, most commonly the right upper pulmonary vein. Inferior sinus venosus defects are rare. They occur at the mouth of the IVC and may have right-to-left shunting and cyanosis due to preferential shunting of IVC blood to the LA. The rarest form of ASD is the coronary sinus defect, which may occur at the mouth of the coronary sinus or in the body of the coronary sinus itself (known as unroofing of the coronary sinus). Coronary sinus ASDs are often associated with a persistent left superior vena cava connecting to the LA. Some patients may have absence of most of the interatrial septum, resulting in a common atrium.

Figure 37: X-ray in patient with ASD.



Note: Arrow indicates prominence of pulmonary artery curve

With unrestricted defects, there is no pressure gradient between the atria. Left-to-right shunting across the ASD occurs in late systole and diastole. The magnitude of the shunt depends on the size of the defect and the relative compliance of the right and left ventricles as well as the pulmonary and systemic vascular resistance. Diseases that affect left ventricular (LV) compliance (e.g., hypertension, coronary artery disease) can increase the magnitude of the left-to-right shunt. The left-to-right shunt results in right ventricular volume overload with increased pulmonary blood flow. Large shunts may result in pulmonary hypertension. Spontaneous closure of ASDs may occur. Small ASDs (<3 mm) usually close by 18 months, and as many as 80% of defects in the range of 5 to 8 mm close by 18 months. Larger defects rarely close spontaneously

The cardiac exam demonstrates a right ventricular lift with significant volume overload. S1 is normal. S2 is widely split and does not vary with respiration, although this pathognomonic finding is not universally present. A systolic flow murmur is common due to increased flow across the right ventricular out-flow tract. A diastolic rumble across the tricuspid valve may be heard with large shunts. With the development of pulmonary hypertension, splitting of S2 narrows and the intensity of P2 increases. With shunt reversal (the Eisenmenger syndrome), cyanosis and clubbing develop. Cyanosis may also be seen in the absence of pulmonary hypertension in patients with very large defects, a prominent Eustachian valve, a coronary sinus defect, or in association with pulmonic stenosis, RV dysfunction, or Ebstein's anomaly. Typical ECG findings include right-axis deviation (except in ostium primum defects) and an rSR or rsR pattern in lead V1. There may be evidence of right ventricular hypertrophy (RVH). Some patients have prolongation of the PR interval. Inverted P waves in the inferior leads suggest a sinus venosus type of defect. A superior QRS axis (extreme right- or left-axis deviation) suggests a primum atrial septal defect. The CXR shows right-sided chamber enlargement, a dilated pulmonary artery, and increased pulmonary vascular markings in patients with significant shunts.

The diagnosis is made by echocardiography, which demonstrates the location and size of the defect as well as the direction of shunting. The presence of a dilated RA and RV consistent with right-sided volume overload should suggest the presence

of an ASD, prompting thorough interrogation of the atrial septum and a bubble study. Ostium secundum and primum defects are well visualized by transthoracic imaging, particularly on subcostal views. Sinus venosus defects may be more difficult to demonstrate and require additional views. TEE is frequently used in the adult populations to fully interrogate the interatrial septum.

Cardiac catheterization is not usually required in patients with an ASD unless there is associated pulmonary hypertension or the noninvasive assessment is inconclusive. The presence of an ASD is confirmed by catheter passage across the atrial septum and a step up in oxygen saturation at the level of the atrium. Systemic and pulmonary blood flow, ratio of pulmonary to systemic blood flow (Q_p/Q_s), pulmonary pressure, and pulmonary vascular resistance should be assessed. If anomalous pulmonary venous drainage is suspected, levophase pulmonary artery injections should be obtained. Coronary angiography is usually performed for patients over the age of 40 years if surgical correction is planned. ASDs can also be diagnosed by cardiac MRI, which is also excellent for assessing pulmonary venous connections.

Ventricular Septal Defect

Ventricular septal defects are the most common form of congenital heart defect, accounting for 25% to 30% of all patients with congenital heart disease. The male:female ratio is 1. VSDs are the most common defect seen in the pediatric population. VSDs are usually a single defect, but they can occur in the setting of more complex congenital heart defects. Defects can be divided into restrictive defects (flow restricted between the LV and the RV with right ventricular pressure less than half of systemic levels) or nonrestrictive defects (with equal left and right ventricular pressures). From 70% to 80% of VSDs can be characterized as restrictive, with the potential to close or become smaller. Nearly half of all VSDs are small, and up to 75% may close spontaneously. Even large defects can decrease in size. VSDs usually close by the age of 10 years. Spontaneous closure in adults is rare but has been reported.

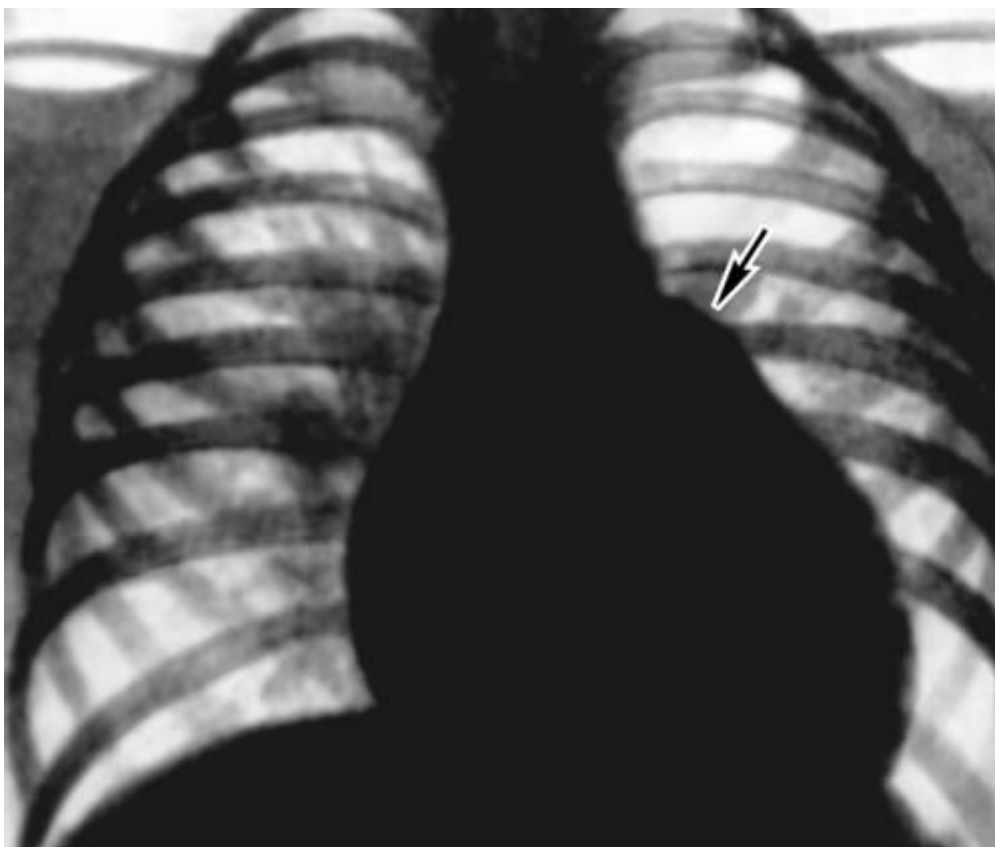
The ventricular septum consists of the trabecular muscular septum, the inlet septum (formed from the endocardial cushion), the outlet or infundibular septum, and

the membranous septum. Failure of growth, alignment, or fusion of these components results in a VSD. Perimembranous VSDs are the most common type, accounting for 75% to 80% of cases. A perimembranous defect occurs at the junction of the inlet, outlet, and trabecular septum and may extend variably into these regions. The perimembranous VSD underlies the septal leaflet of the tricuspid valve and may decrease in size or close spontaneously due to adherence of septal leaflet tissue to the defect, resulting in a ventricular septal aneurysm. Inlet septal defects account for 5% to 10% of VSDs. They occur in the muscular septum, under the mitral and tricuspid leaflets, due to deficiency of tissue from the endocardial cushion. Inlet VSDs rarely close spontaneously. Muscular defects or defects of the trabecular septum account for 20% of all VSDs. They may be located in various positions within the trabecular septum and may be multiple. Muscular VSDs tend to decrease in size with muscle growth and may close spontaneously. Outlet defects (also known as doubly committed subarterial defects or supracristal VSDs) account for 5% of all VSDs. They occur in the right ventricular outlet or conal portion of the septum, underlying both the pulmonary and aortic valves. Outlet defects do not close spontaneously, but their size can decrease due to prolapse of aortic cusp tissue through the defect (also resulting in aortic regurgitation).

The degree of left-to-right shunting depends on the size of the defect and the relative resistance of the systemic and pulmonary vascular beds. VSDs are characterized as small when the defect size is less than one-third of the aortic root size, and these are always restrictive. Pulmonary vascular resistance remains normal. With moderate restrictive defects, the defect is approximately half the size of the aortic valve, and there is moderate to severe left-to-right shunting. Patients with moderate defects may develop symptoms associated with LV volume overload and are at risk for developing pulmonary vascular disease. Large VSDs are nonrestrictive, with equal pressures in the left and right ventricles. There is a large left-to-right shunt initially, and the pulmonary circulation is exposed to systemic pressures early in the course of the disease. Patients with nonrestrictive VSDs usually develop irreversible pulmonary vascular disease within the first decade of life, eventually resulting in shunt reversal and Eisenmenger physiology. ECG findings are nonspecific. The ECG

is normal with small defects. Larger defects are usually associated with the development of left ventricular hypertrophy (LVH) and ST-T wave changes. RVH may be seen with large defects or with the Eisenmenger syndrome. The CXR is normal with small defects, but cardiomegaly and pulmonary plethora are seen with larger defects. Patients with severe pulmonary vascular disease and shunt reversal (Eisenmenger physiology) have mild cardiomegaly or normal heart size with large central pulmonary arteries, peripheral pruning of the pulmonary vessels, and oligemic lung fields. Figure 37 represents X-ray findings in VSD.

Figure 37: X-ray findings in VSD



The diagnosis can be made by echocardiography with Doppler color flow mapping. With careful interrogation of the septum, the site and size of defects can be demonstrated. The pressure gradient between the LV and the RV can be assessed by continuous-wave Doppler interrogation of the VSD jet, and right ventricular systolic pressure can be indirectly estimated from continuous-wave Doppler interrogation of the tricuspid regurgitation (TR) jet. Care must be taken with the latter approach because the TR jet may be contaminated by the VSD jet (particularly with perimembranous defects), resulting in inaccurate right ventricular pressure

estimation. The interventricular pressure gradient may be inaccurate in the setting of tortuous or serpiginous defects where the modified Bernoulli equation is not applicable. Echocardiography may also reveal other associated defects, including aortic regurgitation. Cardiac catheterization is generally reserved for patients in whom there is uncertainty regarding the size of the shunt and the pulmonary vascular resistance. The reversibility of pulmonary hypertension can be assessed with the administration of oxygen, nitric oxide, prostaglandins, or adenosine. Selective coronary angiography is usually performed for patients older than the age of 40 years if surgical repair is planned.

The diagnosis is usually made on the basis of finding a loud holosystolic murmur. Larger shunts may result in symptoms of congestive heart failure in infancy as well as an increased susceptibility to pulmonary infections. The diagnosis of a VSD in adulthood is usually based on the incidental finding of a murmur or the development of a complication related to the VSD (e.g., endocarditis, aortic valve prolapse and regurgitation, or the Eisenmenger syndrome).

Patent Ductus Arteriosus

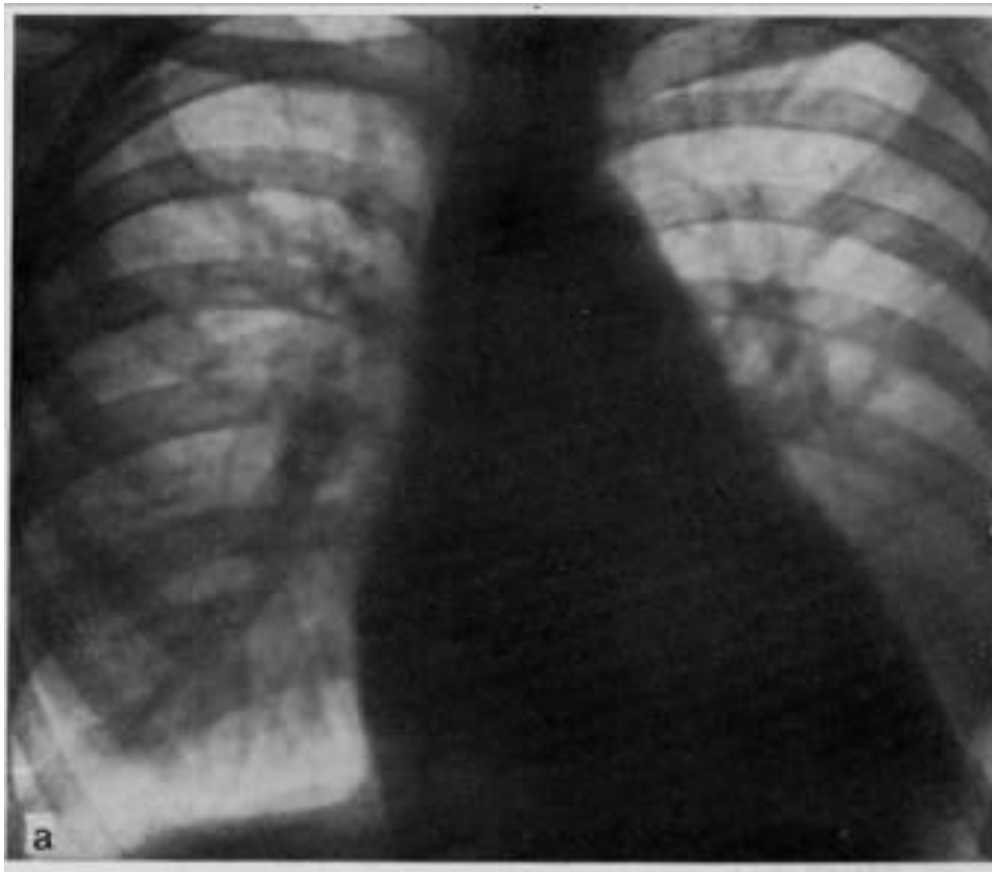
Patent ductus arteriosus (PDA) refers to continued patency of a normal structure in fetal circulation. The ductus arteriosus is derived from the left sixth aortic arch and is usually a left-sided structure, but may be right sided or bilateral. PDA occurs in 5% to 10% of congenital defects and is often present in premature infants. An increased incidence is also seen in cases of maternal rubella. A PDA is associated with a left-to-right shunt that is predominantly systolic in early infancy but becomes continuous as PVR decreases. Thus, in the newborn with a significant shunt, there is an active precordium and only a systolic murmur. In older children and adults, a continuous machinery murmur is present at the left upper sternal border. A PDA may close spontaneously before the age of 6 months.

Echocardiography demonstrates continuous flow from the aorta to the pulmonary artery by color Doppler. Direct visualization of the ductus by echocardiography is usually possible in children but difficult in adults. X-ray may help to receive indirect findings of PDA (Figure 38).

The aortic-to-pulmonary artery pressure gradient can be measured from the

continuous-wave Doppler tracings. The presence of other associated congenital defects should be a routine part of the exam. The diagnosis can also be made and/or confirmed at cardiac catheterization by the presence of an oxygen saturation step-up at the level of the pulmonary artery and demonstration of the ductus by aortography.

Figure 38: X-ray findings of PDA



Atrioventricular Septal Defects

Partial and complete atrioventricular septal defects (AVSDs) are seen in 2% to 3% of patients with congenital heart disease. Also known as AV canal defects or endocardial cushion defects, they are characterized by a common atrioventricular junction guarded by a common atrioventricular valve. There is absence of the atrioventricular septum that separates the RA from the LV. The aorta is unwedged from its usual position between the atrioventricular orifices, which results in a narrowing of the subaortic region and a longer outflow dimension of the interventricular septum. This gives a three-leaflet appearance to the mitral valve, often mistaken as a cleft in the anterior leaflet. On echocardiography, the mitral and tricuspid valves appear at the same level at the AV junction. Partial AVSDs may have

attachment of the bridging leaflets of the common AV valve to the ventricular septum, resulting in only interatrial shunting (the so-called ostium primum defect). Alternatively, the bridging leaflets may be attached to the atrial septum, resulting in only an interventricular shunt (inlet-type VSD). With a complete atrioventricular septal defect (complete AVSD), the common AV valve floats between the atrial and ventricular septum, allowing shunting at both atrial and ventricular levels. Patients with a complete AVSD may have a common valve with a single orifice or may have separate left and right orifices. When the common AV valve is equally committed to both ventricles, this is referred to as a balanced defect. In unbalanced forms, there is commitment of the common AV valve to one ventricle with resultant hypo-plasia of the other ventricle. Many other associated malformations may coexist, including left ventricular outflow obstruction, other congenital deformities of the AV valve, and association with other forms of congenital heart disease (e.g., tetralogy of Fallot, double-outlet right ventricle, etc.). There is a distorted arrangement of atrioventricular node (located in the posterior atrial wall) and the bundle of His (located under the inferior bridging leaflet), which makes these patients prone to conduction block.

AVSDs are particularly common in patients with Down syndrome (seen in 30% to 40% of Down patients with CHD), usually as the complete form of AVSD. Conversely, Down syndrome is present in 70% to 80% of patients with a complete AVSD. The risk of developing associated pulmonary vascular disease appears to be greater and more rapidly progressive in patients with Down syndrome. This is due, at least in part, to a tendency toward airway obstruction (due to macroglossia, a small hypopharynx, and poor pharyngeal muscle tone), abnormal capillary bed morphology in the lungs, and possible pulmonary hypoplasia.

The ECG in patients with a complete AVSD shows left-axis deviation due to an abnormal activation sequence of the ventricles (due to deficiency of intermediation radiation of left bundle branch). First-degree AV block is common, and right-bundle-branch block and right ventricular hypertrophy (RVH) are invariably present. Left ventricular hypertrophy (LVH) may be present as well. The CXR shows cardiomegaly and pulmonary plethora.

Echocardiography places a critical role in the diagnosis, including the anatomy

and function of the common AV valve, the location and degree of intracardiac shunts, the balance of the ventricles, and the presence of other associated conditions. Cardiac catheterization with angiography is often warranted to assess hemodynamic parameters and the magnitude of the intracardiac shunts. In patients with significant pulmonary hypertension, a lung biopsy is occasionally required to determine operability.

Surgical repair should be undertaken at the time of diagnosis if pulmonary vascular disease is not prohibitive. Surgical repair of complete AV septal defects is complex, requiring closure of the shunts and creation of two competent AV valves. In some cases, a pulmonary artery band is placed to prevent pulmonary hypertension if repair of the defect cannot be performed. When diagnosis is made in adolescence or adulthood, there is usually a partial AV septal defect or the patient has developed severe pulmonary vascular obstructive disease. Patients who present in adulthood with a partial AVSD are usually candidates for surgery. Device closure is not an option. Patients with a complete AVSD and severe pulmonary hypertension should be treated as having Eisenmenger physiology once the diagnosis is confirmed. The long-term outcome after surgical repair is good. All patients are at risk for endocarditis and require antibiotic prophylaxis. Despite a good prognosis after surgery, patients remain at risk for left-sided AV valve regurgitation and need long-term follow-up. Surgical series have indicated that as many as 10% to 12% of patients will need further surgery for left-sided AV valve regurgitation. Patients may also have a residual VSD, may develop subaortic or subpulmonary obstruction, or may develop progressive pulmonary vascular disease (especially with late closure of VSD). Patients are also at risk for development of complete heart block, sinus node dysfunction, and atrial arrhythmias. Sudden death has been reported, although the risk is largely unknown.

Aortopulmonary Window

The aortopulmonary window is a rare form of congenital heart disease, manifested by a communication between the ascending aorta and the pulmonary trunk above the level of the coronary arteries. An aortopulmonary window can occur as an isolated defect but is often associated with other anomalies. The defect is

usually very large, resulting in a large left-to-right shunt and a high likelihood of developing pulmonary hypertension. Thus, patients usually present in infancy with symptoms of heart failure or with cyanosis due to pulmonary hypertension with right-to-left shunting. The diagnosis is made by echocardiography demonstrating the defect and the associated shunting. Occasionally, defects may be small enough to be closed with catheter intervention, but surgical closure is required for the majority. Presentation in adulthood is nearly always associated with the Eisenmenger syndrome.

Partial Anomalous Pulmonary Venous Connection

Partial anomalous pulmonary venous connection is defined as one or more (but not all) pulmonary veins connecting to a systemic vein, the RA, or the coronary sinus. Examples include connection of the right upper lobe and right middle lobe veins to the SVC, right upper lobe and right middle lobe veins to the RA, right pulmonary veins to the IVC, right lower lobe vein to the IVC (scimitar syndrome), left upper or lower pulmonary veins to the coronary sinus, and left lower pulmonary veins to the RA or IVC. Partial anomalous pulmonary venous connection is relatively uncommon, accounting for less than 1% of all congenital defects. An ASD is usually present, and the clinical presentation is similar to that of an uncomplicated ASD. Partial anomalous pulmonary venous connection can be seen with any type of ASD but is most commonly associated with the sinus venosus type of ASD. Other associated defects may occur. The exam findings, ECG, and CXR findings in patients with partial anomalous pulmonary venous connection are similar to those of a secundum ASD. The CXR findings in the scimitar syndrome are addressed later.

The diagnosis can be made by echocardiography if care is taken to identify the pulmonary vein connections. TEE is usually required in adult patients to adequately define the pulmonary vein anatomy. Cardiac MRI is an excellent tool for the diagnosis of partial anomalous pulmonary venous connections.

Scimitar Syndrome

The scimitar syndrome refers to the presence of anomalous drainage of the right pulmonary veins to the IVC with a characteristic appearance on CXR resembling a scimitar or Turkish sword. There is usually some degree of hypoplasia

of the right lung and the right pulmonary artery, usually with an aberrant systemic artery from thoracic aorta supplying part of the right lung. Surgical correction removes the left-to-right shunt and may improve blood flow to the right lung. There is a risk of postoperative pulmonary venous obstruction.

Obstructive Lesions

Pulmonary Stenosis

Pulmonary stenosis (PS) is a common defect, occurring in 7% to 10% of patients with congenital heart disease. Obstruction may be subvalvular, valvar, or supra-valvular. Valvar stenosis is the most common (90%). The pulmonary valve morphology varies. The valve may be unicommissural with an eccentric orifice (extremely rare), bicuspid or trileaflet with commissural fusion, or dysplastic. Dysplastic valves have markedly thickened leaflets with disorganized myxomatous tissue but minimal commissural fusion. Bicuspid or trileaflet valves with commissural fusion are usually amenable to balloon dilation or surgical valvotomy, whereas dysplastic valves are less amenable to these procedures. Dysplastic valves are commonly associated with Noonan syndrome. PS is usually an isolated lesion. Associated cardiac and noncardiac malformations are more common when the valve is dysplastic. Chronic obstruction of the right ventricular outflow tract leads to RVH, which may be particularly prominent in the infundibular region, further contributing to RV outflow tract obstruction. Severe PS presenting in infancy is associated with severe RVH and a small right ventricular cavity size. Lesser degrees of PS are associated with RVH, but the RV cavity is usually well formed. The degree of stenosis is classified by peak systolic gradient, with trivial stenosis defined as a peak gradient less than 25 mm Hg, mild stenosis with a gradient of 25 to 49 mm Hg, moderate stenosis with a gradient of 50 to 79 mm Hg, and severe stenosis with a peak gradient above 80 mmHg.

Infants with critical PS present in neonatal period, usually with cyanosis due to right-to-left shunting across a PFO or ASD. Mortality is high in neonates with critical PS unless intervention is prompt. Lesser degrees of stenosis usually present later in childhood or in adulthood. Patients with trivial or mild stenosis with a peak gradient of less than 25 mm Hg have a good outcome. There is usually no significant

progression of disease, and therefore no treatment is warranted. Patients with more significant stenosis may present with exertional dyspnea, chest pain, fatigue, or syncope, occasionally with cyanosis.

The ECG reflects the degree of RVH (except in the neonatal period). The ECG is normal with mild degrees of obstruction and shows right-axis deviation and RVH with moderate to severe obstruction. Poststenotic dilation of the main pulmonary artery and the left pulmonary artery (due to a more parallel take-off of the left pulmonary artery) may be seen on CXR with all degrees of PS. Heart size is normal with mild to moderate obstruction, but right-sided enlargement is seen with severe stenosis. Echocardiography is the diagnostic method of choice and can demonstrate valvular and infundibular anatomy. Continuous-wave Doppler is used to quantitate the transvalvular gradient. A complete study includes an assessment of the integrity of atrial septum as well as assessment of RV size and function. In the Second Natural History Study of Congenital Heart Defects, patients with mild PS (peak gradient 25 to 49 mm Hg) had a 20% chance of requiring intervention at some point. Patients with moderate stenosis treated medically were at risk for progressive obstruction with symptoms warranting intervention. Most patients with a peak gradient greater than 50 mm Hg required intervention, with better outcomes demonstrated in those patients undergoing intervention than in those treated medically.

The earliest surgical interventions on the pulmonary valve were performed using a closed technique with blunt dilation of the right ventricular out-flow tract (Brock procedure). Currently, pulmonary valvotomy is performed using cardiopulmonary bypass. Transcatheter intervention with balloon valvuloplasty has now largely replaced operative intervention and has become the therapy of choice. Balloon valvuloplasty can be performed with a low rate of complications and outcomes similar to surgery with a similar reduction in gradient. An infundibular gradient may be present after successful pulmonary valvotomy but often regresses over 3 to 12 months. Long-term outcomes for both surgical and balloon valvotomy are excellent. Long-term complications of both procedures include pulmonary regurgitation and residual or recurrent RV outflow tract obstruction. Reintervention is required in some cases for recurrent RV outflow obstruction with symptoms or

significant arrhythmias. The presence of severe pulmonary regurgitation with decreasing exercise capacity, deteriorating RV function, or the development of significant arrhythmias is an indication for pulmonary valve replacement. Subpulmonary stenosis is usually seen in complex defects, such as tetralogy of Fallot. Isolated subpulmonary stenosis is rare.

Supravalvular obstruction with pulmonary arterial stenosis may be seen in rubella syndrome and Williams syndrome and in association with other complex congenital cardiac defects (e.g., tetralogy of Fallot). Pulmonary arterial stenosis may also occur as an isolated defect. Stenosis may occur in the main pulmonary artery, at the bifurcation of the pulmonary artery branches, and at the secondary or more distal branches. The obstruction may be focal or diffuse (often a manifestation of more widespread vasculopathy such as rubella, cutis laxa, or Ehlers-Danlos syndrome).

The clinical presentation is similar to that of valvar PS. Patients have a systolic ejection murmur, but there is no ejection click, and P2 is normal. The ECG and CXR findings are usually nonspecific. Echocardiography may demonstrate the presence of RV pressure overload and may demonstrate the site of stenosis, but the branch pulmonary arteries may be difficult to visualize by TTE. Doppler study of the main and branch pulmonary arteries is used to quantitate the severity of stenosis. CT or MRI scans offer excellent visualization of the main pulmonary artery trunk and the pulmonary artery branches. Angiography can also be used to demonstrate the obstruction, and the localized pressure gradient can be demonstrated at catheterization. Perfusion imaging helps in assessing perfusion imbalance. Although pulmonary artery stenosis may be managed surgically with pericardial or prosthetic patch repair to enhance stenotic vessels, stenting of pulmonary vessels is playing an increasing role.

Obstruction of the Left Ventricular Outflow Tract

Left ventricular outflow tract obstruction may occur at the level of the valve, below the valve, or in the ascending aorta. Valvar aortic stenosis (AS) is the most common cause of congenital LV outflow obstruction, and bicuspid valves are by far the most common type. The bicuspid aortic valve is usually not included in epidemiologic studies of congenital heart disease but is the most common type of

congenital cardiac defect, seen in 1% to 2% of the general population. A bicuspid aortic valve results from fusion of two commissures, resulting in two rather than three valve leaflets. There is a high incidence of bicuspid valves in a mouse model of nitric oxide synthase deficiency, suggesting a role of nitric oxide in the development of the normal trileaflet aortic valve. Bicuspid aortic valves may be familial, but most appear to be spontaneous mutations. Bicuspid valves and coarctation of the aorta are the most common defects found in patients with Turner syndrome (XO).

Considered a normal variant by some, a bicuspid aortic valve may function normally throughout life or may develop either stenosis or regurgitation. There are autopsy reports of normally functioning bicuspid valves in octogenarians. The abnormal opening of the valve leaflets is presumed to cause an abnormal flow profile across the valve, resulting in valve thickening, fibrosis, and calcification. This, in turn, may result in either progressive stenosis or regurgitation. Although it is usually an isolated abnormality, associated cardiac defects are seen in up to 20% of patients (including coarctation of the aorta, PDA, and VSD). Left-dominant coronary circulation is seen in 30% to 60% of cases. Patients with bicuspid aortic valves may have associated abnormalities within the media of the aorta, placing them at risk for aortic root dilation and dissection. The degree of aortic root abnormality may be out of proportion to the severity of the valvular dysfunction. Congenital AS presenting in infancy is unusual (occurs in 10% to 15% of patients with congenital AS) and may be associated with other lesions. The valve morphology in isolated valvar AS in the neonate may be bicuspid, unicuspid, or severely dysplastic. Neonates with severe AS typically present with severe decompensation, and prompt intervention is required. Children with less severe degrees of AS are usually asymptomatic, and the diagnosis is usually made based on the presence of a murmur. Bicuspid aortic valves are often seen in adults as an incidental finding.

The ECG may be normal or may demonstrate LVH. There is poor correlation between the degree of stenosis and the ECG findings. The CXR may demonstrate a normal heart size or cardiomegaly. Poststenotic dilation of the ascending aorta may be seen.

Echocardiography is the diagnostic tool of choice for the diagnosis of AS.

Patients with a bicuspid aortic valve typically have two unequal-size aortic cusps with an eccentric closure line. Valve anatomy can be determined, and the presence of associated regurgitation or stenosis can also be demonstrated and quantitated, with assessment of the transvalvular gradient, and calculation of valve area. LVH and LV function (both systolic and diastolic) should be assessed. Cardiac catheterization is usually reserved for patients in whom either surgical or catheter intervention is contemplated or for additional quantitation of the severity of valvular disease. Coronary angiography is usually performed in patients older than the age of 40 years. Visualization of the aortic root by echo, angiography, or MRI is an important part of the diagnostic evaluation. All patients with congenital AS need bacterial endocarditis prophylaxis. The indications for catheter or surgical intervention differ between the pediatric and adult populations. In children, there is a risk of sudden death in the absence of definable symptoms related to the aortic valve disease. For this reason, catheter or surgical intervention is recommended for those patients with severe stenosis as defined by a valve area of less than $0.5 \text{ cm}^2/\text{m}^2$ or a mean gradient of greater than 50 mm Hg. Exercise testing is also used, with the development of ST-segment depression or significant ventricular ectopy considered to be a reasonable indication for intervention. For mild stenosis (gradient <40 mm Hg), observation is recommended because the risk of sudden death is low. In the adult population, the indications for surgical intervention are the same as for those patients with acquired forms of AS, namely chest pain, congestive heart failure, and syncope. Unlike the pediatric population, sudden death occurs rarely in asymptomatic adult patients with AS. In symptomatic adults, survival is poor without surgical intervention, with 5-year survival rates ranging from 15% to 50%. Because of the associated aortic root abnormalities, the initial presentation of a patient with a bicuspid aortic valve may be in the setting of aortic dissection or rupture.

Echocardiography is a good technique for the diagnosis of coarctation, demonstrating the area of obstruction in the aorta and demonstrating disturbed flow by Doppler techniques. Continuous-wave Doppler with the expanded Bernoulli equation is needed to accurately assess the degree of obstruction. For patients with severe stenosis and extensive collaterals, the Doppler gradient may underestimate the

degree of obstruction due to decreased blood flow through the coarctation segment. MRI is excellent for demonstrating aortic anatomy and is particularly useful in the adult population in whom echocardiographic imaging of the aortic arch and descending thoracic aorta may be difficult.

Interruption of the Aortic Arch

Interruption of the aortic arch is defined as the absence of continuity between the transverse arch and the descending thoracic aorta. This uncommon defect produces symptoms in the neonatal period as the ductus arteriosus closes. There are rare cases of survival to adulthood. Interrupted aortic arch may be associated with DiGeorge syndrome and is nearly always associated with other defects (e.g., VSD, PDA, and complex defects). The diagnosis is made by echocardiography.

Other Obstructive Lesions

Shone Syndrome

Left ventricular inflow and outflow obstructive lesions frequently occur together. Shone syndrome was originally described as supralvalvular mitral membrane, parachute mitral valve, subaortic stenosis, and coarctation of the aorta. Currently, the term Shone syndrome is applied to patients with some or all of these features.

Congenital Mitral Stenosis

Congenital mitral stenosis is rare. When present, it often coexists with other left-sided stenotic lesions (i.e., LV outflow tract obstruction and coarctation of the aorta). The obstruction may be supralvalvular, at the annulus, at the leaflet margins, or at the level of the chordae and papillary muscle. Typically, congenital mitral stenosis has rolled leaflet edges, short, thick chordae, and hypoplastic papillary muscles. If the papillary muscles fuse to form a single papillary muscle, the term parachute mitral valve is applied. The age at presentation depends on the severity of obstruction and the presence of other associated lesions. Congenital mitral stenosis is usually diagnosed in childhood, rarely in adulthood. Patients typically present with symptoms of heart failure and signs of pulmonary hypertension. Echocardiography is diagnostic. Treatment consists of medical management, with surgery for symptoms refractory to medical management. Balloon valvotomy may be considered, but results are less

satisfactory than for rheumatic mitral stenosis. There are limited data on long-term surgical outcomes.

Cor Triatriatum

Cor triatriatum is a rare congenital defect in which a membrane divides the LA into a superior pulmonary venous chamber and an inferior chamber including the LA appendage and inflow portion of the LA. This occurs due to embryologic failure of the common pulmonary vein to become incorporated into the LA. An associated ASD is common, either above or below the membrane, but the atrial septum may be intact. From 70% to 80% of patients have other associated defects. The clinical presentation depends on the severity of obstruction (size of the orifice) and the presence of associated defects.

Patients may present in infancy or adulthood. Patients presenting in infancy have dyspnea, cyanosis, exercise intolerance, and failure to thrive. Patients who present in adulthood may have atrial arrhythmias, dyspnea, syncope, chest pain, or symptoms caused by pulmonary hypertension. The diagnosis may also be made incidentally during echocardiography. TTE or TEE demonstrates a nonmobile membrane in the left atrium. Echocardiography is also used to define the location, size, and number of membrane openings, the transmembrane gradient, and the presence of associated defects including anomalies of pulmonary venous connection. In some cases, it may be necessary to volume load the patient in order to assess the significance of the transmembrane gradient. Surgical excision is therapy of choice. There is a high mortality in symptomatic patients who do not undergo intervention. Reoperation is rarely necessary.

Pulmonary Vein Stenosis

Congenital pulmonary vein stenosis and atresia is uncommon, usually consisting of diffuse hypoplasia of the pulmonary veins. Surgical results are disappointing, with recurrence of stenosis and progressive pulmonary hypertension commonly seen after surgery. Transcatheter approaches with balloon dilation have also been disappointing. There is some preliminary data suggesting that cutting balloon technology may be helpful.

Vascular Rings

Vessels encircling the trachea and the esophagus cause vascular rings. In contrast, vascular slings partially encircle these structures. Compression of the trachea and esophagus may cause dysphagia, wheezing, and respiratory distress, or these vascular abnormalities may be incidental findings. Imaging by echocardiography or magnetic resonance imaging is usually diagnostic.

Complex Lesions

Transposition Complexes

In transposition complexes, the great arteries arise from the wrong ventricles (ventriculoarterial discordance), with the aorta arising from the RV and the pulmonary artery from the LV. The aorta is usually anterior to the pulmonary artery, and there are many variations in the spatial relationship of the two great vessels. The terms D and L refer to the cardiac loop or position of the ventricles.

Complete Transposition

In complete transposition of the great arteries (also known as D-transposition), there is atrioventricular concordance (the RA connected to the RV and the LA to the LV) but ventriculoarterial discordance (the RV connected to the aorta and the LV to the pulmonary artery). This results in two parallel circulations. Complete transposition is the second-most-common cyanotic lesion overall and the most common cyanotic lesion presenting in neonates. Two thirds of patients are male.

Most cases are not associated with a specific gene defect. There is an increased incidence in infants of diabetic mothers, leading to speculation that complete transposition may be related to a maternal intrauterine hormone imbalance. Associated defects are common. From 60% to 70% of patients with complete transposition have an intact ventricular septum, whereas 30% to 40% have a moderate to large VSD. Other abnormalities may be present, including LV outflow tract obstruction (subpulmonary obstruction), which is seen in 25% of cases, and coarctation of the aorta, which is seen in 5%.

With complete transposition and intact ventricular septum, there is complete separation of the pulmonary and systemic circulations, and the only intracardiac mixing occurs through the foramen ovale and the ductus arteriosus. Because the

foramen ovale allows only limited interatrial shunting, the infant is dependent on shunting through the ductus arteriosus. These infants are severely cyanotic within hours to days after birth. Without intervention, mortality is 90% in the first year of life. Treatment involves prostaglandin E1 to maintain patency of ductus and balloon atrial septostomy to improve oxygenation by increasing intracardiac mixing. Patients with complete transposition and a VSD tend to have less cyanosis and be less critically ill in the neonatal period.

Congenitally Corrected Transposition

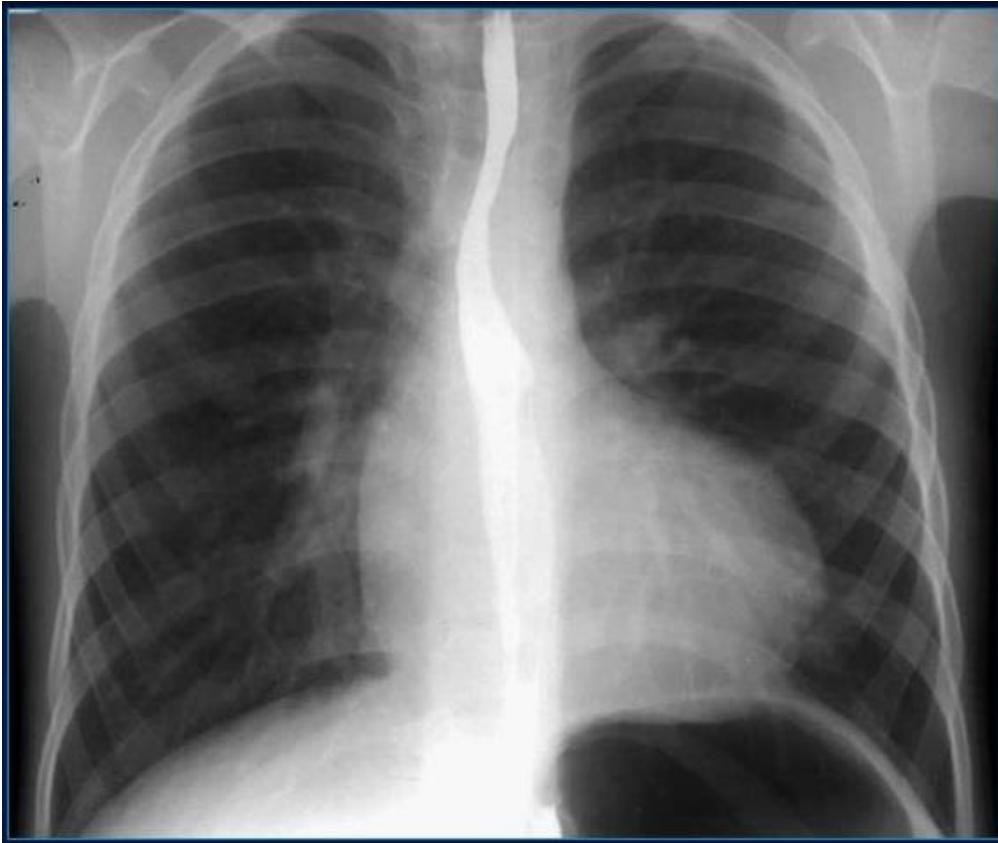
Congenitally corrected transposition is characterized by atrioventricular and ventriculoarterial discordance, resulting in systemic venous return to the RA, LV, and pulmonary artery, and pulmonary venous return to the LA, RV, and aorta. Thus, the tricuspid valve and the RV are in the systemic circulation. The aorta is positioned anterior and leftward of the pulmonary artery. Also known as L-transposition or ventricular inversion, congenitally corrected transposition is uncommon, occurring in less than 1% of patients. Associated defects are common, with VSD, pulmonary outflow tract obstruction, and morphologic abnormalities of the tricuspid valve seen most commonly. An Ebstein-type malformation of the tricuspid valve may be seen, and tricuspid regurgitation (systemic AV valve regurgitation) is likely to progress with time. Other defects may occur, including ASD, PDA, double-outlet right ventricle, and subaortic stenosis. The AV node and bundle of His are abnormally located in patients with congenitally corrected transposition, placing patients at risk for conduction system abnormalities. Patients are particularly prone to develop spontaneous heart block (occurs in 2% to 4% of patients per year) or complete heart block with surgery. Left-sided accessory bypass tracts with preexcitation and AV reentrant tachycardia are seen in 2% to 4% of cases. Dextrocardia is present in 20%. The diagnosis may be made by echocardiography, angiography, and cardiac MRI.

Tetralogy of Fallot

Tetralogy of Fallot is the most common cyanotic malformation, accounting for 10% of all congenital heart disease. There is a slight male preponderance. Fifteen percent of patients with tetralogy of Fallot have a deletion on chromosome 22q11. Tetralogy of Fallot is characterized by malalignment of the infundibular outlet

septum, which results in a VSD, obstruction of the right ventricular outflow tract, and an aorta that overrides the VSD. Right ventricular hypertrophy, the fourth component, occurs as a consequence of both RV outflow obstruction and the large nonrestrictive VSD (Figure 39).

Figure 39: X-ray findings in tetralogy of Fallot



Multiple variations of RV outflow obstruction can be seen, including infundibular stenosis, hypoplastic pulmonary valve annulus, bicuspid pulmonary valve, and varying degrees of hypoplasia of the main pulmonary trunk and its branches. The branch pulmonary arteries may be confluent or nonconfluent, with origin of one vessel from the ductus or from the aorta. Alternatively, one branch pulmonary artery may be absent. Extreme variants of tetralogy of Fallot may be seen with an absent pulmonary valve (seen in DiGeorge syndrome and velocardiofacial syndrome) or with pulmonary atresia. Coronary anomalies are present in 3% of cases. The most significant of these is origin of the left coronary artery from the right coronary artery, with the left coronary artery crossing the right ventricular outflow tract (important surgical implications). From 25% to 30% of cases have a right-sided aortic arch. Multiple VSDs are seen in 5% to 7% of cases. An ASD or PFO may be present as well (pentalogy of Fallot).

Most patients present with cyanosis in infancy. Cyanosis occurs due to the right-to-left shunt across the nonrestrictive VSD and the obstruction to pulmonary blood flow. The severity of the RV outflow tract obstruction determines the severity

of cyanosis. With mild degrees of RV outflow tract obstruction, patients usually have minimal cyanosis (pink tetralogy) and may present in adulthood. In most cases, survival to adolescence and adulthood is uncommon without treatment. Only 10% of patients with unoperated tetralogy of Fallot survive to 10 years of age.

Pulmonary Atresia with Intact Ventricular Septum

Pulmonary atresia with intact ventricular septum is another rare congenital defect. There is either an imperforate pulmonary valve (80%) or muscular obliteration of the RV infundibulum with no pulmonary valve. There are varying degrees of hypoplasia of the tricuspid valve and the RV cavity. Pulmonary blood flow is provided through the ductus (or, less commonly, through aortopulmonary collaterals) with an obligatory right-to-left shunt at the atrial level. The severity of the defect ranges. Some patients have a nearly normal RV cavity with mild infundibular narrowing that is amendable to pulmonary valvotomy or catheter perforation of valve. Other patients have more significant RV hypoplasia with tricuspid stenosis. In other patients, the tricuspid valve is dysplastic or absent, with severe tricuspid regurgitation and a thinned, underdeveloped RV. In patients with severe RV hypoplasia, the high-pressure RV is decompressed through a dilated coronary circulation, the coronary sinusoids. Echocardiography is critical in the initial diagnosis, but cardiac catheterization is usually required to define the coronary circulation. Surgical options are complicated, and long-term survival is poor, with only 30% to 35% survival at 15 to 20 years of age. There are preliminary reports of intervention in the fetus (perforation of pulmonary valve) to permit normal growth of RV and improve long-term outcome.

Double-Chambered Right Ventricle

Double-chambered RV is an uncommon defect. The RV is divided or septated by muscular or fibrous structures into a high-pressure proximal chamber and a lower-pressure distal chamber (397). The RV outflow obstruction appears to be an acquired lesion, but probably results from a congenitally abnormal substrate. A double-chambered RV is often associated with a perimembranous VSD (seen in >75% of cases). A double-chambered RV may also be seen with other abnormalities of the RV outflow tract, including valvar PS, tetralogy of Fallot, and double-outlet right

ventricle. The degree of RV outflow obstruction ranges from trivial to severe. The clinical presentation depends on the size of the VSD and the degree of RV outflow obstruction, with a clinical appearance similar to that of tetralogy of Fallot. In some cases, the VSD may close spontaneously, and these patients present similarly to patients with isolated PS.

Tricuspid Atresia

Tricuspid atresia is defined as the absence of a right-sided atrioventricular connection, usually associated with underdevelopment of the RV (absence of inlet portion). An ASD is invariably present for the obligatory right-to-left shunt. If the interatrial communication is restrictive, patients have severe cyanosis in infancy. A nonrestrictive ASD may become restrictive over time. The great arteries may be normally related (70%) or transposed (30%). With normally related great arteries, the pulmonary artery arises from the RV and there is usually valvular or subvalvular PS. With transposed great arteries, the aorta arises from the RV and there may be associated PS, pulmonary atresia, and subaortic obstruction (due to a small VSD restricting blood flow into the RV).

Tricuspid atresia is an uncommon lesion (seen in 1% to 3% of all congenital defects) and is usually sporadic, although some familial cases have been described. The diagnosis is suspected in a cyanotic infant with decreased pulmonary blood flow on CXR. Echocardiography is diagnostic. Catheterization may be required to define hemodynamics before surgical intervention.

Total Anomalous Pulmonary Venous Connection

Total anomalous pulmonary venous connection is defined as connection of all of the pulmonary veins to one or more of the systemic veins, draining to the RA or coronary sinus. There is no direct communication of the pulmonary veins to the LA. Pulmonary venous drainage may return to the heart above the level of the diaphragm (supracardiac type) or below the diaphragm (infracardiac type), or it may occur in a mixed pattern. An ASD or PFO is necessary for survival, allowing blood to enter the LA and LV. There may be associated obstruction of the common pulmonary venous channel, which is more commonly seen with the infracardiac types. Patients with obstructed forms of total anomalous pulmonary venous connection present in the

neonatal period with progressive hypoxemia, marked pulmonary edema, and a small heart on chest x-ray. Patients with unobstructed total anomalous pulmonary venous connection usually present in infancy with congestive heart failure and mild hypoxemia. Less commonly, they may present later in childhood or adolescence, rarely in adulthood.

The diagnosis is made by echocardiography. Cardiac catheterization with angiography is usually not required unless pulmonary venous drainage patterns are complex. MRI is an excellent tool for defining the pulmonary venous connections. Corrective surgery to redirect the pulmonary venous return to the LA and close the associated ASD is necessary for all patients with this condition (427). For severely ill infants with the obstructed form, medical therapy with digoxin, diuretics, and mechanical ventilation may help to stabilize the patient until corrective surgical repair can be accomplished. The development of postoperative pulmonary venous obstruction is uncommon but carries a poor prognosis.

Ebstein's Anomaly

Ebstein's anomaly is an uncommon defect (<1.0% of all congenital defects), and is characterized by varying degrees of dysplasia and apical displacement of the septal and mural (posterior) leaflets of the tricuspid valve. The anterior leaflet is often malformed and excessively large and may be adherent to the RV free wall. Tricuspid leaflet displacement results in atrialization of the inlet portion of the RV. The true RV or functional RV (apical and outflow segments) may be quite small. The degree of leaflet displacement varies, resulting in wide differences in the clinical presentation. Patients have varying degrees of tricuspid regurgitation, whereas tricuspid stenosis is unusual. There is an increased incidence in Ebstein's malformation in the offspring of mothers treated with lithium carbonate in the first trimester of pregnancy.

Ebstein's malformation may occur as an isolated defect or in association with other complex congenital heart defects (e.g., tetralogy of Fallot, AV septal defect, etc.). Ebstein's anomaly is commonly seen with congenitally corrected transposition. The most common associated congenital defect is an ostium secundum ASD or a PFO, which is present in greater than 50% of patients.

Double-Outlet Right Ventricle

Double-outlet right ventricle (DORV) is an uncommon defect in which more than half of each great artery is connected to the morphologic RV. DORV is nearly always associated with a large, nonrestrictive VSD, which provides the only outlet from the LV. There is a wide variety of spatial orientations of the great arteries, as well as variation in the location of the VSD. The VSD may be subaortic, subpulmonary, doubly committed (beneath both great arteries), or noncommitted. Patients may have pulmonary or aortic outflow obstruction, abnormalities of the atrioventricular junction, and ventricular hypoplasia.

There are four major types of DORV, each of which requires a different type of surgical repair. The most common form is the subaortic VSD without associated PS. In this case, oxygenated blood from the LV is directed through the VSD into the aorta. These patients present with mild or no cyano-sis. Their clinical presentation resembles that of a large VSD, with patients at risk for congestive heart failure and pulmonary hypertension. Surgical treatment involves a primary repair, tunneling left ventricular blood through the VSD to the aorta. Surgery is performed early in infancy to prevent the development of pulmonary hypertension. Patients with a subaortic VSD may have valvar or subvalvar PS (so-called Fallot type), causing desaturated blood to enter the aorta.

Single Ventricle

Single ventricle is an uncommon defect in which both atria are connected to one ventricle. There are usually two atrioventricular valves (double inlet), although rarely there may be a common atrioventricular valve (common inlet). The morphology of the single ventricle is usually that of an LV with a rudimentary RV (outlet chamber). On occasion, the single ventricle may have the morphology of an RV, often associated with a double outlet (both aorta and pulmonary artery arising from the RV). In some cases, the ventricular morphology is indeterminate. The great arteries are transposed in the majority of cases, with the aorta arising anteriorly from the rudimentary outlet chamber. The connection between the single ventricle and the outlet chamber (the bulboventricular foramen) may become obstructed, causing decreased systemic blood flow and increased pulmonary blood flow.

There is complete mixing of blood in the common ventricle, and the degree of

cyanosis is determined by the amount of pulmonary blood flow. Infants without PS have markedly increased pulmonary blood flow with symptoms of heart failure. These patients are at risk for the development of pulmonary vascular obstructive disease and have a high mortality in infancy. Infants may have valvar or subvalvar PS, which protects the pulmonary circulation by limiting pulmonary blood flow but results in more severe cyanosis.

Common Arterial Trunk

Common arterial trunk or persistent truncus arteriosus is an uncommon defect, and is characterized by a single great vessel arising from the ventricular mass that gives rise to the coronary arteries, at least one pulmonary artery, and the brachiocephalic arteries. A VSD is invariably present, directly below the truncus. The pulmonary arteries may arise from a common pulmonary trunk off the ascending portion of the arterial trunk or may have separate origins of the branch pulmonary arteries from either the ascending portion of the truncus, the descending aorta, the ductus arteriosus, or an aortopulmonary collateral. The truncal valve may be bicuspid, tricuspid, or quadricuspid and may be stenotic, regurgitant, or both. The coronary artery origins have a variety of abnormalities. Some forms are associated with other severe anomalies of the aorta, including coarctation, aortic arch atresia, and aortic interruption.

Miscellaneous Defects

Congenital Anomalies of the Coronary Arteries

Congenital anomalies of the coronary arteries may occur in isolation or in association with other congenital anomalies. Multiple variations exist. A rare but potentially lethal condition is the anomalous origin of the left coronary artery from the pulmonary artery. As pulmonary pressures fall in newborns with this condition, myocardial perfusion becomes dependent on collaterals from the right coronary circulation. These infants may present with ischemic symptoms or symptoms of heart failure from an ischemic cardiomyopathy. They may present in the neonatal period or later in infancy or childhood. This coronary anomaly is rarely seen in adults. In children, the diagnosis of coronary anomalies may often be made by echocardiography with color flow Doppler. Other patients may require

catheterization with aortography and angiography. The treatment is surgical, with reimplantation of the anomalous coronary or aortocoronary bypass. Postoperatively, patients may have persistent problems with abnormal myocardial perfusion.

Congenital Pericardial Defects

Congenital pericardial defects may be partial or complete. Partial absence of the left side of the pericardium may cause chest pain. An unusual cardiac silhouette may be seen on CXR due to herniation of the left atrial appendage or the ventricles through the defect. Herniation of the right lung through a partial right-sided defect may result in obstruction of the SVC. Alternatively, right heart structures may herniate through right-sided defects.

Sinus of Valsalva Aneurysms

Sinus of Valsalva aneurysms are defined as enlargement of one of the aortic sinuses between the valve annulus and sinotubular ridge. Absence of the elastic lamellae results in focal weakening of the aortic wall. This leads to aneurysmal dilation of the weakened portion and may ultimately lead to rupture. Sinus of Valsalva aneurysms are rare, and are seen in 0.09% of the general population at autopsy. They are four times more common in male individuals. Aneurysms occur in the right coronary sinus in 65% to 85% of cases, in the noncoronary sinus in 10% to 30%, and in the left coronary sinus in less than 5%. Sinus of Valsalva aneurysms may be associated with VSD, AR, bicuspid aortic valve, or connective tissue disorders such as Marfan syndrome or Ehlers-Danlos syndrome. The diagnosis can be made by echocardiography demonstrating the aneurysm and color flow mapping to demonstrate flow in ruptured aneurysms. Patients are usually asymptomatic until the aneurysm ruptures, which usually occurs in the third and fourth decades. A sinus of Valsalva aneurysm may cause local obstructive symptoms (compression of the right ventricular outflow tract or the coronary ostium).

Classically, rupture of a sinus of Valsalva aneurysm occurs with exertion or after trauma. The usual site of rupture is into the RV (in 90% of cases). Patients typically present with chest pain, cough, and breathlessness. Over time, they may develop LV volume overload and symptoms of congestive heart failure and may present late. Patients often have a continuous/machinery murmur, but this is not

invariably present. Without surgical intervention, there is usually progressive deterioration with LV failure. Surgical repair is recommended for ruptured aneurysms or symptomatic aneurysms with compression, arrhythmias, or evidence of infection. Unruptured aneurysms without symptoms do not warrant surgical intervention.

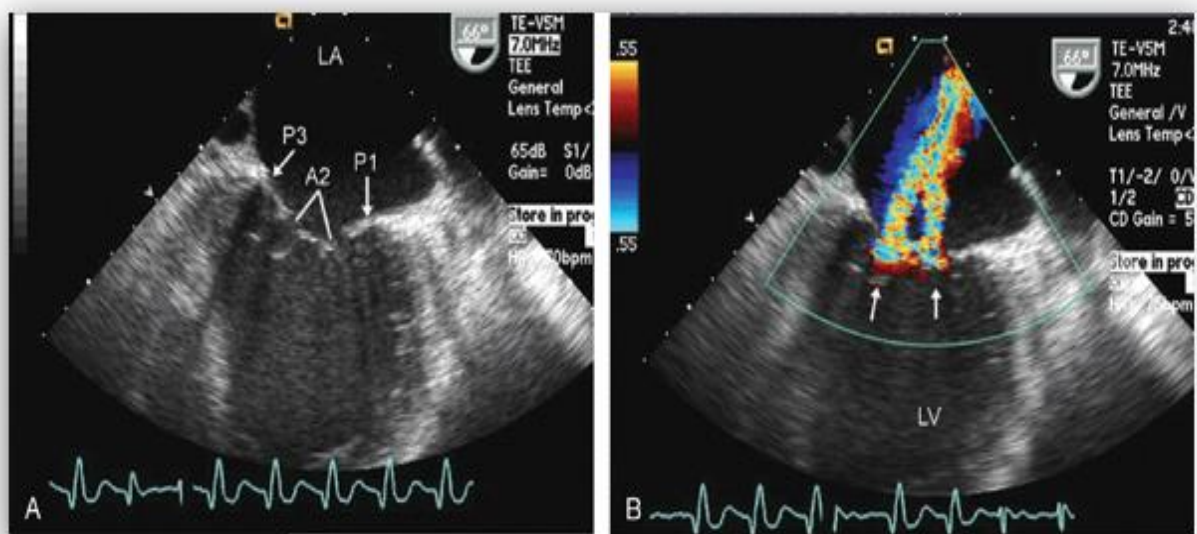
1.2. Acquired heart disease

Mitral valve regurgitation

The pathophysiologic consequences of acute severe mitral regurgitation (MR) such as that observed in patients following rupture of a papillary muscle differ from those of chronic MR due to rheumatic fever or endocardites.

With acute MR, a sudden volume overload is imposed on the nondilated, nonhypertrophied left ventricle and left atrium causing a sudden increase in left atrial pressure. Preload is increased, whereas afterload decreases as a result of the newly developed low-pressure runoff to the left atrium during systole. Overall LV pump function declines in acute MR. The clinical impact of acute MR is largely determined by the compliance of the left atrium. Diagnosis is based on echocardiography (Figure 40). Therefore, transesophageal and transthoracic echocardiography, as well as right heart catheterization (measurement of right-sided and capillary wedge pressures, as well as cardiac index) can be useful for the diagnosis. X-ray findings associated with LV dilation.

Figure 40: Echocardiography findings of acute mitral regurgitation

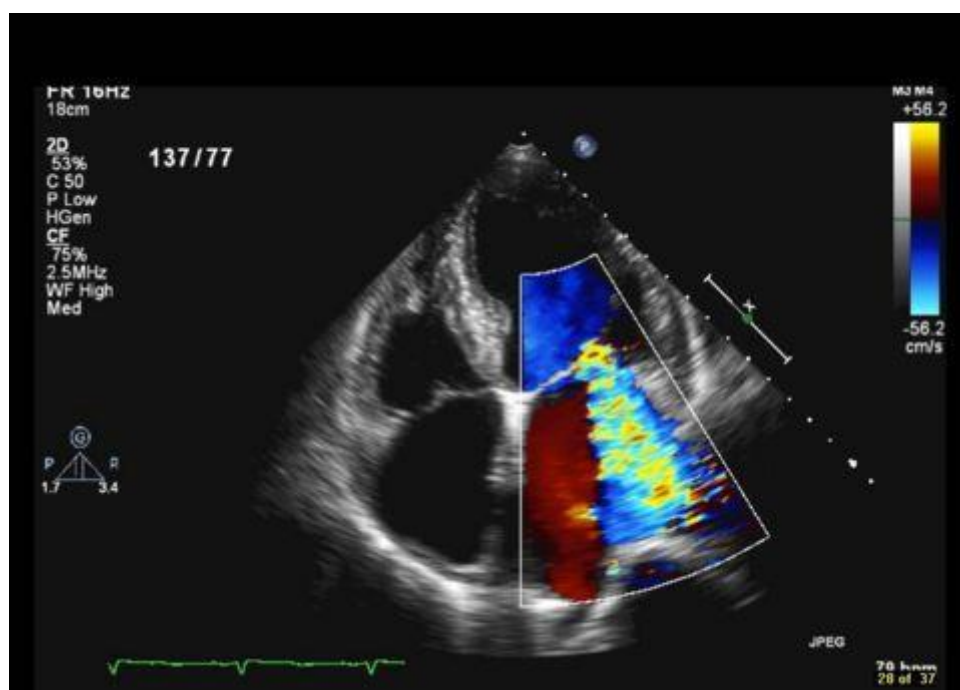


The vast majority of patients present with chronic MR at the time of diagnosis with

LV and left atrial adaptation to volume overload , the main causes of which are inflammatory and degenerative diseases. MR causes LV and left atrial volume overload. The degree of volume overload depends on the regurgitant volume. Initially, as the severity of MR increases there is progressive enlargement of the left atrium and left ventricle to compensate for the regurgitant volume. LV dilatation occurs as a result of remodeling of the extracellular matrix with rearrangement of myocardial fibers, in association with the addition of new sarcomeres in series and the development of eccentric LV hypertrophy. In patients with severe, chronic MR, the left atrium is markedly dilated and atrial compliance is increased. There is fibrosis of the atrial wall, left atrial pressure can be normal or only slightly elevated.

Echocardiography is the main diagnostic tool in patients with MR (Figure 41), while X-ray may produce signs of LV dilation at late stage (Figure 42). On the X-ray there is the signs regarding both LV and LA dilation. The complete mitral valve apparatus must be interrogated by two-dimensional echo and Doppler. Transesophageal echocardiography offers a better definition of the anatomy, and is indicated in cases with suboptimal transthoracic windows or unclear etiology, mechanism, or severity of the MR

Figure 41: Ech-CG findings in chronic mitral regurgitation



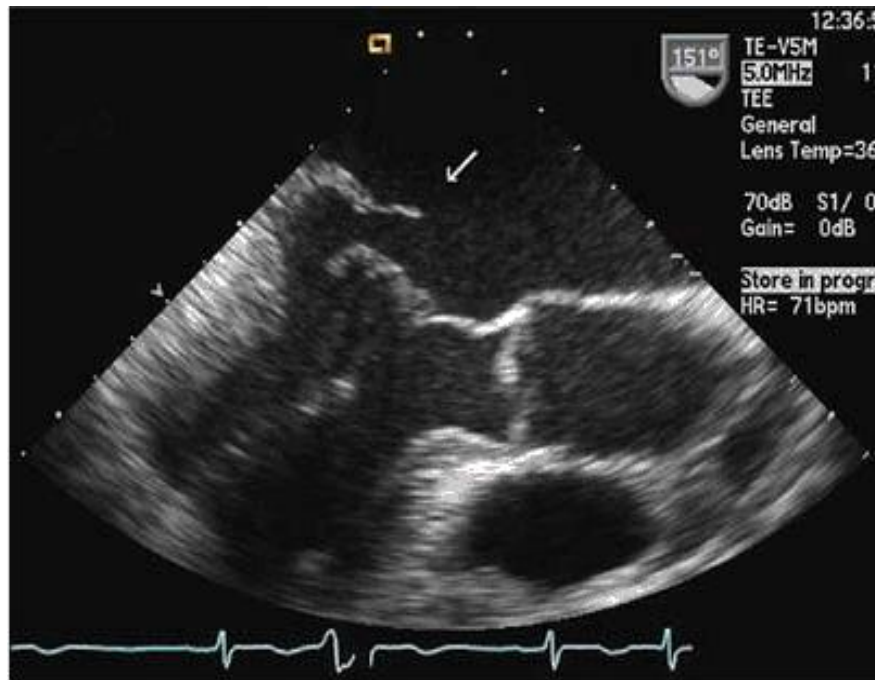
Mitral valve prolapse is a common and frequent findings associated with chronic MR in children and adolescents.

Figure 42: X-ray findings in chronic mitral regurgitation



Mitral valve prolapse has been associated with a number of different conditions, including Marfan syndrome, Ehlers-Danlos syndrome, acute rheumatic carditis, and a variety of congenital cardiac anomalies. A number of these entities are the result of genetic defects in connective tissue structure that produce, among other anatomic abnormalities, mitral valve prolapse. Although most cases of degenerative mitral valve disease are sporadic, a familial basis for the condition has been recognized. This form of mitral valve prolapse has an autosomal dominant mode of inheritance with variable penetrance and is influenced by age and gender. There is marked heterogeneity of clinical presentation. The main diagnostic tool with high diagnostic value is EchoCG (Figure 43), which allow determining abnormal moving of mitral leaflets and MR with different stages.

Figure 43: The Eco-CG findings in patients with mitral valve prolapse

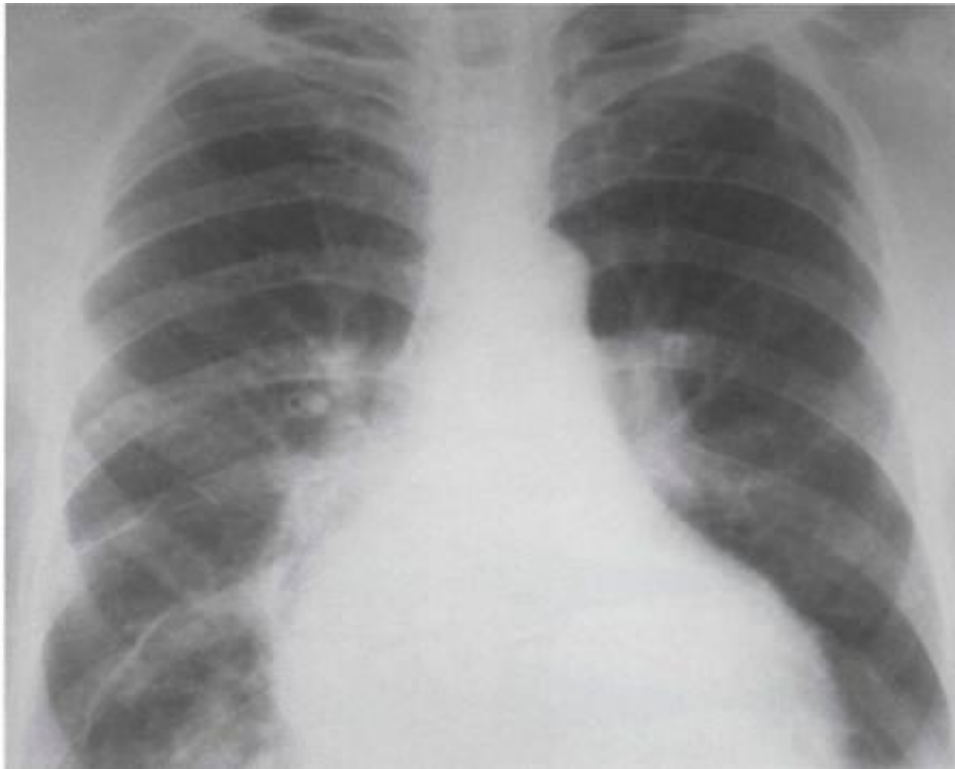


Severe cases associated with advance chronic heart failure might be determoned with echocardiogramm anmd X-ray on which increase both LV and RV dimensions are detected (Figure 44 and 45).

Figure 44: Severe MV regurgitation in patients with severe congestive heart failure



Figure 45: X-ray findings in patients with severe chronic MR and congestive heart failure

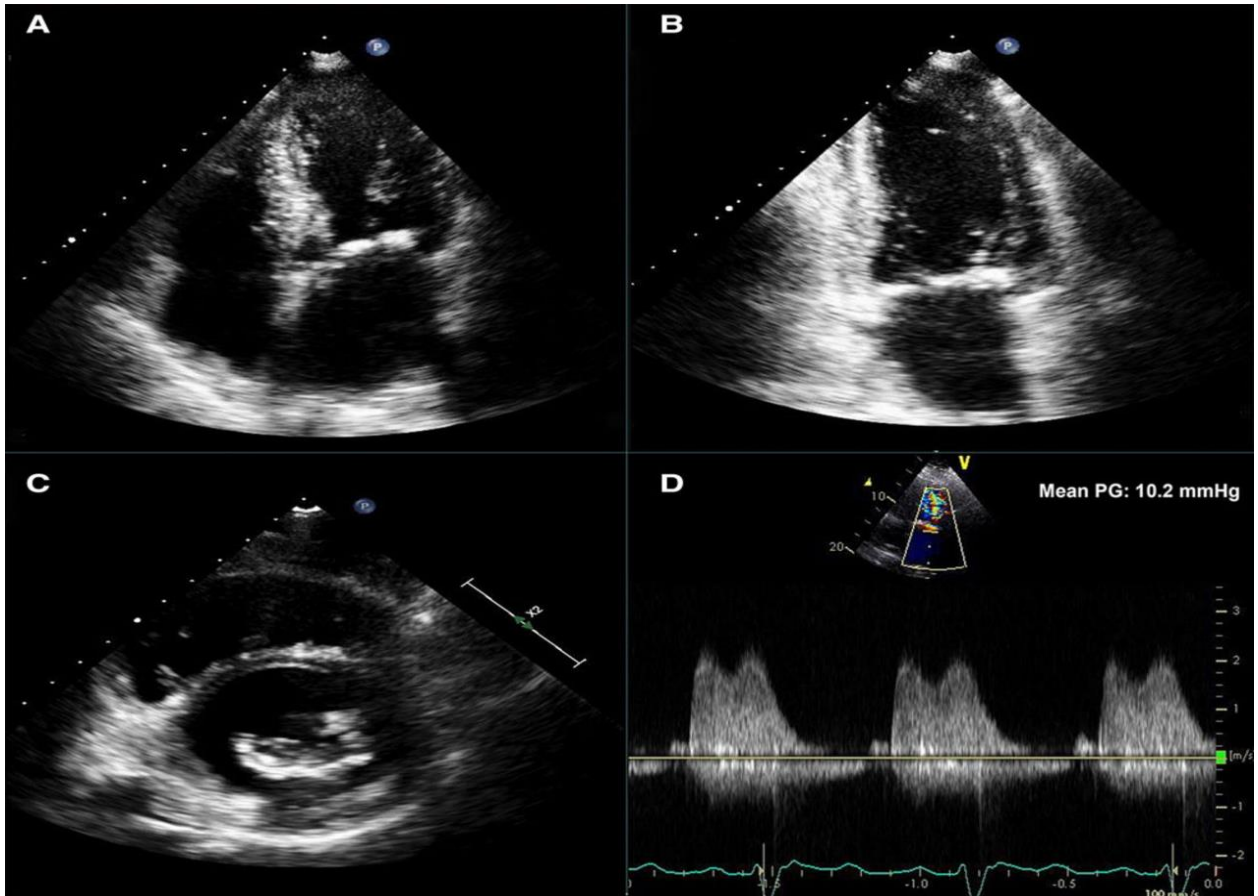


Acquired mitral stenosis

Rheumatic cardiac disease is an immunologic phenomenon that may affect any of the heart valves and the myocardium and is by far the most common cause of mitral stenosis. Pathologic features of rheumatic mitral valve disease include thickening of the leaflets with fusion of the edges at the commissures. The initial valvular pathologic lesion in acute rheumatic fever consists of inflammation manifesting as a series of translucent nodules along the line of closure of the mitral valve. Rarely, mitral stenosis is the result of entities other than rheumatic heart disease.

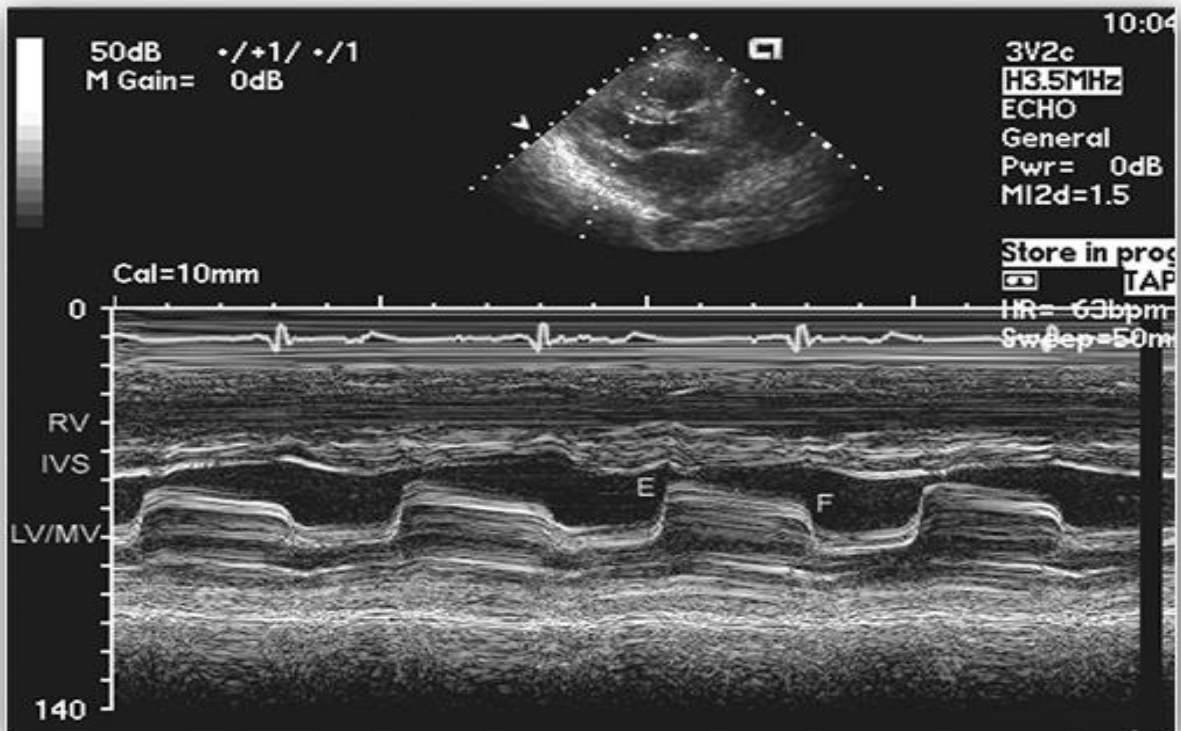
The progression of mitral stenosis is generally slow. Recent serial hemodynamic and Doppler echocardiographic studies have demonstrated annual mitral valve area loss ranging from 0.09 to 0.32 cm², deformation of mitral leaflets and calcification mitral root. The rate of progression of mitral valve narrowing is variable among individuals, and difficult to predict based on initial valve area or gradients (Figure 46). Complications of rheumatic mitral disease are attributable to the abnormal hemodynamic state produced by severe mitral stenosis

Figure 46: Echocardiogram in patients with rheumatic mitral stenosis.



M-mode echocardiogram represents frequently specific type of moving MV leaflets like letter ‘TP’, which is most known early sign of the disease (Figure 47)

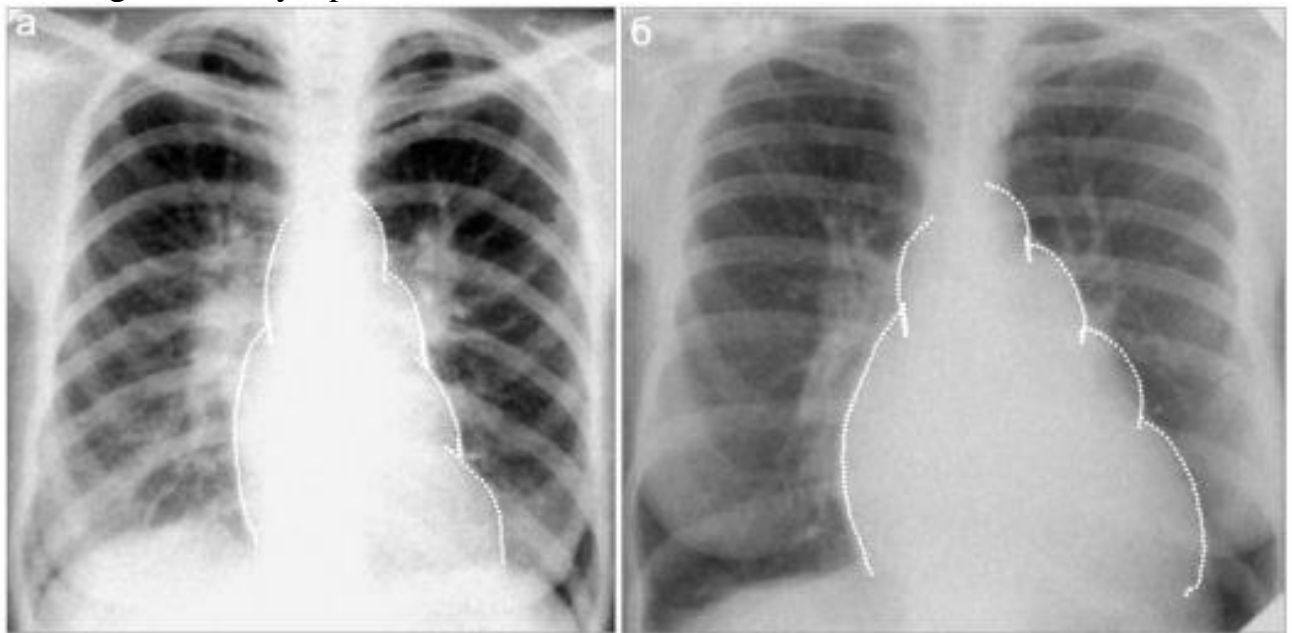
Figure 47: Rheumatic mitral stenosis. M-mode echocardiogram



X-ray examination reveals increase of both LA and RV dimensions that might interpret as

progression of chronic heart failure due to mitral valve stenosis gradient (Figure 48).

Figure 48: X-ray in patients with rheumatic mitral stenosis



Acquired aortic stenosis

Aortic stenosis is the narrowing of the exit of the left ventricle of the heart (where the aorta begins), such that problems result. It may occur at the aortic valve as well as above and below this level. It typically gets worse over time. Among symptomatic patients with medically treated moderate-to-severe aortic stenosis, mortality from the onset of symptoms is approximately 25% at 1 year and 50% at 2 years. Symptoms of aortic stenosis usually develop gradually after an asymptomatic latent period of 10-20 years.

The main causes are senile calcific valve, bicuspid form of aortic valve, rheumatic processes and congenital varieties. The most common cause of adult-acquired aortic stenosis is a chronic inflammatory and fibrotic process of the aortic valve similar to arterial atherosclerosis. The progressive fibrosis and calcification can occur on a bileaflet or a trileaflet valve, it just occurs earlier in life in the bicuspid valve. The rheumatic aortic stenosis occurs rarely today.

The reduction in aortic orifice area from its normal 3.0 to 4.0 cm² to approximately 1.5 cm² results in only a small gradient. After that degree of stenosis has developed, small additional reductions in the orifice area lead to progressively more dramatic increases in gradient. The average increase in gradient is 7 to 10 mm Hg per year but with a large and unpredictable individual variation, as much as 25

mm Hg in 1 year in occasional patients. A rapid rate of progression of stenosis, as reflected by an increase in aortic-jet maximum velocity of more than 0.3 m/second in the course of a year, occurs more often in patients who have clinical cardiac events.

Diagnosis is based on specific findings after Echoardiography providing (Figure 49) and X-ray examination (Figure 50).

Figure 49: Aortic stenosis: B-mode echocardiogramm

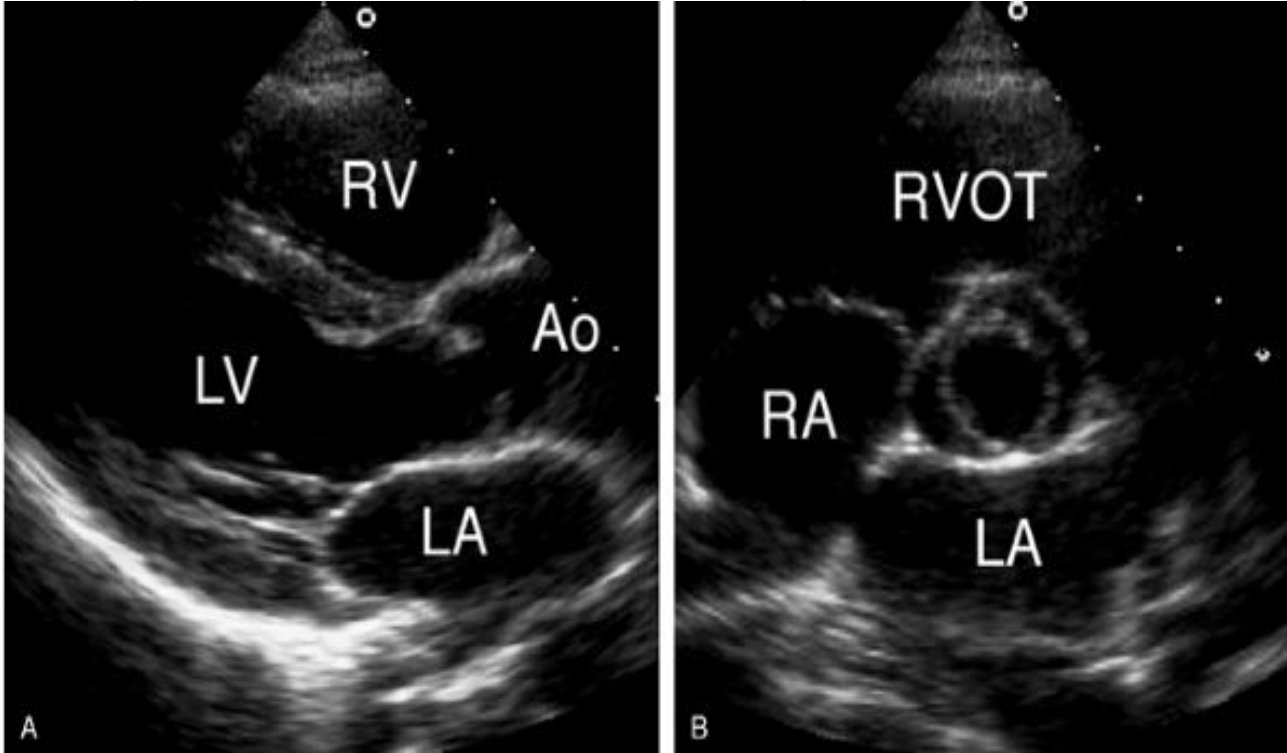
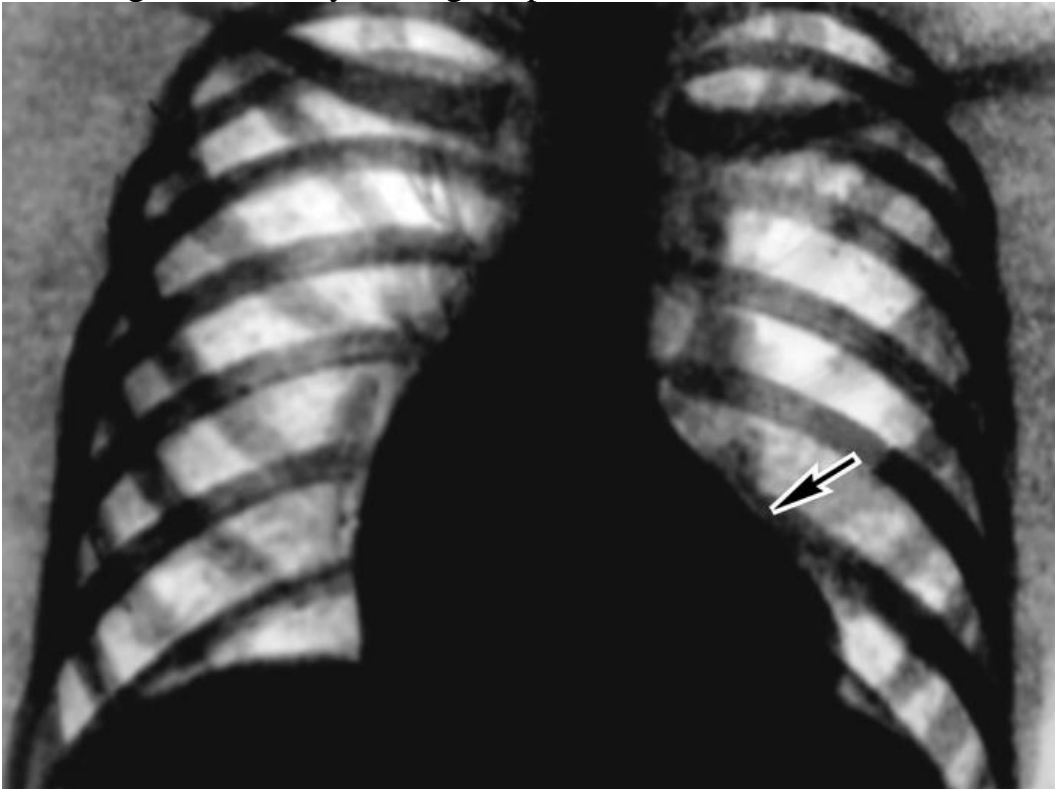


Figure 50: X-ray findings in patients with aortic stenosis



Note dilatation of the ascending aorta, increased convexity of the left ventricle, and normal pulmonary vascularity. The systolic aortic pressure gradient was 100 mmHg.

Chronic Aortic Valve Regurgitation

The incidence of clinically significant aortic regurgitation (AR) increases with age, typically peaking in the fourth to sixth decade of life. It is more common in men than women. The prevalence of AR in the Framingham study was reported to be 4.9%, with regurgitation of moderate or greater severity occurring in 0.5%.

Aortic Valve Regurgitation (AR) may be caused by malfunction of the valve leaflets themselves, by dilatation of the aortic root and annulus, or may be due to a combination of these factors (table 11.). Rheumatic disease is still the most common aetiology of AR in developing countries; however, in Western Europe and North America the leading cause of AR is either congenital (particularly due to bicuspid leaflets) or degenerative disease, including annuloaortic ectasia. Understanding the mechanism leading to AR is essential for proper patient management, including the surgical approach. Thus, knowledge of the morphology of the valve leaflets, the annulus and the ascending aorta are essential

Common causes of Chronic Aortic Valve Regurgitation

- congenital bicuspid aortic valve,
- rheumatic heart disease,
- infective endocarditis,
- all causes of fibrosis and calcification of the leaflets

AR causes volume overload of the left ventricle (LV). The total stroke volume ejected by the LV (sum of effective stroke volume plus regurgitant volume) is increased; in severe AR regurgitant volume may equal or even exceed effective stroke volume. An increase in LV end-diastolic volume is the main compensatory mechanism needed to maintain a normal effective stroke volume. Left ventricular ejection fraction is initially normal, however, LV end-diastolic pressure rises. In time LV end-diastolic volume continues to increase further and ejection fraction drops; these changes may actually precede the development of clinical symptoms. Considerable eccentric myocardial hypertrophy can occur with chronic AR and at autopsy heart weights of up to 1000 g have been reported.

Acute AR can be life threatening, as LV dilatation and other compensatory mechanisms cannot develop rapidly enough to avoid haemodynamic deterioration. The same regurgitant volume that would be well tolerated in chronic AR can lead to notable increases in LV end-diastolic pressure and a drop in effective stroke volume, leading to pulmonary oedema, hypotension and even cardiogenic shock.

In AR there is not only volume overload but also an increase in afterload and therefore of systolic wall stress. This distinguishes AR from mitral regurgitation (MR),¹ where LV volume overload is also present, but where systolic wall stress is normal or even low, since the regurgitant blood is ejected into the low pressure left atrium. Thus valve surgery in MR usually results in an increase in afterload and commonly in worsening of the LV ejection fraction, while surgical correction of AR results in a decrease in afterload and frequently an improvement of the ejection fraction. The differences in afterload between the two disorders could also explain why vasodilator treatment may be beneficial in AR, but not in MR.

Patients with chronic AR typically remain asymptomatic for many years, with symptoms developing only in the late stages of the disease. The most common clinical complaint is shortness of breath, initially occurring during exercise, but later also at rest. Patients may be aware of a prominent, bounding heart beat and may experience sinus tachycardia at minimal exertion as well as palpitations, which can be caused by ventricular or supraventricular arrhythmias. In some instances angina can be present even in the absence of coronary artery disease.

Physical examination reveals a characteristic high-pitched, blowing decrescendo diastolic murmur and - as soon as AR becomes moderate to severe—low diastolic arterial blood pressure, widened pulse pressure, and bounding pulses. Often an increase in systolic pressure also takes place. Widened pulse pressure is a useful indicator of haemodynamically significant AR; however, its absence does not reliably exclude severe regurgitation.

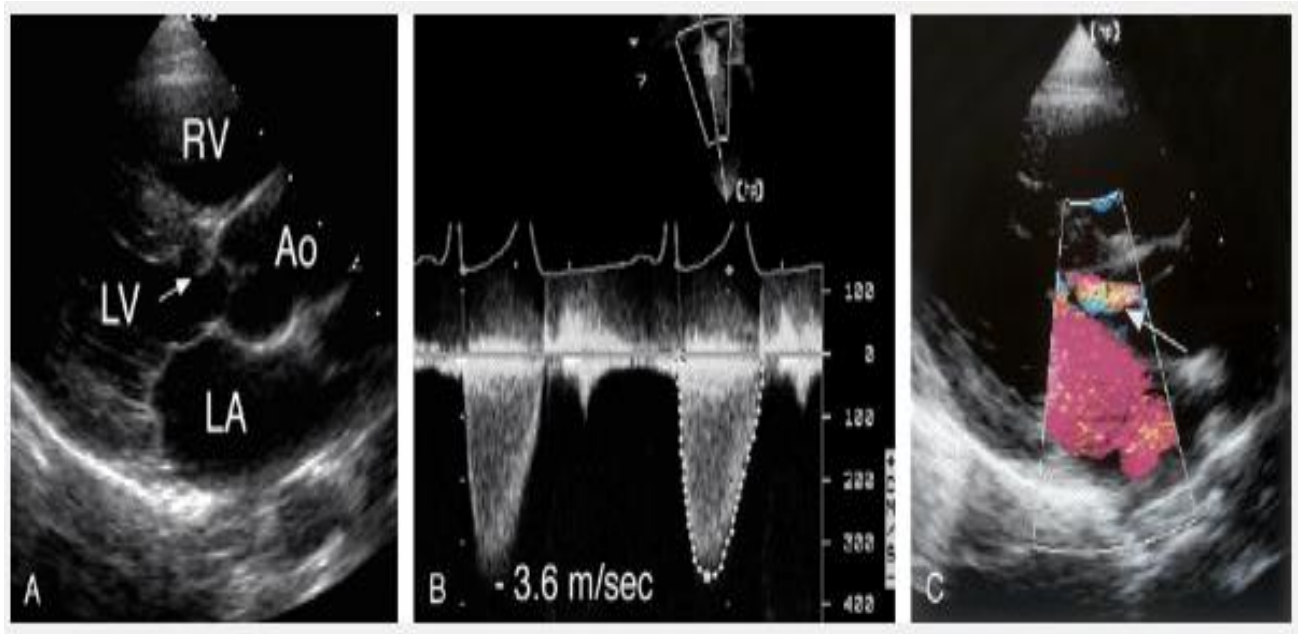
The ECG may be normal in mild AR. With greater degrees of regurgitation LV hypertrophy with or without strain pattern can be seen.

Chest x ray shows evidence of LV enlargement. Dilatation of the ascending aorta and aortic knob may be seen. Aneurysmal dilatation of the aorta can be present,

particularly in patients in whom the AR is related to primary disease of the aortic wall.

Echocardiography (Fig 51) presently is the principal tool for diagnosis and grading of AR severity as well as for serial follow-up. Colour Doppler is a highly sensitive and specific technique for detecting AR and provides visualisation of the regurgitant jet. Continuous and pulsed wave Doppler offer additional haemodynamic information and aid quantitation. Importantly, two dimensional echocardiography permits evaluation of LV size and function as well as visualisation of valve structures and of the aorta. Three dimensional echocardiography may play an increasing role in obtaining more precise measurements of ventricular volumes and may offer enhanced images of valve morphology

Figure 51: Echo- Doppler in patient with aortic regurgitation



Aortic root angiography and cardiac magnetic resonance imaging are alternative imaging techniques, particularly in rare instances when echocardiography is technically impossible or technically limited. Radionuclide ventriculography can be used to serially assess LV ejection fraction at rest and during exercise.

A valuable and simple parameter for grading AR is measurement of the narrowest width of the proximal regurgitant jet (vena contracta) by Colour Doppler. In very eccentric jets this measurement becomes unreliable.

Evaluation of the flow pattern in the proximal descending aorta using PW-Doppler yields additional important information.² Holodiastolic flow reversal is specific for severe AR, while no or only brief diastolic flow reversal indicates mild AR.

CW-Doppler can be used to measure regurgitant flow velocity of the AR jet, which reflects the diastolic pressure gradient between the aorta and the LV. The rate of deceleration and the derived pressure half-time correspond to the rate of equalisation of these pressures. With increasing AR severity, aortic diastolic pressure decreases more rapidly, the late diastolic jet velocity becomes lower, and pressure half-time becomes shorter. These measurements are not always reliable, as they are affected by other causes of elevated LV diastolic pressure or low aortic diastolic pressure.

References:

1. Хемптон Д. Р. ЕКГ у практиці = The ECG in Practice = ЭКГ в практике : навч. посіб. / Д. Р. Хемптон ; пер. 6-го англ. вид. О. І. Ромаскевича. - пер. 6-го вид. - Київ : ВСВ Медицина, 2018. - 560 с. - тримовне вид.
2. 2019 ESC Guidelines for the diagnosis and management of chronic coronary syndromes The Task Force for the diagnosis and management of chronic coronary syndromes of the European Society of Cardiology (ESC). European Heart Journal (2019) 00, 1-71
3. Guidelines on the management of valvular heart disease / European Heart Journal. – 2012. – Vol. 33. – P. 2451–2496.
4. Guidelines on the Management of Valvular Heart Disease. The Task Force on the Management of VHD of the ESC/ Eur Heart J 2007; 28: 230-268.
5. Iung B, Gohlke-Barwolf C, Tornos P. et al Recommendations on the management of the asymptomatic patient with valvular heart disease. Eur Heart J 2002;23:1253–1266.
6. Bonow R, Carabello B, DeLeon A C., Jr et al Guidelines for the management of patients with valvular heart disease: executive summary: a report of the American College of Cardiology/American Heart Association task force on practice guidelines (committee on management of patients with valvular heart disease). Circulation 1998; 98: 1949–1984